THESIS APPROVAL

GRADUATE SCHOOL, KASETSART UNIVERSITY

Master of Engineering (Chemical Engineering)
DEGREE

Chemical Engineering
FIELD

Chemical Engineering
DEPARTMENT

TITLE: Stability Analysis of Heat Exchanger Networks Using the Passivity Theorem

NAME: Mr. Nitipat Chaiwattanapong

THIS THESIS HAS BEEN ACCEPTED BY

.... **THESIS ADVISOR**
(Associate Professor Thongchai Srinophakun, Ph.D.)

.... **THESIS CO-ADVISOR**
(Assistant Professor Chanin Panjapornpon, Ph.D.)

.... **DEPARTMENT HEAD**
(Associate Professor Phungphai Phanawadee, D.Sc.)

APPROVED BY THE GRADUATE SCHOOL ON ....

.... **DEAN**
(Associate Professor Gunjana Theeragool, D.Agr.)

THESIS

STABILITY ANALYSIS OF HEAT EXCHANGER NETWORKS USING THE PASSIVITY THEOREM

NITIPAT CHAIWATTANAPONG

A Thesis Submitted in Partial Fulfillment of

the Requirements for the Degree of

Master of Engineering (Chemical Engineering)

Graduate School, Kasetsart University

2011

Nitipat Chaiwattanapong 2011: Stability Analysis of Heat Exchanger Networks Using the Passivity Theorem. Master of Engineering (Chemical Engineering), Major Field: Chemical Engineering, Department of Chemical Engineering. Thesis Advisor: Associate Professor Thongchai Srinophakun, Ph.D. 162 pages.

Passivity theorem as the stability analysis tool of the interconnected systems was studied and implemented in this thesis through both a single bypass heat exchanger and heat exchanger networks (HENs). A single bypass heat exchanger from Westhalen *et al*. (2003) was implemented with the passivity approach. Firstly, a state space model was developed along with its transfer function to test the passivity with the passivity index. This case study showed either passivity or non-passivity behavior depending upon its possible pairing schemes. Therefore, the magnitude of passivity index was used to rank the pairing schemes. Consequently, the passivity based decentralized unconditional stability (DUS) PI controllers for this system were designed and also verified with Aspen Dynamics simulator. This system was tested by making $\pm 10\%$ of setpoint temperatures and $\pm 10\%$ inlet hot flowrates. The results illustrated that the passivity approach gave better setpoint tracking than conventional PI controllers from the simulator.

The extension to HENs from Glemmestad *et al*. (1996) was further implemented. Likewise, this network was followed the passivity based DUS PI controller synthesis procedure. This network was tested by disturbing $\pm 1\%$ inlet hot flowrates. In addition, fault-tolerant control was tested by letting one of controllers failed during the network was facing disturbances. As a result, the proposed controllers could capably achieve fault-tolerant control while the other PI controllers had some deficiency and could not be controllable.

____________________ Student's signature

____________________ Thesis Advisor's signature

____ / ____ / ____

ACKNOWLEDGEMENTS

It is my pleasure to acknowledge those who have helped make this thesis possible. Firstly, I would like to express my gratitude to my advisor, Associate Professor Thongchai Srinophakun for advice, valuable suggestion, encouragement, enthusiasm, and great support throughout this work. He has been my most important mentor, and has greatly influenced my perspective in process control. Secondly, I would like to gratefully thank to Associate Professor Tony Paterson for the opportunity to visit his research group at School of Engineering and Advanced Technology, Massey University, Palmerston North, New Zealand during July to August 2010, and also gives me valuable suggestions for writing up a research manuscript to be published in the international journal.

Appreciation is also extended to Assistant Professor Chanin Panchapornpon, Dr.Veerayut Lersbamrungsuk, and Associate Professor Paisan Kongkachuichay for my kindly committee and giving me useful recommendations.

Acknowledgement is given to the Graduate school, Kasetsart University for giving me the scholarship to implement the research, given to the Department of Chemical Engineering, Kasetsart University for all facilities provided to accomplish this thesis, and also given to the Centre of Excellence for Petroleum, Petrochemicals, and Advanced Materials; Centre for Advanced Studies in Industrial Technology, for supporting this research.

My sincere thank is also given to my friends, colleagues, and teams in Centre of Process Control and Operation (CPCO), Kasetsart University, Thailand, and in School of Engineering and Advanced Technology, Massey University, New Zealand for their helps, their suggestions and their moral supports.

Most of all, I would like to express my deepest gratitude to my family for their loves and continuing encouragements.

Nitipat Chaiwattanapong

February 2011

TABLE OF CONTENTS

LIST OF TABLES

Table **Page**

LIST OF FIGURES

LIST OF FIGURES (Continued)

Figure **Page**

LIST OF FIGURES (Continued)

Figure **Page**

LIST OF FIGURES (Continued)

Figure **Page**

LIST OF FIGURES (Continued)

Appendix Figure **Page**

LIST OF ABBREVIATIONS

Abbreviations

Diag	=	Diagonal
CU	=	Cold Utility
CV	=	Controlled Variable
CW	=	Cooling Water
DIC	=	Decentralized Integral Controllability
DUS	=	Decentralized Unconditional Stability
EMAT	=	Exchanger Minimum Approach Temperature
HE	=	Heat exchanger
HENs	=	Heat Exchanger Networks
HU	=	Hot Utility
LMI	=	Linear Matrix Inequality
LTI	=	Linear Time Invariant
Max	=	Maximum
Min	=	Minimum
MIMO	=	Multi-Input Multi-Output
MINLP	=	Mixed Integer Nonlinear Programming
MV	=	Manipulated Variable
NS	=	Number of Stage
PI	=	Proportional Integral
PR	=	Positive Real
RGA	=	Relative Gain Array
RHP	=	Right Half Plane
SISO	=	Single Input Single Output
SPR	=	Strictly Positive Real

Greek Letters

LIST OF ABBREVIATIONS (Continued)

C, β	=	Area cost coefficient and exponent of area cost
ϵ	=	Arbitrarily small positive number
ρ	=	Density
ω	=	Frequency
ω_b	=	Frequency bandwidth
ν	=	Passivity index
ν_s	=	Diagonal scaling passivity index
k_c	=	Proportional gain of PI controller
τ_I	=	Time integral of PI controller
γ	=	Scalar decision variable
Ω	=	Upper bound for heat exchange
Γ	=	Upper bound for temperature difference
L_2	=	L_2 space
L_{2e}	=	Extended L_2 space
Σ	=	Time invariant dynamical system
$\subset$	=	Subset
$\triangleq$	=	Defined as
$\lambda_{\min}$	=	Minimum eigenvalue
Λ	=	Relative gain array
$\forall$	=	For all
$\in$	=	For some

Sets

HP	=	$\{ i \mid i$ is a hot process stream, $i = 1, \ldots, NH \}$
CP	=	$\{ j \mid j$ is a cold process stream, $j = 1, \ldots, NC \}$
ST	=	$\{ k \mid k$ is a stage, $k = 1, \ldots, NS \}$

LIST OF ABBREVIATIONS (Continued)

Subscripts

C	=	Cold process stream
H	=	Hot process stream
i	=	Input
m	=	m matrix dimension
n	=	number of cell
o	=	Output
0	=	Initial state

Superscripts

in	=	Input
out	=	Output
T	=	Transpose
n	=	n matrix dimension
m	=	m matrix dimension
*	=	Conjugate transpose

Symbols

$\bar{A}$	=	Numerical value of A at steady state condition
A^T	=	Transpose of matrix A
$A > 0$	=	Matrix A is positive definite
$A \geq 0$	=	Matrix A is positive semidefinite
D(ω)	=	A frequency dependent diagonal scaling matrix
f_T(t)	=	Truncation operator of function f(t)
$G(s)$	=	Transfer function of process
$h(x(t))$	=	Function of $x(t)$

LIST OF ABBREVIATIONS (Continued)

K(s)	=	Transfer function of controller
Re(A)	=	Real part of complex matrix A
w(s)	=	Weighting function
w(t)	=	Supply rate

Units

atm	=	Atmosphere
BTU	=	British thermal unit
ºC	=	Degree celsius
F	=	Degree fahrenheit
ft^2	=	Square feet
ft^3	=	Cubic feet
hr	=	Hour
K	=	Kelvin
kg	=	Kilogram
kW	=	Kilowatt
m^2	=	Square meter
m^3	=	Cubic meter

Variables

a, b, c, k	=	Decision variables of weighting function
A	=	Heat exchanger area
A, B, C, D	=	Matrix coefficient of state space equation
C	=	Cold process stream
CCU	=	Unit cost of cold utility
CF	=	Fixed charge for exchangers
CHU	=	Unit cost of hot utility

LIST OF ABBREVIATIONS (Continued)

C_p	=	Specific heat capacity
dt_{ijk}	=	Temperature approach for match (i,j) at temperature location k
$dtcu_i$	=	Temperature approach for match of hot stream i and cold utility
$dthu_j$	=	Temperature approach for match of cold stream j and hot utility
f	=	Bypass fraction of stream
F	=	Volumetric flowrate
FC_p	=	Heat capacity flowrate
h	=	Heat transfer coefficient
H	=	Hot process stream
I	=	Identity matrix
Im	=	Imaginary number
j	=	Square root of minus one (-1)
k	=	Stage of superstructure of heat exchanger networks
n	=	Matrix dimension
p	=	Pole of transfer function
q_{ijk}	=	Heat exchange between hot and cold stream (i,j) in stage k
qcu_i	=	Heat exchanged between hot stream i and cold utility
qhu_j	=	Heat exchanged between cold stream j and hot utility
R	=	Real number
s	=	Frequency domain (or called s-domain)
S	=	Storage function
t	=	Time
t_{ik}	=	Temperature of hot stream i at hot end of stage k
t_{jk}	=	Temperature of cold stream j at hot end of stage k
T	=	Temperature
TIN	=	Supply temperature
u	=	Manipulated variable
U	=	Overall heat transfer coefficient
U	=	Space of control

LIST OF ABBREVIATIONS (Continued)

U	=	Diagonal matrix with either -1 or 1 along the diagonal
v	=	Volumetric flowrate
V	=	Volume of compartment of a heat exchanger
x	=	State variable
X	=	Space of state
y	=	Output variable
Y	=	Space of output
z_{ijk}	=	Binary variable to denote existence of match (i,j) in stage k
zcu_i	=	Binary variable denoting CU exchanges heat with stream i
zhu_j	=	Binary variable denoting HU exchanges heat with stream j

STABILITY ANALYSIS OF HEAT EXCHANGER NETWORKS USING THE PASSIVITY THEOREM

INTRODUCTION

Heat exchanger networks (HENs) are the most important part dealing with energy recovery in many chemical process industries. Generally, a HEN consists of a number of heat exchangers which hot process streams are integrated with cold process streams in order to achieve the highest energy recovery as possible. The energy integration, however, introduces interactions, and may make the process more difficult to control and operate (Mathisen, 1994). Interactions and other effects such as disturbance or setpoint variations, which are normally encountered in the HEN operations, may deteriorate the performance and lead to the instability of the HENs. These effects result the undesirable target temperatures. Consequently, a control point of view of a HEN becomes a main motivation in this work. Up to present, a number of researches on HENs have been published since the last two decades (Furman and Sahinidis, 2002). They are not only hardly focused on the control but also mainly concentrated on steady state optimal design and operation of HENs. Therefore, the point of dynamics behaviors of the HENs is of interest. A way that commonly uses to describe the dynamics behavior of the system is *state space* (Ogata, 1967) which is adopted throughout this work.

A state space equation or dynamics equation is the set of equations that describes the unique relations between the input, output, and state (Chi-Tsong, 1984). In practice, models of HENs are formidably presented, thus, the model of single heat exchanger is preferred to primarily concern. After that, a number of single heat exchangers will be expanded to the network of heat exchangers. For a single heat exchanger, its state space has been available in many woks (Varga *et al*., 1995; Hangos *et al*., 2004; Mathisen, 1994); however, they concerned only a single heat exchanger which is not realistic in industrial processes that regularly equip a bypass with the heat exchanger. As Glemmestad *et al*. (1996) mentioned, for optimal operation of a HEN, bypasses should be manipulated in order to maintain the target temperatures. Hence, the state space equation for a single heat exchanger with a single bypass will be presented and for the network also.

As mentioned above, the stability of HENs is very indispensable in the field of an energy integration process. For example, if one of a heat exchanger in a HEN fails, all of the HEN may be accordingly failed. Therefore, the stability analysis of this system should be concerned.

The one technique to analyze the stability of general processes is the passivity theorem (Van Der Schaft, 1997) which is the most useful method to stability analysis. Generally speaking, passive systems are the systems that do not generate energy with respect to the given input and output ports (Willems, 1972a). Linear passive systems are phase bounded, and a strictly passive system combined with another passive system is stable without necessarily satisfying the small gain condition. Therefore, the passivity theorem provides another approach to robust control which may be less conservative than the small-gain based approaches (Bao, 1998).

The stability analysis of HENs using the passivity theorem has not been reported yet. However the single heat exchanger was already implemented with the passivity theorem by Bao and Lee (2007). They addressed that the heat exchanger was inherently passive because the passivity condition was valid for any design parameters, types of fluid, and operating conditions. Although the heat exchanger is physically passive, there is a specific case to take heat exchanger to be non-passive. Normally, a heat exchanger accompanied with a bypass is the well-known fashion used in many chemical process industries (*e.g.* Westhalen *et al*., 2003; Glemmestad *et al*., 1996; Escobar and Trierweiler, 2009). This design can probably take the heat exchanger to be non-passive. Consequently, it is of interest to study, and drives a motivation for this thesis.

OBJECTIVES

1. To apply the passivity theorem with heat exchanger networks.

2. To design the passivity based DUS PI controllers for this process.

3. To study the heat exchanger networks using bypasses as manipulation.

4. To develop the state space equation of heat exchanger networks.

Scopes of Work

1. The lump dynamic models of a single heat exchanger presented in this thesis are applied from Hangos *et al*. (1994).

2. The concepts of passive system and their relations are referred from Bao *et al.* (2000; 2002) and Boonkhao (2004).

3. The water is used as the only one component in HENs and no phase changes.

4. The results are verified via Aspen Dynamics.

5. Single bypasses are assumed to be used and only placed on either hot or cold side of a heat exchanger.

6. Economic objective of HENs is not concerned in this work.

Thesis Contribution

1. Embed the stability analysis of HENs

2. Obtain more knowledge of dynamic models of HENs in the state space form.

3. Clearly understand the relations between HENs and passivity.

LITERATURE REVIEW

This section is divided into two main parts. The first part is reviewed the literatures relating with HENs and the passivity theorem, and the second part is reviewed the theory related.

1. Literature Review

For the literature review section, the first part is reviewed the works related to HENs and another one is reviewed the works related to passivity theorem (and/or passivity properties).

1.1 Heat exchanger networks (HENs)

Wolff *et al*. (1991) presented various dynamic models of single heat exchangers and the HEN which may also include stream splitting, mixing and bypasses. They studied where bypasses should be placed in the network by dynamics considerations, and investigated interaction and pairing considerations when placing bypasses.

Mathisen and Morari (1994) described model features which are important to assess controllability of heat exchangers and HENs. They discriminated between important and less important model features by order of magnitude argumentation, comparison of controllability measures and dynamic simulations. Important model features for single heat exchangers are model order (number of cell-model), wall capacitance and fluid compressibility, whereas flow configuration and temperature driving force have only a small effect on the dynamics. The most important model feature for HENs is residence time of the connecting pipes.

Glemmestad *et al*. (1996) discussed a procedure for optimal operation of HENs. This procedure is based on structural information of the HENs, and is used to find which bypass manipulation that should be adjusted in order to compensate for deviation in the output temperature so that utility consumption is minimized. The procedure is used to pair output temperatures and manipulated inputs in a decentralized control structure that "automatically" will find the optimal bypass fractions at steady state. It has been demonstrated by dynamic simulations of the controlled HENs that the procedure works well. However, in this work, the trade-off between steady-state and dynamic performance is not considered.

Gonzalez *et al*. (2006) presented a method to control HENs where both the control objective and the economics objective are taken into account. It is assumed that they have a two-layer structure in which the steady state economic optimization is performed in the upper level, and the model predictive control (MPC) controller is used to enforce the optimal operating point defined by the economic layer. In this approach, integration is achieved through the definition of an extended cost-function that provides the controller with the ability of driving the system to optimal conditions.

Lersbamrungsuk *et al*. (2007) studied a simple split-range control scheme to implement the optimal operation of HENs when only single bypasses and utility duties are used as manipulations. The optimal operation of HENs can be formulated as a linear programming implying the operation always lies at some input constraints. They mentioned that this technique is not only able to be applied for constraint (vertex) optimal operation problem, but also for unconstraint (nonvertex) optimal operation problem (e.g., simplifying an online optimization task)

1.2 Passivity theorem (and/or passivity properties)

The concept of passive systems originally arose in the context of electrical circuit theory. In such electrical systems, no energy is generated, e.g. a network consisting of only inductors, resistors and capacitors (Guillemin 1957; Weinberg 1962).

Willems (1972) studied the dissipative systems. It is defined in term of an inequality of storage function and the supply rate function. The storage function is bounded from below by the available storage and from above by the required supply. These ideas were applied to the interconnected system and stability.

Desoer and Vidyasagar (1975); Willems (1972) analyzed the stability of interconnected passive systems. The important theorem which can be used to determine the input-output stability of passive systems is the Passivity Theorem, which can be simply stated as: a system formed by the negative feedback of a passive system and a feed-forward strictly passive system with finite gain is asymptotically stable.

Bao *et al*. (2000b) proposed the passivity-based conditions for closed-loop stability, and also the tuning method for multi-loop PI controllers was developed satisfying the above conditions. This leads to a failure-tolerant design, as each control loop can be arbitrarily and independently detuned even switched off, without affecting the closed-loop stability.

Bao *et al*. (2002a) provided a new approach to stability analysis for multi-loop control systems. The passivity index not only used to check whether the system is passive but also used to decide pairing schemes. The decentralized unconditional stability condition, which implies closed-loop stability of decentralized control systems under control loop failure, was derived.

Bao *et al*. (2002c) proposed a new pairing method for multi-loop control for multivariable processes. Based on the passivity theorem, a new pairing rule does not imply general diagonal dominance. The passivity index was used to indicate the performance of the closed-loop system under decentralized control. The advantages of this proposed method are: (1) It is an open-loop dynamic analysis and does not need to assume closed-loop transfer function; (2) It indicates the total destabilizing effects of both interactions and process dynamics and does not imply the diagonal dominance conditions; (3) The analysis procedure is entirely mechanical and thus can be performed automatically by a computer.

Sirisak (2002) implemented the passivity theorem to milk-powder plant in New Zealand. He adopted the passivity index to indicate the best paring of manipulate and output of decentralized control and then found the controllers which stabilize the process based on passivity theorem.

Lengsukchai (2003) studied the measure of the passivity-based interaction on the process system with time delay, RHP zeros and large interaction. This passivity-based interaction measure predicted the stability of decentralized control systems and also evaluated their performance losses. The steady state value of the measure provided a sufficient condition for offset free decentralized control. And the controllers were designed by H_∞ synthesis procedure. The simulation results show that the passivity-based interaction measure of all case studies at steady state was less than unity. Therefore the controllers can be designed to achieve the offset-free condition as can be considered in the closed-loop response of each case study process.

2. Theories

In this theoretical part, there are two major topics, HENs and passivity and its relation properties, to describe some necessary definitions or equations that may be used to carry out this thesis.

2.1 Heat exchanger networks (HENs)

2.1.1 Dynamic models of a heat exchanger network

In order to assess controllability (in case of applying passivity theorem to stability analysis) of HENs, a dynamic model of a heat exchanger is required. Although heat exchangers are usually distributed parameter process systems, they can be built as approximate lumped parameter models using finite difference approximations of their spatial variables (as in the method of lines approximation scheme) (Hangos *et al*., 2004). A heat exchanger can then be seen as a composite lumped parameter process system consisting of elementary dynamic units as depicted in Figure 1.

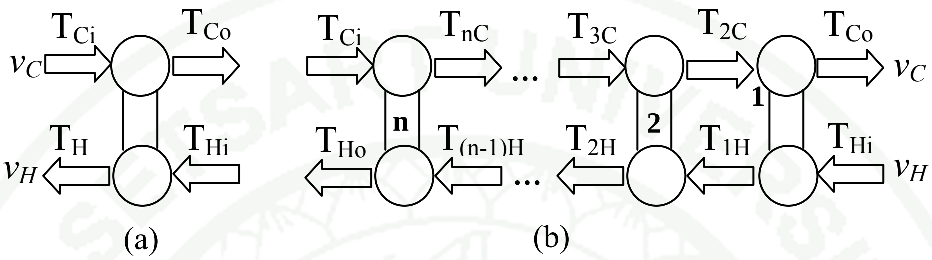

Figure 1 A cascade model of a heat exchanger

Source: Hangos *et al*. (2004)

For lumped heat exchanger model, let one of the lumps be $j = H$ (hot side) or $j = C$ (cold side) which their lumped variables are shown in Figure 1a

2.1.1.1. Modeling assumptions

In order to obtain a simple model with only two state equations, the following simplifying modeling assumptions are used (Hangos *et al*., 2004):

1. Constant volume and mass hold-up in both of the lumps $j = C; H$.
2. Constant physico-chemical properties, such as density ρ_j, specific heat C_{Pj}.
3. Constant heat transfer coefficient U and area A.
4. Completely observable states, i.e. $y(t) = x(t)$.

2.1.1.2. Conservation balances

The continuous time state equations of the heat exchanger cell above are the following energy conservation balances (Hangos *et al*., 2004):

$$\dot{T}_{Co}(t) = \frac{v_C(t)}{V_C}(T_{Ci}(t) - T_{Co}(t)) + \frac{UA}{\rho_C C_{pC} V_C}(T_{Ho}(t) - T_{Co}(t)) \tag{1}$$

$$\dot{T}_{Ho}(t) = \frac{v_H(t)}{V_H}(T_{Hi}(t) - T_{Ho}(t)) + \frac{UA}{\rho_H V_H C_{pH}}(T_{Co}(t) - T_{Ho}(t)) \tag{2}$$

where T_{ji} and T_{jo} are the inlet and outlet temperatures, V_j is the volume and v_j is the volumetric flow rate of the two sides ($j = C; H$), respectively.

2.1.1.3. System variables

The state vector is therefore composed of the two outlet temperatures:

$$x_1 := T_{Co}, x_2 := T_{Ho} \tag{3}$$

There are a number of possible time-dependent variables on the right-hand side of the above equations which may act as manipulable input variables or disturbances, depending on the measurement and actuator settings and on any additional modeling assumptions we may have. These are as follows:

1. The inlet temperatures: T_{Ci} and T_{Hi},
2. The volumetric flowrates: v_C and v_H.

The special cases of the heat exchanger cell models are obtained by specifying assumptions on their variations in time. For every case, the output equation is

$$y(t) = h(x(t)) = [x_1(t) \;\; x_2(t)]^T \tag{4}$$

2.1.1.4 Additional modeling assumptions

From this step, the state space of a heat exchanger model can be either linear or nonlinear model depending on the following additional assumptions.

1. The model will be linear model if volumetric flowrates are assumed to be constant, and inlet temperatures are manipulable.

2. The model will be nonlinear model for more realistic case of heat exchanger if inlet temperatures are assumed to be constant, and volumetric flowrates are manipulable.

When each heat exchanger is considered, the system can be extended to the network.

2.1.2 Mathematical model for heat exchanger network synthesis

In synthesizing a HEN using the formulation of the mathematical model, it is proposed into two main techniques. The first one is the sequential synthesis whereas the minimum utility cost (operating cost) is considered following by the minimization of the number of units and investment cost. The second one is the simultaneous synthesis in which the tradeoff between the operating cost and the investment cost is taken into account to minimize the total annual cost, simultaneously. Many researches are reported that the optimal result from the simultaneous synthesis is more efficient than the sequential synthesis in the way of reporting the lower total annual cost of the network. This part, hence, will show the mathematical model to synthesize the HEN using the simultaneous synthesis technique.

The simultaneous synthesis technique is described based on the stage-wise superstructure representation proposed by Yee and Grossmann (1990). The two-stage superstructure for the problem with two hot and cold streams is shown in Figure 2. However, in most cases, the number of stages is selected as the maximum of hot and cold process stream i.e. number of stages ≥ max (number of hot streams, number of cold streams).

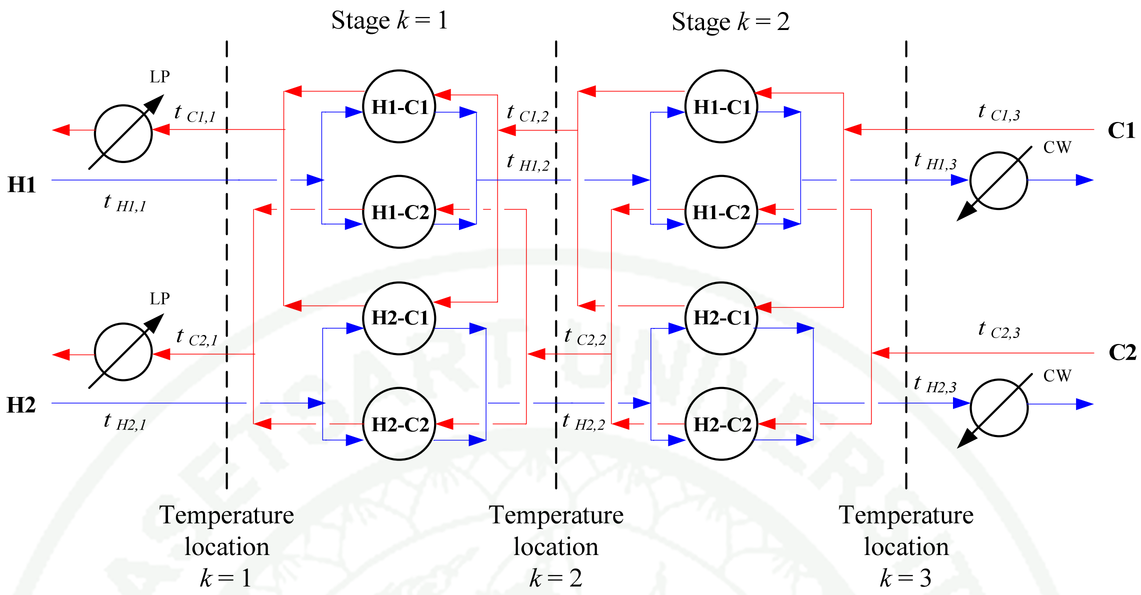

Figure 2 Two-stage superstructure for heat exchanger networks

Source: Yee and Grossman (1990)

Within each stage of the superstructure, heat exchanges between any pair of hot and cold streams can occur. In each stage, the hot (cold) process stream is split and directed to an exchanger in order to match with each cold (hot) stream. Obviously, the two-stage superstructure for the problem containing two hot and cold streams involves eight exchangers with four possible matches in each stage e.g. in stage $k = 1$ possible matches are H1 – C1, H1 – C2, H2 – C1, and H2 – C2.

For the model formulation of the simultaneous synthesis of HENs, it can be formulated as a mixed integer nonlinear programming (MINLP) model. The definition of parameters and variables in the model are provided in the following part.

Indices:

i = Hot process stream

j = Cold process stream

k = Index of stage, 1,…, NS, and temperature location, 1,…, $NS + 1$

Sets:

HP = $\{ i \mid i$ is a hot process stream, $i = 1, \ldots, NH \}$

CP = $\{ j \mid j$ is a cold process stream, $j = 1, \ldots, NC \}$

ST = $\{ k \mid k$ is a stage, $k = 1, \ldots, NS \}$

Parameters:

T^{in} = Inlet temperature of stream

T^{out} = Outlet temperature of stream

FCp = Heat capacity flow rate

U = Overall heat transfer coefficient

CCU = Unit cost of cold utility

CHU = Unit cost of hot utility

CF = Fixed charge for exchangers

C, β = Area cost coefficient and exponent of area cost

Ω = Upper bound for heat exchange

Γ = Upper bound for temperature difference

Variables:

dt_{ijk} = Temperature approach for match (i,j) at temperature location k

$dtcu_i$ = Temperature approach for match of hot stream i and cold utility

$dthu_j$ = Temperature approach for match of cold stream j and hot utility

q_{ijk} = Heat exchange between hot and cold process stream (i,j) in stage k

qcu_i = Heat exchanged between hot stream i and cold utility

qhu_j = Heat exchanged between cold stream j and hot utility

t_{ik} = Temperature of hot stream i at hot end of stage k

t_{jk} = Temperature of cold stream j at hot end of stage k

z_{ijk} = Binary variable to denote existence of match (i,j) in stage k

zcu_i = Binary variable to denote that cold utility exchanges heat with stream i

zhu_j = Binary variable to denote that hot utility exchanges heat with stream j

With the above declaration, the formulation can now be presented. The objective function of this task is the minimum total annualized cost of the network subjecting to the following seven constraints.

Constraint 1: *Overall heat balance for each stream*

This constraint is needed to ensure sufficient heating or cooling of each process stream. The constraints specify that the overall heat transfer requirement of each stream must equal to the sum of the heat it exchanges with other process streams at each stage plus the exchange with the utilities streams

$$(T_i^{in} - T_i^{out})FCp_i = \sum_{k \in ST} \sum_{j \in CP} q_{ijk} + qcu_i \qquad i \in HP \tag{5}$$

$$(T_j^{out} - T_j^{in})FCp_j = \sum_{k \in ST} \sum_{i \in HP} q_{ijk} + qcu_j \qquad j \in CP \tag{6}$$

Constraint 2: *Heat balance at each stage*

An energy balance is also needed at each stage of the superstructure to determine the temperatures. Temperatures for the streams are the highest at temperature location k = 1 and the lowest at last temperature location.

$$(t_{i,k} - t_{i,k+1})FCp_i = \sum_{j \in CP} q_{ijk} \qquad k \in ST \quad i \in HP \tag{7}$$

$$(t_{j,k} - t_{j,k+1})FCp_j = \sum_{i \in HP} q_{ijk} \qquad k \in ST \quad j \in CP \tag{8}$$

Constraint 3: *Assignment of superstructure inlet temperatures*

Fixed supply temperatures (*TIN*) of the process streams are assigned as the inlet temperatures to the superstructure. In Figure 2, for hot streams the superstructure inlet corresponds to temperature location k = 1, while the cold streams, the inlet corresponds to location k = 3.

$$TIN_i = t_{i,1} \qquad \text{and} \qquad TIN_j = t_{j,NS+1} \tag{9}$$

Constraint 4: *Feasibility of temperatures*

Constraints are also needed to specify a monotonic decrease of temperature at each successive stage. In addition, a bound is set for the outlet temperatures of the superstructure at the specific stream's target temperature. Note that the temperature of each stream at its last stage does not necessarily correspond to the stream's target temperature since utility exchanges can occur at the outlet of the superstructure.

$$t_{i,k} \ \geq \ t_{i,k+1} \qquad k \in ST \quad i \in HP \tag{10}$$

$$t_{j,k} \ \geq \ t_{j,k+1} \qquad k \in ST \quad j \in CP \tag{11}$$

$$TOUT_i \ \leq \ t_{i,NS+1} \qquad i \in HP \tag{12}$$

$$TOUT_j \ \geq \ t_{j,1} \qquad j \in CP \tag{13}$$

Constraint 5: *Hot and cold utility load*

Hot and cold utility requirements are determined for each process stream in term of the outlet temperature in the last stage and the target temperature for that stream. The utility heat load requirements are determined as follows:

$$(T_{i,NS+1} - T_i^{out})FCp_i = qcu_i \qquad i \in HP \tag{14}$$

$$(T_j^{out} - t_{j,1})FCp_i = qhu_j \qquad j \in CP \tag{15}$$

Constraint 6: *Logical constraints*

Logical constraints and binary variables are needed to determine the existence of process match between streams *i,j* in stage *k* and also any match involving utility streams. The binary variables, 0-1, are represented by z_{ijk} for process stream matches, and zcu_i and zhu_j for matches involving cold and hot utility, respectively. An integer value of one for any binary variable designates that the match is presented in the optimal network.

$$q_{ijk} - \Omega z_{ijk} \leq 0 \qquad i \in HP \quad j \in CP \quad k \in ST \tag{16}$$

$$qcu_i - \Omega zcu_k \leq 0 \qquad i \in HP \tag{17}$$

$$qhu_j - \Omega zhu_j \leq 0 \qquad j \in CP \tag{18}$$

$$z_{ijk},\ zcu_i,\ zhu_j = 0,1$$

Constraint 7: *Calculation of approach temperatures*

The area requirement of each match will be incorporated in the objective function. Calculation of these areas requires that approach temperatures be determined. To ensure feasible driving forces for exchangers that are selected in the optimization procedure, the binary variables are used to activate or deactivate the following constraints. Nevertheless, the approach temperature between the hot and cold streams at any point of any exchangers will be at least exchanger minimum approach temperature (EMAT).

$$dt_{ijk} \leq t_{i,k} - t_{j,k} + \Gamma(1 - z_{ijk}) \qquad i \in HP \quad j \in CP \quad k \in ST \tag{19}$$

$$dt_{ijk+1} \leq t_{i,k+1} - t_{j,k+1} + \Gamma(1 - z_{ijk}) \qquad i \in HP \quad j \in CP \quad k \in ST \tag{20}$$

$$dtcu_i \leq t_{i,NS+1} - TOUT_{CU} + \Gamma(1 - zcu_i) \qquad i \in HP \tag{21}$$

$$dthu_i \leq TOUT_{HU} - t_{j,1} + \Gamma(1 - zhu_j) \qquad j \in CP \tag{22}$$

$$dt_{ijk} \geq EMAT \tag{23}$$

Objective Function: *Minimum Total Annualized Cost*

The objective function can be defined as the annual cost for the network. The annual cost is the combination of the utility cost, the fixed charges for the exchangers, and the area cost for each exchanger. The objective function is derived as follows:

$$\text{Minimize} \quad \sum_{i\in HP} CCU\ qcu_i + \sum_{j\in CP} CHU\ qhu_j$$

$$+\sum_{i\in HP}\sum_{j\in CP}\sum_{k\in ST} CF_{ij} z_{ijk} + \sum_{i\in HP} CF_{i,CU} zcu_i + \sum_{j\in CP} CF_{j,HU} zhu_j$$

$$+\sum_{i\in HP}\sum_{j\in CP}\sum_{k\in ST} C_{ij}\left[q_{ijk} / \left(U_{ij}\left[\left(dt_{ijk} dt_{ijk+1} \right)\left(dt_{ijk} + dt_{ijk+1} \right)/2 \right]^{1/3} \right) \right]^{\beta_{ij}}$$

$$+\sum_{i\in HP} C_{i,CU}\left[qcu_i / \left(U_{i,CU}\left[\left(dtcu_i \right)\left(TOUT_i - TIN_{CU} \right)\left[dtcu_i + \left(TOUT_i - TIN_{CU} \right) \right]/2 \right]^{1/3} \right) \right]^{\beta_{i,CU}}$$

$$+\sum_{j\in CP} C_{HU,j}\left[qhu_j / \left(U_{HU,j}\left[\left(dthu_j \right)\left(TIN_{HU} - TOUT_j \right)\left[dthu_j + \left(TIN_{HU} - TOUT_j \right) \right]/2 \right]^{1/3} \right) \right]^{\beta_{j,CU}} \quad (24)$$

where $\dfrac{1}{U_{ij}} = \dfrac{1}{h_i} + \dfrac{1}{h_j}$; $\dfrac{1}{U_{i,CU}} = \dfrac{1}{h_i} + \dfrac{1}{h_{CU}}$; $\dfrac{1}{U_{HU,j}} = \dfrac{1}{h_j} + \dfrac{1}{h_{HU}}$

2.2 Passivity theorem (and/or passivity properties)

2.2.1 Passivity theorem

The basic concepts of passive systems are introduced in this section. Since this concept is fundamentally connected with dissipativeness and is a special case of dissipativeness. Let start from the definition of dissipative systems and consider the time invariant dynamical system Σ:

$$\dot{x} = f(x) + g(x)u \quad (25)$$

$$y = h(x) \quad (26)$$

where $x \in X \subset R^n$, $u \in U \subset R^m$ and $y \in Y \subset R^m$ are state, control and output vectors respectively, and X, U and Y are state, control and output spaces respectively. The representation $x(t) = \phi(t, t_0, x_0, u)$ is used to denote the state at time t reached from the initial state x_0 at t_0.

***Definition 1**: Supply Rate* (Willems, 1972a)

The supply rate w(t) = w(u(t), y(t)) is a real valued function defined on U × Y, such that for any $u \in$ U and $x_0 \in$ X and output y(t) = h(ϕ(t, x_0, u)), w(t) satisfies

$$\int_{t_0}^{t_1} |w(t)| dt < \infty \tag{27}$$

for all $t_1 \geq t_0 \geq 0$, and usually can be an inner product of u(t) and y(t), which is an abstract concept of input power.

***Definition 2**: Dissipative Systems* (Willems, 1972a)

A system Σ with supply rate w(t) is said to be dissipative if exists a nonnegative function S: X → R^+, called the storage function, such that for all (t_1, t_0) ∈ R_2^+, $x_0 \in$ X, and u ∈ U,

$$S(x_0) + \int_{t_0}^{t_1} w(t) dt \geq S(x_1) \tag{28}$$

where $x_1 = \phi(t_1, t_0, x_0, u)$ and w(t) = w(u(t), y(t)), with $y = y(t_0, x_0, u)$.

***Definition 3**: Available Storage Function* (Willems, 1972a)

The available storage, S_a, of a dynamical system Σ with supply rate is the function from X into R^e defined by

$$S_a(x) = \sup_{\substack{x\rightarrow \\ t_1 \geq 0}} - \int_{0}^{t_1} w(t) dt \tag{29}$$

where the notation $x \rightarrow$ denotes the supremum over all motions starting in state x at time 0 and where the supremum is taken over all u ∈ U.

The available storage function plays an important role in dissipative/passive systems. If a system is dissipative, the available storage function $S_a(x)$ is finite for each $x \in$ X. Moreover, any possible storage function S(x) satisfies

$$0 \leq S_a(x) \leq S(x) \tag{30}$$

for each $x \in$ X. If S_a is continuous (C^0) function, then S_a itself is a possible storage function.

Definition 4: Linear Passive Systems (Willems, 1972b)

A linear time invariant system $\sum : G(s) := C(sI - A)^{-1}B + D$, (G(s) is a n×n transfer function matrix, and A, B, C, D are coefficients of a state space) is *passive* if and if G(s) is *positive real* (PR), or equivalently,

1. $\mathrm{Re}[\lambda_i(A)] \leq 0$ for i = 1,…, n,
2. $G(j\omega)+G^*(j\omega) \geq 0$ for all real ω, $j\omega \neq \lambda_i(A)$,
3. Imaginary eigenvalues of *A* are nonrepeated and the residue matrix at those eigenvalues is Hermitian and nonnegative definite.

G(s) is said to be *Strictly Passive* or *Strictly Positive Real* (SPR) if :

1. $\mathrm{Re}[\lambda_i(A)] < 0$ for i = 1,…, n,
2. $G(j\omega)+G^*(j\omega) > 0$ for all real ω, $j\omega \neq \lambda_i(A)$

For the multi-loop control system as shown in Figure 3, if the multivariable process G(s) is strictly passive, then the closed loop is stable if the multi-loop controller K(s) is passive, regardless of loop interactions.

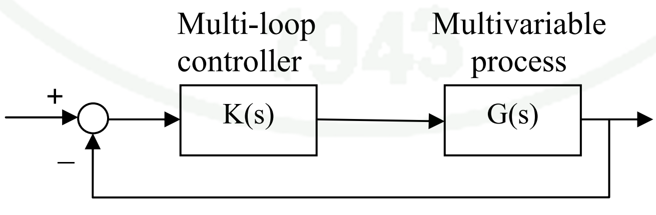

Figure 3 Multi-loop control system

Source: Bao *et al*. (2002a)

Theorem 1: *Passivity Theorem* (Van Der Schaft, 1997)

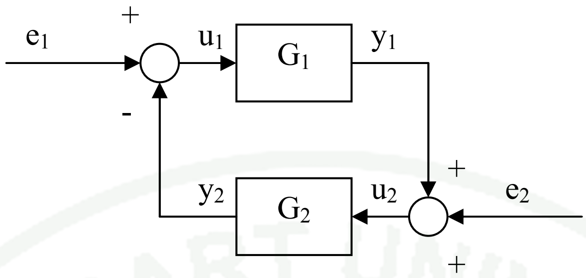

Figure 4 Passivity Theorem

Source: Van Der Schaft (1997)

Consider the closed-loop system of G_1, G_2 (as shown in Figure 4) with $e_2 \equiv 0$ so that

$$u_1 = e_1 - G_2(u_2) \tag{31}$$

$$u_2 = G_1(u_1) \quad e_1 \in L_2 \tag{32}$$

with G_1, G_2 : $L_{2e} \to L_{2e}$ Assume that for any $e_1 \in L_2$ there are solutions $u_1, u_2 \in L_{2e}$. If G_1 is passive and G_2 is strictly passive, then $u_2 = G_1(u_1) \in L_2$ where L_{2e} is the extended L_2 space, which consists of all measurable signals f(t) such that its truncation $f_T(t) \in L_2$.

2.2.2 Passivity index and passivity based stability conditions

2.2.2.1 Extended passivity condition for non-passive systems

Many chemical processes are not passive (Bao *et al.*, 2002a), and thus, the passivity based condition given in Theorem 1 cannot be directly used to analyze decentralized unconditional stability for those systems. Therefore, the passivity index is introduced and the passivity based condition is extended to cope with both passive and non-passive processes. As any stable non-passive process can be rendered passive by adding a nonnegative feedforward, the minimum feedforward required can be used to measure how far the process is from being passive and thus defined as the passivity index.

Theorem 2: (Bao and Lee, 2007) For a given stable non-passive process with a transfer function matrix of G(s), there exists a diagonal, stable, and passive transfer function matrix W(s) = *w(s)I* such that H(s) = G(s) + W(s) is passive. This full theorem proof is shown in Appendix D.

Definition 5: *Passivity Index ν* (Bao *et al*., 2000a)

Given a stable linear time invariant system $\sum : \mathrm{G(s)} := \mathrm{C}(\mathrm{sI}-\mathrm{A})^{-1}\mathrm{B}+\mathrm{D}$, the passivity index is defined as:

$$\nu(\mathrm{G}) \triangleq \inf\{\nu \in \mathrm{R}:(\mathrm{A,B,C,D}+\nu I) \text{ is strictly positive real}\} \tag{33}$$

The ν-index can also be defined as a function of frequency *ω*.

$$\nu(G,\omega) \triangleq -\lambda_{\min}\left(\frac{1}{2}\left[G(j\omega)+G^*\left(j\omega\right)\right]\right) \tag{34}$$

Passive systems are phase bounded (Haddad and Bernstein, 1991; Bao *et al.,* 1996). The phase of passive system lies in [-π/2,+π/2] and therefore, the small gain condition is not required for a closed-loop system comprising of two passive systems.

Index ν(G,ω) indicates how far the system G(s) is from being passive and is negative if G(s) is passive. Apparently, for a system G(s) with its passivity index $\nu(\mathrm{G(s)},\omega)$, if a stable and minimum phase transfer function w(s) is chosen such that

$$\nu(\mathrm{w(s)},\omega) < -\nu(\mathrm{G(s)},\omega) \tag{35}$$

then G(s)+w(s)I is strictly passive.

The passivity index of a linear system comprises both phase and gain information about the system in question (Bao *et al*., 1998). This can be seen from a simple SISO example. Given a system G(s), its passivity index at frequency ω is given by

$$\nu\left[G(s),\omega\right] = -\{\mathrm{Re}\}\left[G(j\omega)\right] = -\left|G(j\omega)\right|\cos(\phi) \qquad (36)$$

where

$$\phi = \tan^{-1}\left(\frac{\mathrm{Im}\left(G(j\omega)\right)}{\mathrm{Re}\left(G(j\omega)\right)}\right) \qquad (37)$$

It is possible to use the passivity index as a single index, rather than use both phase and gain margins, to study unconditional stability.

To facilitate future stability analysis, $G^+(s) = G(s)U$ (Bao *et al*., 2002a) is defined, where U is a diagonal matrix with either 1 or –1 along the diagonal. The signs of U elements are determined such that the diagonal elements of $G^+(s)$ are positive at steady state, that is $G^+_{ii}(0) \geq 0$, i = 1, … , n, Let denote

$$K^+(s) = U^{-1}K(s) = UK(s) \qquad (38)$$

$$G^+(s) = G(s)U \qquad (39)$$

Theorem 3: (Bao *et al*., 2002a) For an interconnected system (as shown in Figure 3) comprising a stable subsystem G(s) and a decentralized controller K(s) = diag{$k_i(s)$}, i = 1, ..., n, if a stable and minimum phase transfer function $w(s)$ is chosen such that $\nu(\mathrm{w}(s),\omega) < -\nu(G^+(s),\omega)$, then the closed-loop system will be decentralized unconditionally stable if for any loop i = 1, ..., n, $k'_i(s) = k^+_I(s)[1-w(s)k^+_I(s)]^{-1}$ is passive, where $k_I^+(s) = U_{ii}k_I(s)$ and U = diag{U_{ii}}, i = 1, …, n. This full theorem proof is shown in Appendix D.

Similar to the diagonal scaling treatment for calculating maximum stability gain margins (Safonov, 1982), the conservativeness of the sufficient stability condition given in Theorem 3 could be reduced by using a constant, real, and positive-definite diagonal rescaling matrix (as matrix D shown in Figure 5).

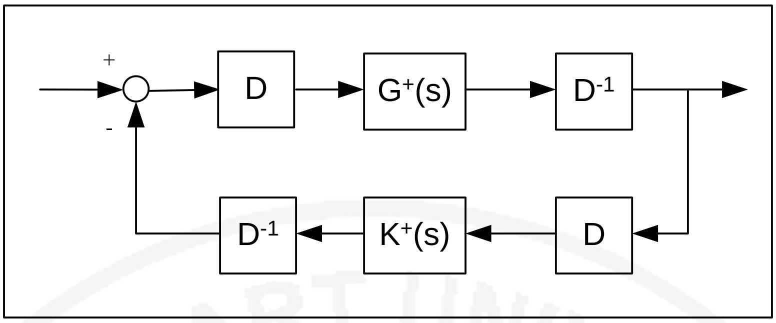

Figure 5 Rescaling

Source: Bao *et al*. (2002a)

The closed-loop system in Figure 3 is stable if and only if the feedback system shown in Figure 5 is stable. Note that, for any diagonal system $K^{+}(s)$, $K^{+}(s) = D^{-1}K^{+}(s)D$. However, the passivity index of $D^{-1}G^{+}(s)D$ can be significantly reduced by using an appropriate D matrix:

$$\nu(D^{-1}G^{+}(s)D,\omega) < \nu(G^{+}(s),\omega) \tag{40}$$

The rescaling matrix D can be chosen such that the rescaled $G^{+}(s)$ at steady state is positive-real; that is, the following inequality is satisfied:

$$D^{-1}G^{+}(0)D + D[G^{+}(0)]^{T}D^{-1} > 0 \tag{41}$$

Because D is nonsingular, thus,

$$D\{D^{-1}G^{+}(0)D + D[G^{+}(0)]^{T}D^{-1}\}D > 0 \tag{42}$$

$$G^{+}(0)DD + DD[G^{+}(0)] > 0 \tag{43}$$

Define M = DD; thus, M is a constant, real, and positive-definite diagonal matrix. Inequality (41) is equivalent to the following inequality:

$$G^{+}(0)M + M[G^{+}(0)]^{T} > 0 \tag{44}$$

Equation (44) is a typical linear matrix inequality (LMI) problem and can be solved by using any semi-definite programming tools such as MATLAB^{TM}: LMI

Toolbox. The continuity of the transfer function $G^{+}(s)$ implies that inequality (44) holds not only at steady state but also for a certain frequency range $[0,\omega_1]$:

$$G^{+}(j\omega)M + M[G^{+}(j\omega)]^{T} > 0, \quad \forall\ \omega \in [0, \omega_1] \tag{45}$$

The following theorem can be derived directly from Theorem 3.

***Theorem 4*:** Given a stable and rational LTI MIMO process with its transfer function matrix $G(s) \in C^{nxn}$, if the rescaled passivity index of $G^{+}(s) = G(s)U$ is bounded by

$$\nu_s\left(G(s),\omega\right) = \max\left\{-\min_{D}\nu\left(D^{-1}G^{+}(s)D,\omega\right),\epsilon\right\} \tag{46}$$

then any multi-loop controller

$$K(s) = \operatorname{diag}\{k_i(s)\},\ i = 1, \ldots, n \tag{47}$$

satisfying the following conditions will stabilize the closed-loop system and achieve decentralized unconditional stability:

$$1\ \operatorname{Re}\left\{\frac{k_i^{+}(j\omega)}{1-\nu_s(G(s),\omega)k_i^{+}(j\omega)}\right\} \geq 0 \qquad \forall\omega \in R,\ i = 1,\ldots,n \tag{48}$$

2 K(s) is analytic in Re(s) > 0 (49)

where ϵ is an arbitrarily small positive number, and D is positive-definite and $\nu_s(\omega)$ is a frequency-dependent real positive function, $k_i^{+}(s) = U_{ii}k_i(s) = 0$.

The (i,i)th element in matrix U indicates whether the corresponding ith loop is direct acting or reverse acting.

Theorem 5: (Necessary condition for decentralized integral controllability (DIC)) (Morari and Zafiriou, 1989). An $m \times m$ LTI stable process G(s) is DIC only if

$$\Lambda_{ii}(G(0)) \geq 0, \forall i = 1,\ldots,m \tag{50}$$

where $\Lambda_{ii}(G(0))$ is the ith diagonal element of the RGA matrix of G(0).

Note: This theorem proof is shown in Appendix D.

2.2.2.2 Diagonal scaling of the passivity index

The passivity index can be diagonally scaled to reduce the conservativeness of the passivity based control (Bao *et al*., 2002a). Let define "*D*" as a diagonal positive definite matrix. In this section, a frequency dependent diagonal scaling matrix $D(\omega)$ is implemented such that the passivity indices at different frequencies can be reduced. For a given stable process with signs adjusted $G^+(s) \in C^{n\times n}$, the problem of diagonally scaling for passivity index at frequency ω can be described as:

Problem 1 (Bao *et al*., 2002a)

$$\min_{D}\{t\} \tag{51}$$

subject to:

$$D(\omega)^{-1} G^+(j\omega) D(\omega) + D(\omega)\left[G^+(j\omega)\right]^* D(\omega)^{-1} + tI > 0 \tag{52}$$

$$D(\omega) > 0 \tag{53}$$

where $D(\omega) \in R^{n\times n}$ is a diagonal matrix and *t* is a real scalar variable. This is an optimization problem with a constraint of complex matrix inequality which cannot be handled directly by semi-definite programming solvers because Equation (52) is nonlinear and complex. However, this equation can be converted into a real and linear matrix inequality by defining $M = D(\omega)D(\omega)$ as previous part and $G^+(j\omega) = X(\omega) + jY(j\omega)$, the above problem can be converted into the following linear matrix inequality (LMI) problem as its derivation is shown Appendix D.

Note: more details about LMI information is described in Gahinet *et al*. (1995).

Problem 2 (Bao *et al*., 2002b)

$$\min_{M}\{t\} \tag{54}$$

subject to:

$$\begin{bmatrix} -X(\omega)M - MX^T(\omega) & Y(\omega)M - MY^T(\omega) \\ -Y(\omega)M + MY^T(\omega) & -X(\omega)M - MX^T(\omega) \end{bmatrix} < t\begin{bmatrix} M & 0 \\ 0 & M \end{bmatrix} \tag{55}$$

$$M \text{ is diagonal and } M > 0 \tag{56}$$

For each frequency ω, a diagonal and real matrix of M(ω) can be obtained by solving the above optimization problem, using any semi-definite programming solver. Then the diagonally scaled passivity index can be calculated as (Bao *et al*., 2002b):

$$\nu_s\left(G^+(s),\omega\right) = -\lambda_{\min}\left(\frac{1}{2}\left[M^{-\frac{1}{2}}G^+(j\omega)M^{\frac{1}{2}} + M^{\frac{1}{2}}\left(G^+(j\omega)\right)^* M^{-\frac{1}{2}}\right]\right) \tag{57}$$

In the passivity based stability conditions, the passivity indices $\nu\left(G^+(s),\omega\right)$ can be replaced with the diagonally scaled passivity index $\nu_s\left(G^+(s),\omega\right)$ to reduce the conservativeness of these conditions.

The passivity index as previously mentioned is used to check whether the system is passive or not. If not, from Theorem 2, a stable minimum phase transfer function called weighting function *w*(s) is the term used to render system to be passive. The weighting function has the following form (Bao *et al*., 2002b):

$$w(s) = \frac{k.s.(s+a)}{(s+b)(s+c)} \tag{58}$$

where the parameters a, b, c and k, decision variable, can be obtained from Problem 3:

Problem 3 (Bao *et al*., 2002b)

$$\min_{a,b,c,k} \sum_{i=1}^{m}\left(\mathrm{Re}\left(w\left(j\omega_i\right)\right) - \upsilon_s\left(G^+(s),\omega_i\right)\right)^2 \tag{59}$$

subject to

$$\mathrm{Re}\left(w\left(j\omega_i\right)\right) > \upsilon_s\left(G^+\left(s\right),\omega_i\right), \quad \forall i = 1...m \,. \tag{60}$$

2.2.3 Passivity based pairing

Different paring schemes result in different transfer function matrices *G*(*s*), which normally have different passivity indices (Bao and Lee, 2007). The passivity indices imply achievable performance of decentralized control systems (with passive controllers). A "more" passive *G*(s) is easier to control by using a multi-loop controller (Bao and Lee, 2007). Therefore, a pairing scheme should be chosen such that (1) the resulting *G*(s) is Decentralized Integral Controllable (DIC); (2) *G*(*s*) has small passivity indices at all frequencies concerned.

For each pairing scheme, its passivity index profile can be obtained using following steps (Bao and Lee, 2007):

1. Determine the transfer function *G*(s) for each possible pairing scheme.

2. Screen out the non-DIC pairing schemes by using the necessary DIC condition given in Theorem 5.

3. Find the sign matrix U and obtain G^+(s) such that $G_{ii}^+\left(0\right) > 0 \ (i = 1,...,m)$.

4. Calculate the diagonally scaled passivity index $\nu_s\left(G^+\left(s\right),\omega\right)$ at a number of frequency points.

5. Compare the passivity index profiles of different pairings. The best pairing should correspond to the one with the largest frequency bandwidth ω_b such that $\nu_s\left(G^+\left(s\right),\omega\right) \le 0$ for any $\omega \in [0,\omega_b]$. This pairing scheme would allow using controllers with integral action and the fastest dynamic response.

2.2.4 Multi-loop PI controller design

Multi-loop PI controllers can be designed based on the passivity based stability conditions (Bao *et al*., 2002a). To achieve decentralized unconditional stability of the closed-loop system as well as good performance, a controller tuning method is proposed to minimize the sensitivity function of each loop, subject to the conditions in Equations (48) and (49). For multi-loop PI controller synthesis, this tuning problem is converted into the following optimization problem:

Problem 4 (Bao *et al*., 2002a)

$$\min_{k^+_{c,i},\,\tau_{I,i}} \left(-\gamma_i\right) \tag{61}$$

subject to

$$\left| \frac{w_i(j\omega)\gamma_i}{1 + G^+_{ii}\left(j\omega\right)k^+_{c,i}\left[1 + \dfrac{1}{\tau_{I,i} \times j\omega}\right]} \right| < 1 \tag{62}$$

and

$$\frac{k^+_{c,i}\nu_s\left(\omega\right)}{\left[1 - k^+_{c,i}\nu_s\left(\omega\right)\right]\omega^2} \le \tau^2_{I,i} \qquad \forall\omega\in R, i = 1,...,n \tag{63}$$

For a given stable process G(s), a multi-loop PI controller can be obtained by solving Problem 4 using the design procedure as follows.

1. Determine the pairing scheme for controlled and manipulated variables according to the procedure to find the best pairing in section 2.2.3.

2. For each subsystem $G^+_{ii}(s)$ (i = 1,…,m), solve Problem 4 for the PI controller parameters $k^+_{c,i}$ and $\tau_{I,i}$.

3. Adjust the sign of the final subcontroller gain $k_{c,i} = k_{c,i}^{+}U_{ii}$ to obtain the final multi-loop controller as Equation (64).

$$K(s) = diag\{k_i(s)\} = diag\left\{k_{c,i}(1+\frac{1}{\tau_{I,i}s})\right\} \tag{64}$$

MATERIALS AND METHODS

Materials

1. Personal computer
   a) CPU (Intel core2Duo CPU 2.0 GHz)
   b) 3.00 GB of RAM
   c) 320 GB of Hard disk
2. Operating System: Microsoft Window Vista
3. Software
   a) MATLAB® version 2007b
   b) ASPEN PLUS V.7 and ASPEN DYNAMICS V.7

Methods

1. Overall Methodology

The aim of this work is to apply the passivity theorem with HENs. The main steps to accomplish this goal are presented as follows.

1.1 Develop a state space equation, which is a state and an output equation, of a single bypass heat exchanger.

1.2 Find a transfer function of a single bypass heat exchanger.

1.3 Apply the passivity theorem with a single bypass heat exchanger

1.4 Verify the results by Aspen Dynamics V.7.

1.5 Analyze the results.

1.6 Extend this system to a network and repeat steps 1.1 to 1.5.

2. Passivity based decentralized controller synthesis

This part shows how to apply the passivity theorem to a single bypass heat exchanger and a HEN. The procedure to obtain the passivity based decentralized unconditional stability (DUS) control system is illustrated in Figure 6.

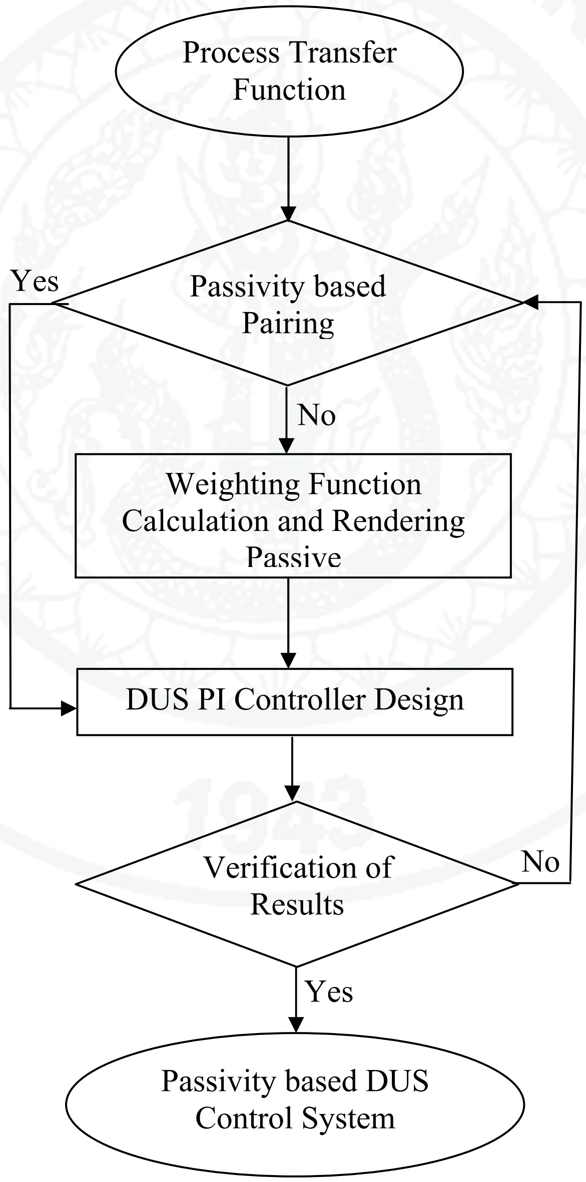

Figure 6 Passivity based decentralized controller synthesis procedure

Note: This procedure was systematically combined by the author from the works of Bao *et al*. (1998; 2000; 2002; 2007).

Firstly, the transfer function of the process needs to be available. After that, this process is checked whether it is passive or not by using passivity index (Bao *et al*., 2002b) which is shown in Equation (65).

$$v_s\left(G^+(s),\omega\right) = -\lambda_{\min}\left(\frac{1}{2}\left[M^{-\frac{1}{2}}G^+(j\omega)M^{\frac{1}{2}} + M^{\frac{1}{2}}\left(G^+(j\omega)\right)^* M^{-\frac{1}{2}}\right]\right) \quad (65)$$

If it is passive (passivity index is less than or equal to zero at a given frequency), it can be directly designed DUS PI controller. If not (passivity index is much more than zero), it has to add mathematically some function called weighting function in the system in order to render the system passive and then can be designed DUS PI controller. However, both ways have to process the passivity based pairing step which is shown as follows.

1. Determine the transfer function *G*(s) for each possible pairing scheme. In this step, there are the numerical symbols to indicate any possible pairing schemes.
u(*i*)-*x*(*i*)/*u*(*i*+1)-*x*(i+1) means that the *i*th manipulated variable (*u*) is used to control the *i*th controlled variable (*x*), and the (*i*+1)th manipulated variable is used to control (*i+1*)th controlled variable. This definition is presented in Table 1.

Table 1 Numerical symbols to indicate any possible pairing schemes

The *i*-th Manipulated Variables (*u*)	**The *i*-th Controlled Variables (*x*)**	**Numerical Symbols**	**Description**
1	1	1-1	u_1 controls x_1
2	2	2-2	u_2 controls x_2
1	2	1-2	u_1 controls x_2
2	1	2-1	u_2 controls x_1

For example, 1-2/2-1 pairing means that the 1st manipulated variable is used to control the 2nd controlled variable, and the 2nd manipulated variable is used to control the 1st controlled variable.

2. Screen out the non-DIC pairing schemes by using the necessary DIC condition given in Theorem 5.

3. Find the sign matrix U and obtain G^{+}(s) such that $G_{ii}^{+}(0) > 0 \ (i = 1, \ldots, m)$. The (*i,i*)-th in matrix U indicates whether the corresponding *i*-th loop is direct or reverse acting.

4. Calculate the diagonally scaled passivity index $\nu_s(G^{+}(s), \omega)$ at a number of frequency points.

5. Compare the passivity index profiles of different pairings. The best pairing should correspond to the one with the largest frequency bandwidth ω_b such that $\nu_s(G^{+}(s), \omega) \leq 0$ for any $\omega \in [0, \omega_b]$. This pairing scheme would allow using controllers with integral action and the fastest dynamic response.

After the passivity based pairing step, the best pairing scheme which is more passive than the others is obtained. Next step for non-passive process called weighting function calculation and rendering passive step, the weighting function which is the stable and minimum phase is added into the system. The weighting function has the following form (Bao *et al*., 2002b):

$$w(s) = \frac{k.s.(s+a)}{(s+b)(s+c)} \tag{66}$$

where the parameters a, b, c and k, decision variable, can be obtained from Problem 3 as shown in the literature review section:

Problem 3 (Bao *et al*., 2002b)

$$\min_{a,b,c,k}\sum_{i=1}^{m}\Big(\mathrm{Re}\big(w(j\omega_i)\big)-\upsilon_s\big(G^+(s),\omega_i\big)\Big)^2 \tag{67}$$

subject to

$$\mathrm{Re}\big(w(j\omega_i)\big)>\upsilon_s\big(G^+(s),\omega_i\big),\quad \forall i=1...m. \tag{68}$$

After weighting function is determined, this function is added mathematically into the system in order to make this system passive which is followed the Theorem 2.

$$H(s) = G(s) + W(s) \tag{69}$$

where W(s) = *w(s)I*

Next step, DUS PI controllers are designed following the multi-loop PI controller design procedure (Bao *et al*., 2002a).

1. Determine the pairing scheme for controlled and manipulated variables according to the procedure to find the best pairing in the passivity based pairing step.

2. For each subsystem $G_{ii}^{+}(s)$ (i = 1,…,m), solve Problem 4 for the PI controller parameters $k_{c,i}^{+}$ and $\tau_{I,i}$.

Problem 4 (Bao *et al*., 2002a)

$$\min_{k_{c,i}^{+},\tau_{I,i}}\left(-\gamma_i\right) \tag{70}$$

such that

$$\left|\frac{w_i(j\omega)\gamma_i}{1+G_{ii}^{+}(j\omega)k_{c,i}^{+}\left[1+\dfrac{1}{\tau_{I,i}\times j\omega}\right]}\right|<1 \tag{71}$$

and

$$\tau_{I,i}^2 \geq \frac{k_{c,i}^{+}\nu_s(\omega)}{\left[1-k_{c,i}^{+}\nu_s(\omega)\right]\omega^2} \qquad \forall\omega \in R, i=1,...,n \tag{72}$$

3. Adjust the sign of the final subcontroller gain $k_{c,i} = k_{c,i}^{+}U_{ii}$ to obtain the final multi-loop controller as Equation (73).

$$K(s) = diag\{k_i(s)\} = diag\left\{k_{c,i}(1+\frac{1}{\tau_{I,i}s})\right\} \tag{73}$$

This multi-loop controller satisfies the following conditions which stabilize the closed-loop system and achieve DUS:

1 $\text{Re}\left\{\frac{k_i^{+}(j\omega)}{1-\nu_s(G(s),\omega)k_i^{+}(j\omega)}\right\} \geq 0 \qquad \forall\omega \in R, i=1,...,n$ (74)

2 K(s) is analytic in Re(s) > 0 (75)

where $k_i^{+}(s)\} = U_{ii}k_i(s)$

However, when DUS PI tuning parameters are designed, the system is performed with these parameters to verify the results compared with the default PI tuning parameters from Aspen Dynamics simulator. In a verification part of the HEN case, there are two works; first, the system is simulated with controllers and disturbed by changing hot flowrate, and second, the system is tested fault-tolerant control by simulating with a failing controller and also is disturbed as the same as the first work. If the results can achieve stability, the passivity based DUS control system is obtained.

RESULTS AND DISCUSSION

This result section is divided into two main parts. The first part covers a single heat exchanger with and without bypass, and the second part extends the study over a HEN. Both systems are studied and implemented with the passivity theorem.

1. A Single Heat Exchanger Applied with the Passivity Theorem

Since a single heat exchanger without bypass referred from Hangos *et al.* (2004) was already applied with the passivity theorem by Bao and Lee (2007), they reported that the model of a single heat exchanger is inherently passive. Therefore, the following section shows the models of a single heat exchanger without bypass tested by passivity index (Bao *et al.*, 2002b) to confirm this heat exchanger model is passive.

1.1 A single heat exchanger model without bypass

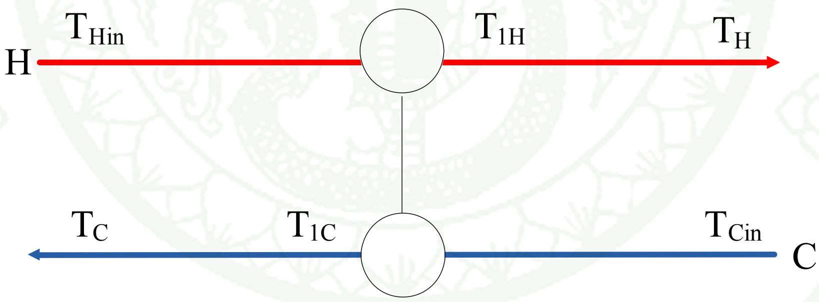

Figure 7 A grid diagram of a single heat exchanger

Source: Hangos *et al.* (2004)

The model of a single heat exchanger referred from Hangos *et al.* (2004) is shown in Figure 7 and Equations (76) to (79) which are developed under the following assumptions.

1. A heat exchanger model is assumed to be an approximate lumped parameter system instead of a distributed parameter system.

2. Volumes of hot and cold streams in the heat exchanger (V_H and V_C) are constant.

3. Physicochemical properties, including density of the hot and cold streams (ρ_H and ρ_C) and their specific heats (C_{pH} and C_{pC}) are constant.

4. Heat transfer coefficient U and area A are constant.

5. Both hot and cold streams are well mixed and the temperatures of the hot and cold streams inside the tube are approximated by the outlet temperatures T_{1H} and T_{1C}.

$$\rho_C V_C C_{pC} \frac{dT_{1C}}{dt} = \rho_C F_C C_{pC} (T_{Cin} - T_{1C}) + UA(T_{1H} - T_{1C}) \tag{76}$$

$$\rho_H V_H C_{pH} \frac{dT_{1H}}{dt} = \rho_H F_H C_{pH} (T_{Hin} - T_{1H}) + UA(T_{1C} - T_{1H}) \tag{77}$$

$$T_C = T_{1C} \tag{78}$$

$$T_H = T_{1H} \tag{79}$$

Equations (76) and (77) are the state equations of the cold and hot streams while Equations (78) and (79) are the output equations of cold and hot streams. These equations are a linear case of a heat exchanger model. These linear heat exchanger models, describing the behavior of the state variables, have two controlled variables and two manipulated variables. The controlled variables are output cold temperature T_{1C} and output hot temperature T_{1H}. The manipulated variables are inlet cold temperature T_{Cin} and inlet hot temperature T_{Hin}. However, this model is mostly ideal case since the manipulated variables are both inlet temperatures by assuming the cold and hot flowrates to be constant. The linear heat exchanger models can be formulated in the state space form as Equations (80) and (81).

$$\begin{bmatrix} \dot{T}_{1C} \\ \dot{T}_{1H} \end{bmatrix} = \begin{bmatrix} \dfrac{-UA-\tau_C F_C}{\xi_C} & \dfrac{UA}{\xi_C} \\ \dfrac{UA}{\xi_H} & \dfrac{-UA-\tau_H F_H}{\xi_H} \end{bmatrix} \begin{bmatrix} T_{1C} \\ T_{1H} \end{bmatrix} + \begin{bmatrix} \dfrac{\tau_C F_C}{\xi_C} & 0 \\ 0 & \dfrac{\tau_H F_H}{\xi_H} \end{bmatrix} \begin{bmatrix} T_{Cin} \\ T_{Hin} \end{bmatrix} \tag{80}$$

$$\begin{bmatrix} T_C \\ T_H \end{bmatrix} = \begin{bmatrix} 1 & 0 \\ 0 & 1 \end{bmatrix} \begin{bmatrix} T_{1C} \\ T_{1H} \end{bmatrix} \tag{81}$$

where $\tau_i = \rho_i C_{Pi}$ and $\xi_i = \rho_i V_i C_{Pi} \quad i = C,H$

The parameters used come from Kern (1950) and are shown in Table 2

Table 2 Parameters used in the linear heat exchanger model

Parameter	Unit	Value
Heat exchanger area (A)	ft^2	521.5
Overall heat transfer coefficient (U)	Btu/(hr.ft^{2o}F)	75
Cold flowrate (F_C)	ft^3/hr	2290
Hot flowrate (F_H)	ft^3/hr	6240
Specific heat capacity of cold stream(C_{PC})	Btu/(lb^{o}F)	0.56
Specific heat capacity of hot stream (C_{PH})	Btu/(lb^{o}F)	0.58
Density of cold stream (ρ_C)	lb/ft^3	44.93
Density of hot stream (ρ_H)	lb/ft^3	47.74
Volume of cold compartment (V_C)	ft^3	5.57
Volume of hot compartment (V_H)	ft^3	20.40

Source: Kern (1950)

When all numerical values are substituted into Equations (80) and (81), the state space equation of this linear heat exchanger model is as follows.

$$\begin{bmatrix} \dot{T}_{1C} \\ \dot{T}_{1H} \end{bmatrix} = \begin{bmatrix} -690.87 & 279.17 \\ 69.254 & -375.29 \end{bmatrix} \begin{bmatrix} T_{1C} \\ T_{1H} \end{bmatrix} + \begin{bmatrix} 411.7 & 0 \\ 0 & 306.03 \end{bmatrix} \begin{bmatrix} T_{Cin} \\ T_{Hin} \end{bmatrix} \tag{82}$$

$$\begin{bmatrix} T_C \\ T_H \end{bmatrix} = \begin{bmatrix} 1 & 0 \\ 0 & 1 \end{bmatrix} \begin{bmatrix} T_{1C} \\ T_{1H} \end{bmatrix} \tag{83}$$

These equations, which have the same form as the state space form shown in Equations (84) and (85), can be transformed into transfer function as Equation (86).

$$\dot{x} = Ax + Bu \tag{84}$$

$$y = Cx \tag{85}$$

Note: All information of state space form is shown in Appendix A.

$$G(s) = \begin{bmatrix} \dfrac{411.7s + (1.545\times10^5)}{s^2 + 1066s + (2.399\times10^5)} & \dfrac{8.543\times10^4}{s^2 + 1066s + (2.399\times10^5)} \\ \dfrac{2.851\times10^4}{s^2 + 1066s + (2.399\times10^5)} & \dfrac{306s + (2.114\times10^5)}{s^2 + 1066s + (2.399\times10^5)} \end{bmatrix} \tag{86}$$

After that, the passivity index (Bao *et al*., 2002b) in Equation (87), indicating how far the system from being passive, is tested with this transfer function of the linear heat exchanger model. The result is shown in Figure 8.

$$\nu_s\left(G^+(s),\omega\right) = -\lambda_{\min}\left(\frac{1}{2}\left[M^{-\frac{1}{2}}G^+(j\omega)M^{\frac{1}{2}} + M^{\frac{1}{2}}\left(G^+(j\omega)\right)^* M^{-\frac{1}{2}}\right]\right) \tag{87}$$

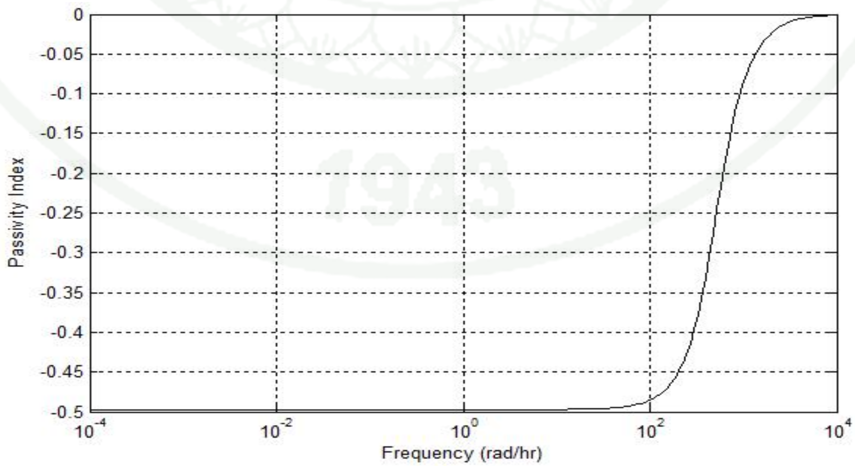

Figure 8 Passivity index of the linear heat exchanger model

Source: Bao and Lee (2007)

Since the passivity index is less than zero along the frequency range 10^{-4}-10^{4} rad/hr, this system is passive (Bao *et al*. 2000a). As all previously mentioned, the model of the heat exchanger is linear in case of inlet temperature of both cold and hot streams being manipulated variables. The another case of a heat exchanger is nonlinear case which the controlled variables are the same as linear case, but the manipulated variables are cold and hot flowrates instead of inlet cold and hot temperatures. The state space equation of nonlinear heat exchanger model is presented in Equations (88) and (89).

$$\begin{bmatrix} \dot{T}_{1C} \\ \dot{T}_{1H} \end{bmatrix} = \begin{bmatrix} \dfrac{-UA-\tau_C \bar{F}_C}{\xi_C} & \dfrac{UA}{\xi_C} \\ \dfrac{UA}{\xi_H} & \dfrac{-UA-\tau_H \bar{F}_H}{\xi_H} \end{bmatrix} \begin{bmatrix} T_{1C} \\ T_{1H} \end{bmatrix} + \begin{bmatrix} \dfrac{\tau_C T_{Cin} - \tau_C \bar{T}_{1C}}{\xi_C} & 0 \\ 0 & \dfrac{\tau_H T_{Hin} - \tau_H \bar{T}_{1H}}{\xi_H} \end{bmatrix} \begin{bmatrix} F_C \\ F_H \end{bmatrix} \tag{88}$$

$$\begin{bmatrix} T_C \\ T_H \end{bmatrix} = \begin{bmatrix} 1 & 0 \\ 0 & 1 \end{bmatrix} \begin{bmatrix} T_{1C} \\ T_{1H} \end{bmatrix} \tag{89}$$

where $\tau_i = \rho_i C_{Pi}$ and $\xi_i = \rho_i V_i C_{Pi} \quad i = C,H$

Note: The full derivation of these equations is shown in Appendix C.

This model was not mentioned in detail from Bao and Lee (2007). Therefore, in order to test this model passive as Bao and Lee (2007) reported, numerical values are required. The simulation conditions, referred from Westhalen *et al*. (2003) as shown in Figure 9 and Table 3, are used to simulate in Aspen Plus to determine the output cold temperature and heat duty by specifying the output hot temperature to be 71.1 ºC.

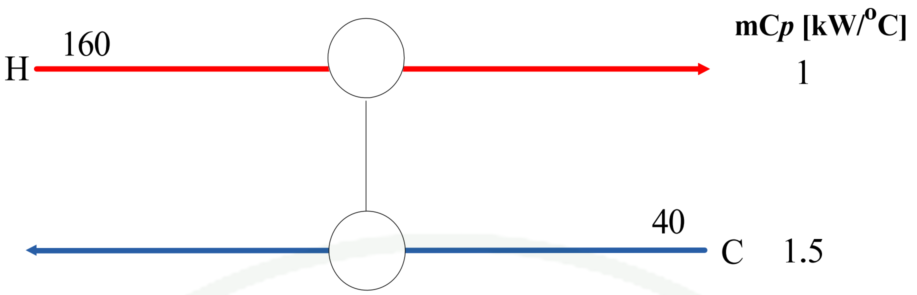

Figure 9 A grid diagram of a heat exchanger with conditions

Source: Westhalen *et al*. (2003)

Table 3 Parameters used in the nonlinear heat exchanger model

Parameter	Unit	Value
Inlet cold temperature	ºC	40
Inlet hot temperature	ºC	160
Output hot temperature	ºC	71.1
Cold mass capacity flowrate	kW/ ºC	1.5
Hot mass capacity flowrate	kW/ ºC	1
Overall heat transfer coefficient	kW/m^2 K	0.85
Heat exchanger area	m^2	0.96
Density	kg/m^3	1000
Volume of cold compartment	m^3	0.1577[a]
Volume of hot compartment	m^3	0.5776[a]

Remark: [a]: assumption referred from linear model (Bao and Lee, 2007; Kern, 1950)

When all numerical values are substituted into Equations (88) and (89), the state space equation of this nonlinear heat exchanger model is as follows.

$$\begin{bmatrix} \dot{T}_{1C} \\ \dot{T}_{1H} \end{bmatrix} = \begin{bmatrix} -5510.15 & 5428.36 \\ 1482.09 & -1483.82 \end{bmatrix} \begin{bmatrix} T_{1C} \\ T_{1H} \end{bmatrix} + \begin{bmatrix} -385.289 & 0 \\ 0 & 153.913 \end{bmatrix} \begin{bmatrix} F_C \\ F_H \end{bmatrix} \qquad (90)$$

$$\begin{bmatrix} T_C \\ T_H \end{bmatrix} = \begin{bmatrix} 1 & 0 \\ 0 & 1 \end{bmatrix} \begin{bmatrix} T_{1C} \\ T_{1H} \end{bmatrix} \qquad (91)$$

These equations can be transformed into transfer function as Equation (92).

$$G(s) = \begin{bmatrix} \dfrac{-385.3s-(5.717\times10^5)}{s^2+6994s+(1.308\times10^5)} & \dfrac{8.355\times10^5}{s^2+6994s+(1.308\times10^5)} \\ \dfrac{-5.71\times10^5}{s^2+6994s+(1.308\times10^5)} & \dfrac{153.9s+(8.481\times10^5)}{s^2+6994s+(1.308\times10^5)} \end{bmatrix} \qquad (92)$$

After that, the passivity index (Bao *et al*., 2002b) is tested with this transfer function of the nonlinear heat exchanger model. The result is shown in Figure 10.

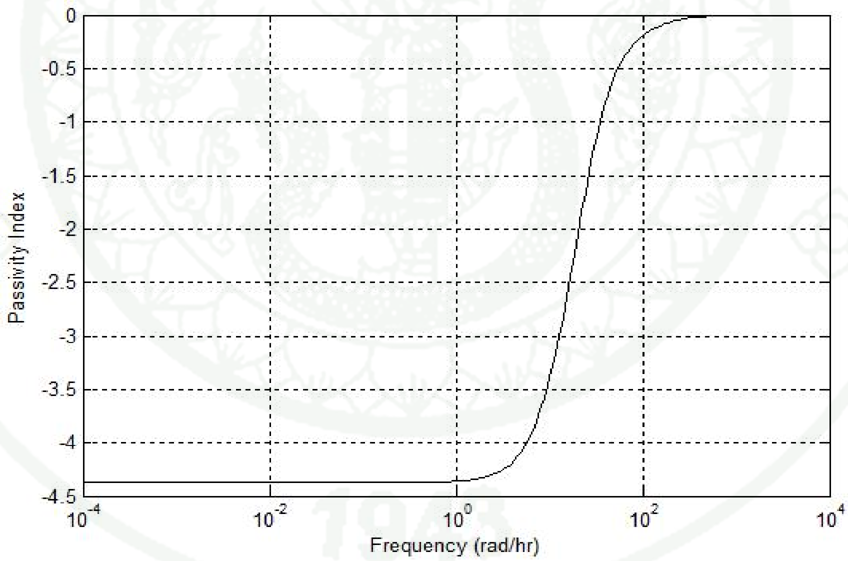

Figure 10 Passivity index of the nonlinear heat exchanger model

1.2 A single bypass heat exchanger

Although single heat exchangers, which both linear and nonlinear models in case of without bypasses, are inherently passive (Bao and Lee, 2007), they are not realistic model since single heat exchangers have generally to be presented with bypass. Single bypasses are assumed to be used throughout this work

(Lersbamrungsuk, 2008; Glemmestad *et al*., 1999; Wolff *et al*., 1991). Therefore, the grid diagram of a single bypass heat exchanger is shown in the following figure.

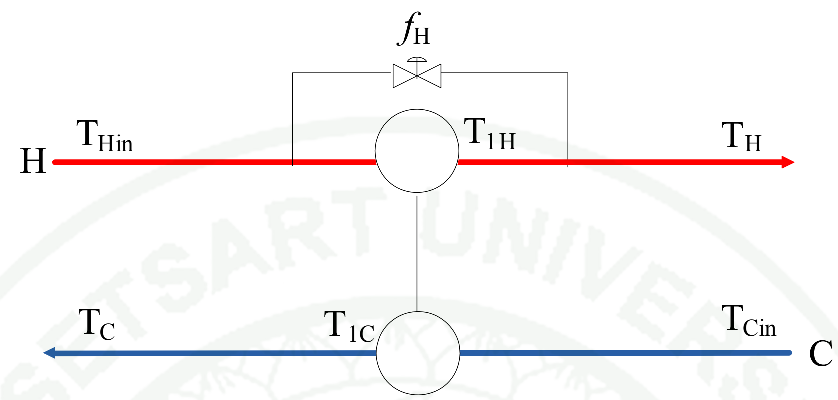

Figure 11 A grid diagram of a single bypass heat exchanger

If a single heat exchanger in Figure 7 is considered carefully, it is found that Equations (76) and (77) are produced from that system which has the boundary system around the heat exchanger shown in Figure 12.

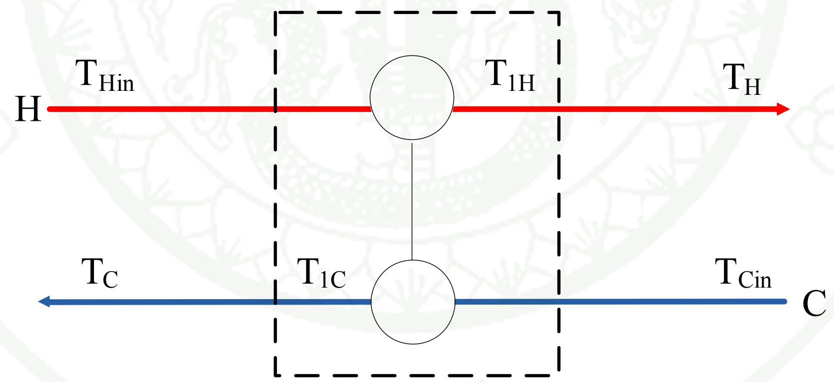

Figure 12 A grid diagram of a single heat exchanger with boundary system

Likewise, the boundary system of a single heat exchanger with bypass is shown in Figure 13.

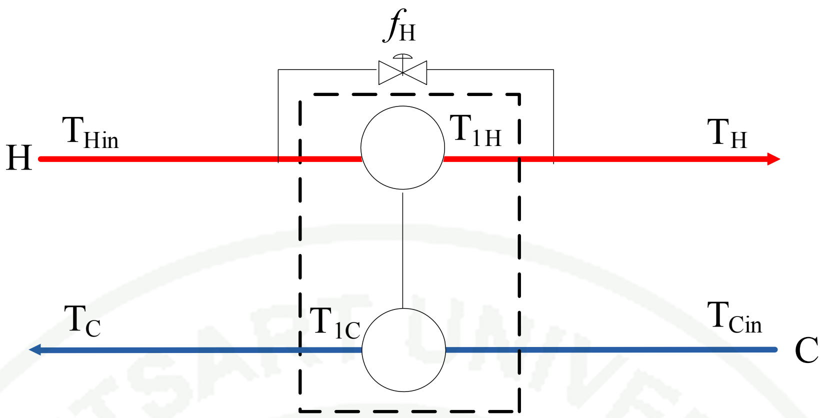

Figure 13 A grid diagram of a single bypass heat exchanger with boundary system

From Figure 13, the dynamic equations of both cold and hot sides governed from energy balance are presented as follows.

$$\rho_H V_H C_{pH} \frac{dT_{1H}}{dt} = \rho_H (1-f_H) F_H C_{pH} (T_{Hin} - T_{1H}) + UA(T_{1C} - T_{1H}) \tag{93}$$

$$\rho_C V_C C_{pC} \frac{dT_{1C}}{dt} = \rho_C F_C C_{pC} (T_{Cin} - T_{1C}) + UA(T_{1H} - T_{1C}) \tag{94}$$

This system has two state variables; outlet cold and hot temperature (T_{1H}, T_{1C}), and two manipulated variables; cold flowrates F_C and bypass fraction on hot side f_H by assuming constant hot flowrate F_H. Due to the nonlinear term which is resulted from the presence of f_H and T_{1H} together, these models need some techniques to develop them. After they are developed, the state equations of this system are in Equations (95) and (96).

$$\frac{dT_{1C}}{dt} = \left(\frac{-UA - \tau_C \bar{F}_C}{\xi_C}\right) T_{1C} + \frac{UA}{\xi_C} T_{1H} + \left(\frac{\tau_C T_{Cin} - \tau_C \bar{T}_{1C}}{\xi_C}\right) F_C \tag{95}$$

$$\frac{dT_{1H}}{dt} = \frac{UA}{\xi_H} T_{1C} + \left(\frac{-UA + \tau_H F_H \bar{f}_H - \tau_H F_H}{\xi_H}\right) T_{1H} + \left(\frac{\tau_H F_H \bar{T}_{1H} - \tau_H F_H T_{Hin}}{\xi_H}\right) f_H \tag{96}$$

where $\tau_i = \rho_i C_{Pi}$ and $\xi_i = \rho_i V_i C_{Pi}$

Note: The full derivation of these equations is shown in Appendix C.

Nevertheless, when this system of a single heat exchanger with a bypass is considered, there is more complicated than without bypass to consider the output equation in order to get the state space form of this single heat exchanger model.

Let consider the output hot temperature after the split stream from the inlet and the exchanged stream from the exchanger are mixed. The mixed temperature equation on hot side, referred from Mathisen (1994) and Glemmestad *et al*. (1999) is in Equation (97).

$$T_H = (1 - f_H)T_{1H} + f_H T_{Hin} \tag{97}$$

There is the nonlinear term $f_H T_{1H}$ presented in Equation (97); therefore, this equation has to be linearized as the same as Equation (94). The complete output hot temperature after mixing is shown in Equation (98).

$$T_H = (1 - \bar{f}_H)T_{1H} + (T_{Hin} - \bar{T}_{1H})f_H \tag{98}$$

Note: The full derivation of these equations is shown in Appendix C.

However, the output cold temperature is also the same as Equation (99).

$$T_C = T_{1C} \tag{99}$$

The new developed output hot temperature equation and the output cold temperature can be written in the state space form as Equation (100), which is the same output equation of the state space form as Equation (101).

$$\begin{bmatrix} T_C \\ T_H \end{bmatrix} = \begin{bmatrix} 1 & 0 \\ 0 & 1 - \bar{f}_H \end{bmatrix} \begin{bmatrix} T_{1C} \\ T_{1H} \end{bmatrix} + \begin{bmatrix} 0 & 0 \\ 0 & T_{Hin} - \bar{T}_{1H} \end{bmatrix} \begin{bmatrix} F_C \\ f_H \end{bmatrix} \tag{100}$$

$$y = Cx + Du \tag{101}$$

Therefore, the developed equations of a single heat exchanger with a single bypass on hot side are compactly summarized in the state space form in Equations (102) and (103).

$$\begin{bmatrix} \dot{T}_{1C} \\ \dot{T}_{1H} \end{bmatrix} = \begin{bmatrix} \dfrac{-UA-\tau_C\bar{F}_C}{\xi_C} & \dfrac{UA}{\xi_C} \\ \dfrac{UA}{\xi_H} & \dfrac{-UA+\tau_H F_H \bar{f}_H - \tau_H F_H}{\xi_H} \end{bmatrix} \begin{bmatrix} T_{1C} \\ T_{1H} \end{bmatrix} + \begin{bmatrix} \dfrac{\tau_C T_{Cin} - \tau_C \bar{T}_{1C}}{\xi_C} & 0 \\ 0 & \dfrac{\tau_H F_H \bar{T}_{1H} - \tau_H F_H T_{Hin}}{\xi_H} \end{bmatrix} \begin{bmatrix} F_C \\ f_H \end{bmatrix} \tag{102}$$

$$\begin{bmatrix} T_C \\ T_H \end{bmatrix} = \begin{bmatrix} 1 & 0 \\ 0 & 1-\bar{f}_H \end{bmatrix} \begin{bmatrix} T_{1C} \\ T_{1H} \end{bmatrix} + \begin{bmatrix} 0 & 0 \\ 0 & T_{Hin} - \bar{T}_{1H} \end{bmatrix} \begin{bmatrix} F_C \\ f_H \end{bmatrix} \tag{103}$$

where $\tau_i = \rho_i C_{Pi}$ and $\xi_i = \rho_i V_i C_{Pi}$

Note: The full derivation of these equations is shown in Appendix C.

The system of a single heat exchanger with a single bypass used to apply with the passivity theorem is referred from Westhalen *et al.* (2003). That system is illustrated in Figure 14.

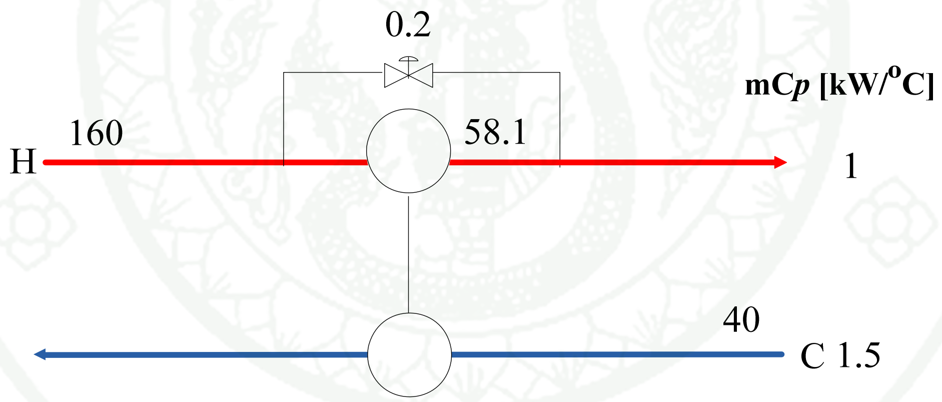

Figure 14 A grid diagram of a single bypass heat exchanger with conditions

Source: Westhalen *et al*. (2003)

This system is simulated by Aspen Plus to determine the necessary variables in the state space equation shown above (Equations (102) and (103)). The simulation conditions are shown in Table 4.

Table 4 Numerical values for a simulation of a heat exchanger with a single bypass

Parameter	Unit	Value
Inlet cold temperature	ºC	40
Inlet hot temperature	ºC	160
Output hot temperature before mixing	ºC	58.1
Cold mass capacity flowrate	kW/ ºC	1.5
Hot mass capacity flowrate	kW/ ºC	1
Bypass fraction	-	0.2
Pressure	atm	1
Density	kg/m^3	1000
Volume of cold compartment	m^3	0.1577[a]
Volume of hot compartment	m^3	0.5776[a]

Source: Westhalen *et al.* (2003)

Remark: [a]: assumption referred from linear model (Bao and Lee, 2007; Kern, 1950)

The results from the simulation are shown in Figure 15 and Table 5.

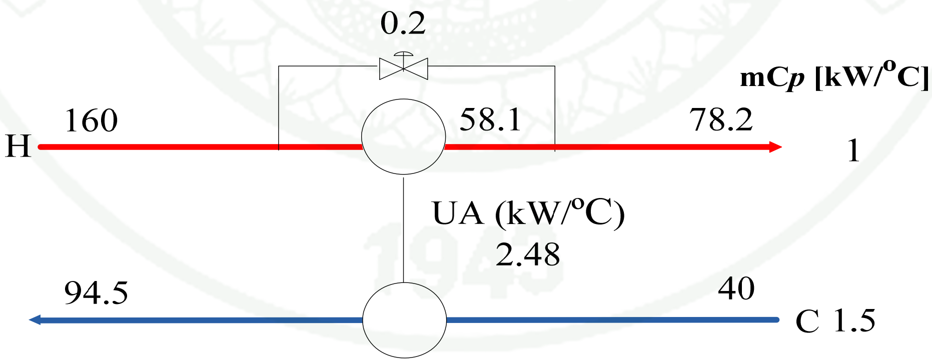

Figure 15 A grid diagram of a single bypass heat exchanger after simulation

Table 5 Simulation results of a single heat exchanger with a single bypass

Parameter	Unit	Value
Output cold temperature	ºC	94.5
Output hot temperature after mixing	ºC	78.2
Heat exchanger area	m^2	2.91
Overall heat transfer coefficient	$kW/m^2{}^oC$	0.85
Heat duty	kW	81.8

When all numerical values in Equations (102) and (103) are available, they are substituted into those equations. Then Equations (102) and (103) become as follows.

$$\begin{bmatrix} \dot{T}_{1C} \\ \dot{T}_{1H} \end{bmatrix} = \begin{bmatrix} -21.66 & 13.49 \\ 3.68 & -4.87 \end{bmatrix} \begin{bmatrix} T_{1C} \\ T_{1H} \end{bmatrix} + \begin{bmatrix} -345.593 & 0 \\ 0 & -151.686 \end{bmatrix} \begin{bmatrix} F_C \\ f_H \end{bmatrix} \tag{104}$$

$$\begin{bmatrix} T_C \\ T_H \end{bmatrix} = \begin{bmatrix} 1 & 0 \\ 0 & 0.8 \end{bmatrix} \begin{bmatrix} T_{1C} \\ T_{1H} \end{bmatrix} + \begin{bmatrix} 0 & 0 \\ 0 & 101.9 \end{bmatrix} \begin{bmatrix} F_C \\ f_H \end{bmatrix} \tag{105}$$

These equations can be transformed into transfer function as Equation (106).

$$G(s) = \begin{bmatrix} \dfrac{-345.6s - 1683}{s^2 + 26.53s + 55.84} & \dfrac{-2046}{s^2 + 26.53s + 55.84} \\ \dfrac{-1017}{s^2 + 26.53s + 55.84} & \dfrac{101.9s^2 - 2582s + 3062}{s^2 + 26.53s + 55.84} \end{bmatrix} \tag{106}$$

After that, the passivity index (Bao *et al*., 2002b) is tested with this transfer function of the single bypass heat exchanger. The result is shown in Figure 16.

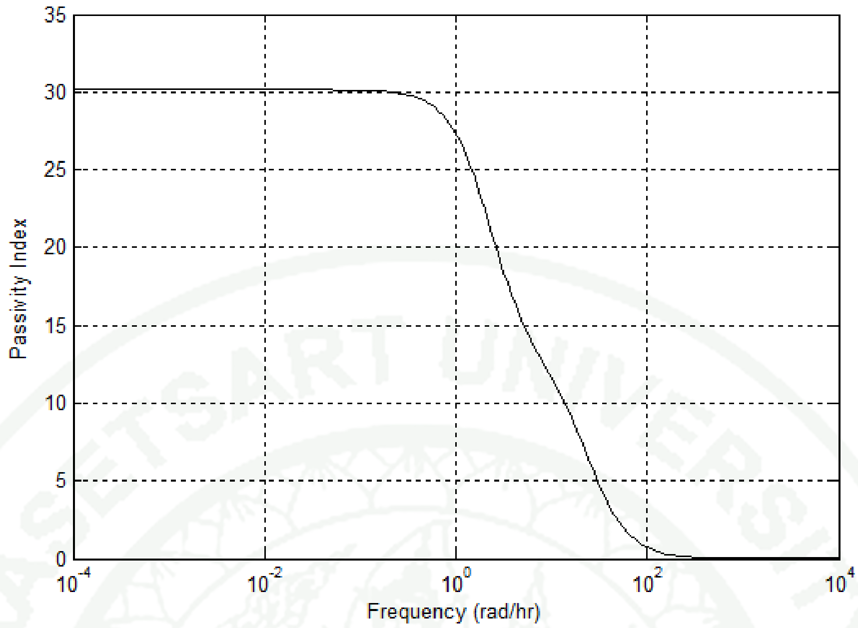

Figure 16 Passivity index of the heat exchanger with a single bypass

From this figure, the passivity index of this system is more than zero along the frequency range 10^{-4}-10^{4} rad/hr; therefore, this system is non-passive (Bao *et al.* 2000a).

Up to this point, we have clearly understood that there are some cases which heat exchangers can be non-passive. In the next section, a single heat exchanger with a single bypass is applied with the passivity theorem following the procedure of Bao and Lee (2007) which is summarized in Figure 17.

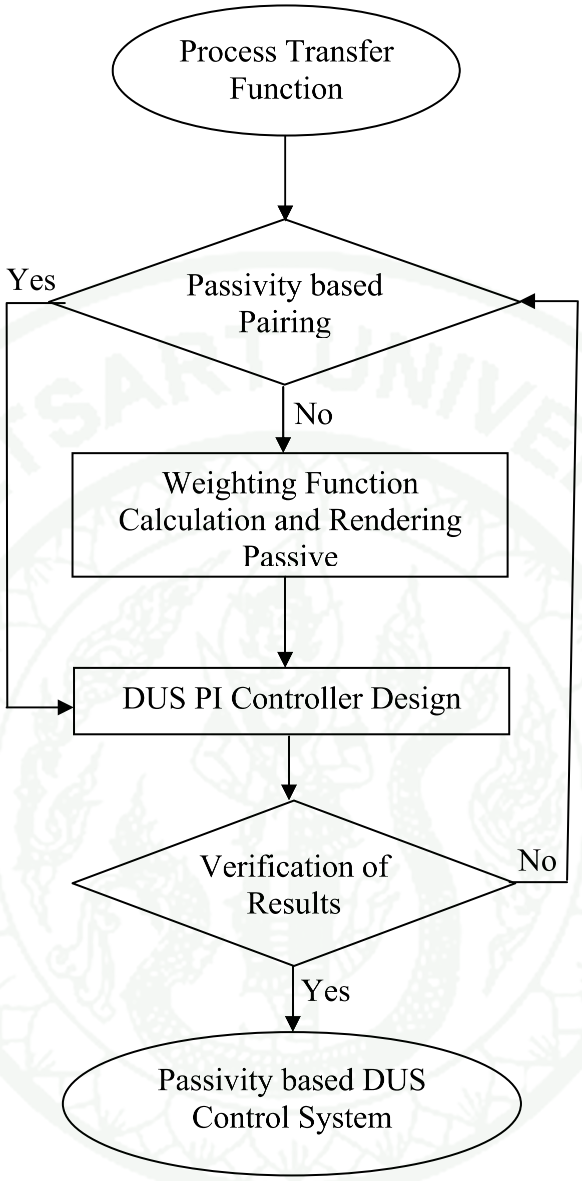

Figure 17 Passivity based decentralized controller synthesis procedure

1.3 Passivity based pairing of the heat exchanger with a single bypass

This section finds the best controlled-manipulated variable pairing of the heat exchanger model following the procedure of passivity based pairing proposed by Bao and Lee (2007).

1.3.1 Determine the transfer function G(s) for each possible pairing scheme

Equations (104) and (105), which are the state space equation of the heat exchanger model with a single bypass, have a transfer function of two-by-two matrix, which has two pairing schemes. The first pairing scheme called 1-1/2-2 uses cold flowrate F_C to control the output cold temperature T_C and bypass fraction f_H on hot side to control the output hot temperature T_H. The second pairing scheme called 1-2/2-1 uses cold flowrate F_C to control the output hot temperature T_H, and bypass fraction f_H on hot side to control the output cold temperature T_C.

1.3.2 Screen out the non-DIC pairing schemes by using the necessary DIC condition given in Theorem 5.

For the steady state of 1-1/2-2 pairing, G(0) of this system is shown in Equation (107).

$$G(0)=\begin{bmatrix} -30.14 & -36.64 \\ -18.21 & 54.84 \end{bmatrix} \tag{107}$$

The relative gain array at steady state ($\Lambda(G(0))$) for 1-1/2-2 pairing is calculated and shown in Equation (108).

$$\Lambda(G(0))=\begin{bmatrix} 0.7124 & 0.2876 \\ 0.2876 & 0.7124 \end{bmatrix} \tag{108}$$

The relative gain array at steady state for 1-2/2-1 pairing is calculated and shown in Equation (109).

$$\Lambda(G(0))=\begin{bmatrix} 0.2876 & 0.7124 \\ 0.7127 & 0.2876 \end{bmatrix} \tag{109}$$

Both relative gain arrays at steady state of two pairing schemes are much more than zero which satisfy the theorem 5, thus, both pairing schemes are DIC.

1.3.3 Find the sign matrix U and obtain G^{+}(s) such that $G_{ii}^{+}\left(0\right)>0\ (i=1,...,m)$

From subsection 1.3.2, the possible pairing schemes remain two pairing schemes which are 1-1/2-2 and 1-2/2-1 pairings. This section determines matrix U defined in the following equation.

$$U = diag\{U_{ii}\}, \quad i=1,...,m \tag{110}$$

where U is a diagonal matrix with either 1 or -1 along the diagonal.
Therefore, U for this 1-1/2-2 pairing is in Equation (111) in order that $G_{ii}^{+}\left(0\right)>0\ (i=1,...,m)$ where $G^{+}\left(s\right)=G(s)U$

$$U=\begin{bmatrix} -1 & 0 \\ 0 & 1 \end{bmatrix} \tag{111}$$

And U for 1-2/2-1 pairing is presented in Equation (112).

$$U=\begin{bmatrix} -1 & 0 \\ 0 & -1 \end{bmatrix} \tag{112}$$

1.3.4 Calculate the diagonally scaled passivity index $\nu_{s}\left(G^{+}\left(s\right),\omega\right)$ at a number of frequency points.

In this step, the diagonally scaled passivity index of each pairing scheme is determined from Equation (87). The passivity index of 1-1/2-2 and 1-2/2-1 pairings of this system are depicted in Figures 18 and 19, respectively.

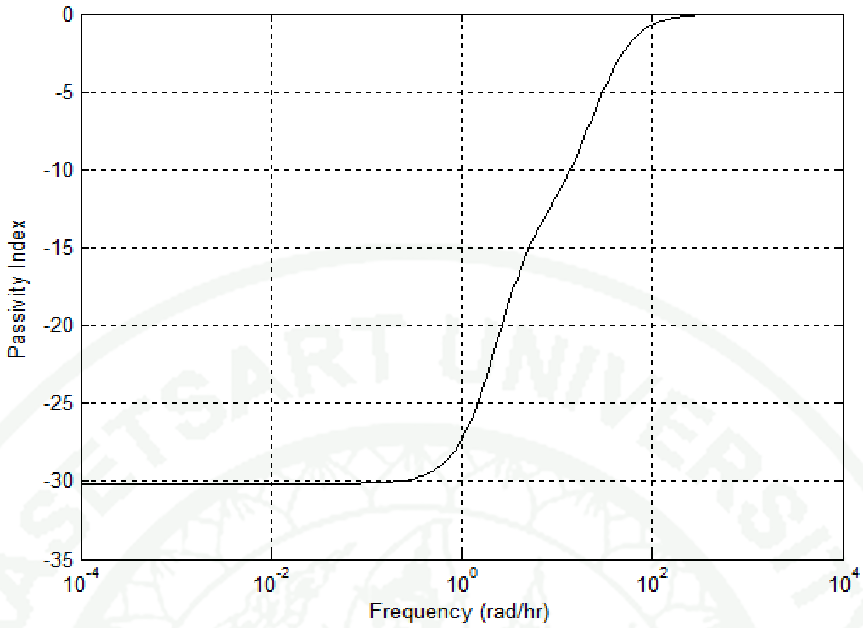

Figure 18 Passivity index of 1-1/2-2 pairing of a single heat exchanger with a single bypass on hot side

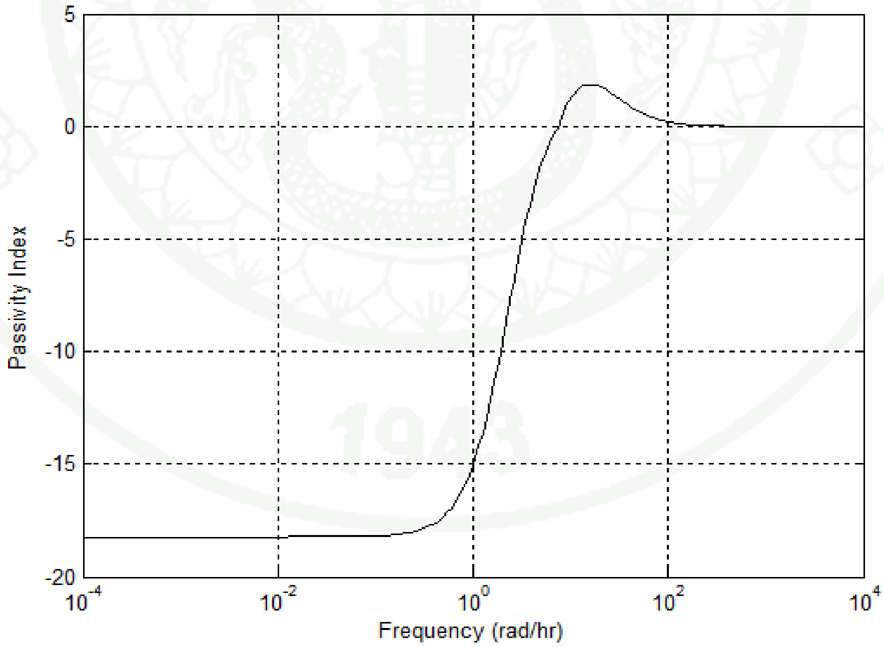

Figure 19 Passivity index of 1-2/2-1 pairing of a single heat exchanger with a single bypass on hot side

1.3.5 Compare the passivity index profiles of different pairings. The best pairing should correspond to the one with the largest frequency bandwidth ω_b such that $\nu_s\left(G^+(s),\omega\right) \le 0$ for any $\omega \in [0,\omega_b]$. This pairing scheme would allow using controllers with integral action and the fastest dynamic response.

In this step, only one pairing scheme is chosen after finding the passivity index of each pairing scheme. Compared the passivity index of both pairing schemes illustrating in Figure 20, 1-1/2-2 pairing is more passive than 1-2/2-1 pairing since the first pairing scheme has the passivity index which is less than zero along the frequency range. Hence, 1-1/2-2 pairing, in which cold flowrate F_C controls the output cold temperature T_C and bypass fraction f_H on hot side controls the output hot temperature T_H, is the best pairing for this single heat exchanger with a single bypass on hot side.

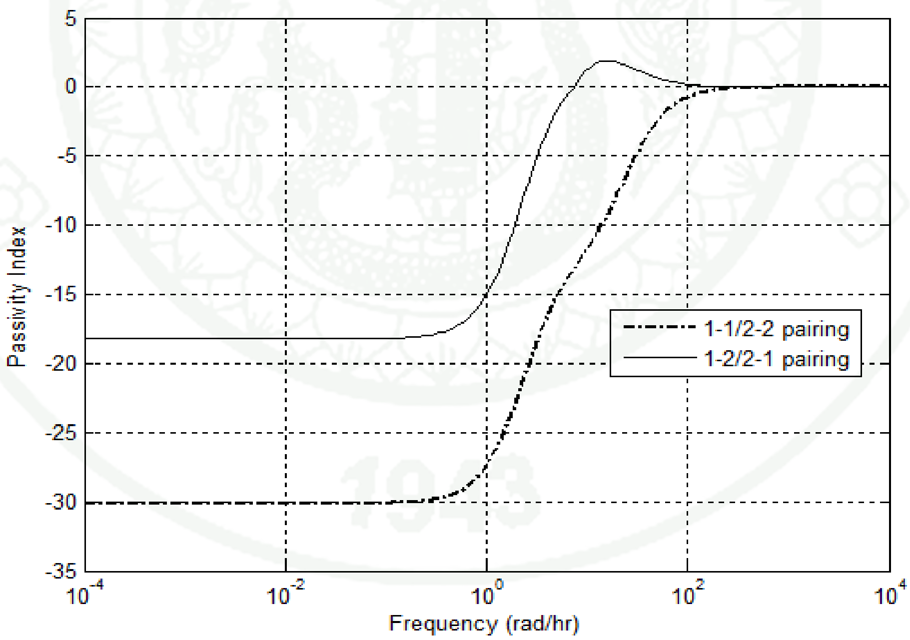

Figure 20 Passivity indices of 1-1/2-2 and 1-2/2-1 pairings of a single heat exchanger with a single bypass on hot side

Although the single bypass heat exchanger has already proved to be non-passive system, the result from the passivity based pairing step shows that the best pairing is 1-1/2-2 pairing which is passive along the frequency range. Therefore, from Figure 17, the DUS PI controllers can be designed directly without concerning the weighting function.

1.4 Multi-loop PI controller design

This section shows the procedure to design multi-loop PI controller following the work of Bao *et al*. (2002a).

1.4.1. Determine the pairing scheme for controlled and manipulated variables according to the procedure to find the best pairing of the system.

For this step, the best pairing has been chosen from section 1.3 which is 1-1/2-2 pairing; cold flowrate F_C controls the output cold temperature T_C, and bypass fraction f_H on hot side controls the output hot temperature T_H.

1.4.2. For each subsystem $G_{ii}^{+}(s)$ (i = 1,…,m), solve Problem 4 for the PI controller parameters $k_{c,i}^{+}$ and $\tau_{I,i}$

Problem 4

$$\min_{k_{c,i}^{+},\tau_{I,i}} \left(-\gamma_i\right) \tag{113}$$

such that

$$\left| \frac{w_i(j\omega)\gamma_i}{1+G_{ii}^{+}\left(j\omega\right)k_{c,i}^{+}\left[1+\dfrac{1}{\tau_{I,i}\times j\omega}\right]} \right| < 1 \tag{114}$$

and

$$\tau_{I,i}^2 \ge \frac{k_{c,i}^{+}\nu_s(\omega)}{\left[1-k_{c,i}^{+}\nu_s(\omega)\right]\omega^2} \qquad \forall\omega \in R, i=1,\ldots,n \tag{115}$$

This step has to find PI tuning parameters for each loop of a single heat exchanger with a single bypass on hot side by solving Problem 4. When this problem is solved, PI tuning parameters are presented in Table 6.

Table 6 PI tuning parameters for a single heat exchanger model with a single bypass on hot side

PI Tuning Parameter	**Loop 1**[a]	**Loop 2**[b]
k_c^+	1940.6	35.0
τ_I	15.48	15

Remark: [a]: 1-1 pairing/ [b]: 2-2 pairing

1.5.3. Adjust the sign of the final subcontroller gain $k_{c,i} = k_{c,i}^{+}U_{ii}$ to obtain the final multi-loop controller as Equation (116).

$$K(s) = diag\{k_i(s)\} = diag\left\{k_{c,i}(1+\frac{1}{\tau_{I,i}s})\right\} \tag{116}$$

When PI tuning parameters for each loop have already been determined, the final multi-loop controller as the same form in Equation (116) is shown in the following equation.

$$K(s) = \begin{bmatrix} -1940.6(1+\dfrac{1}{15.48s}) & 0 \\ 0 & 35(1+\dfrac{1}{15s}) \end{bmatrix} \tag{117}$$

1.6 Verification of results

After getting the PI tuning parameters, the heat exchanger system as displayed in Figure 15 is tested with these tuning parameters via Aspen Dynamics. The following figure shows the control loops for a single heat exchanger with a single bypass on hot side.

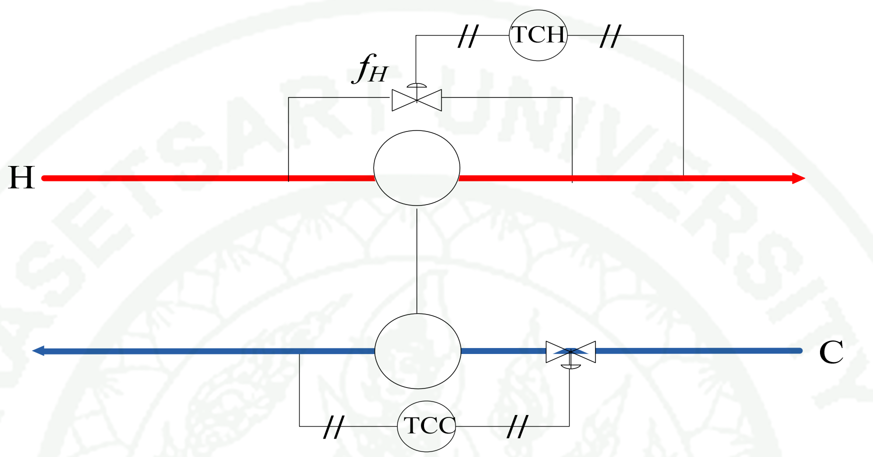

Figure 21 Control loops of a single heat exchanger with a single bypass on hot side

This heat exchanger system with control loops is tested with two main controller classes; controllers with default PI tuning parameters from Aspen Dynamics and controllers with passivity based PI tuning parameters from passivity concept. This system with both controller types is tested by changing its setpoint between -10% and +10% setpoint temperatures of either hot or cold stream, and also tested by disturbing -10% and +10% inlet hot flowrates. Figures 22 to 25 show responses of controllers TCC and TCH when the heat exchanger system with control loops is changed its setpoint.

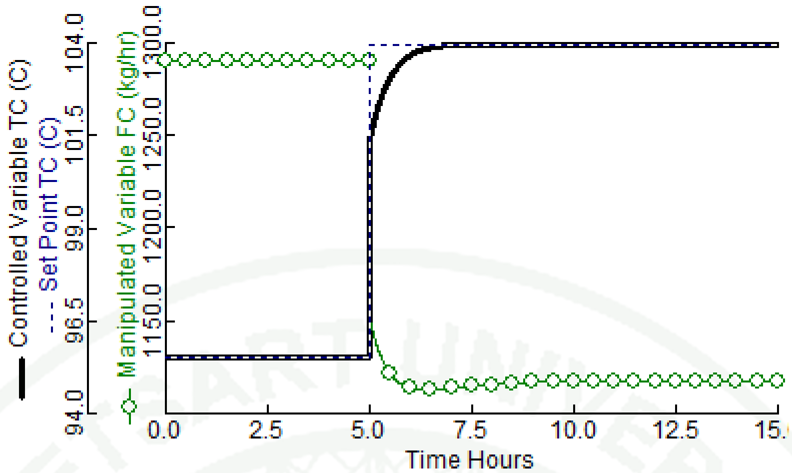

(a)

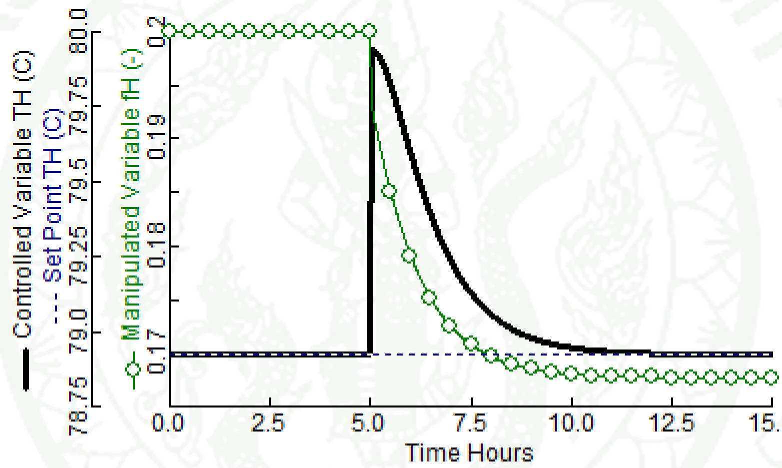

(b)

Figure 22 Responses of controllers TCC (a) and TCH (b) of +10% cold setpoint temperature at hour 5

Figure 22 shows responses of controllers TCC and TCH with default PI tuning parameters when the cold setpoint changed from 94.5 to 103.95 ºC (+10% cold setpoint temperature). When cold setpoint is changed, controller TCC manipulates cold flowrate by decreasing its flowrate in order to reach the new setpoint which takes the time approximately 2.5 hours. Decreasing cold flowrate also affects the higher hot temperature, thus, controller TCH manipulates bypass fraction decreased to obtain the target hot temperature.

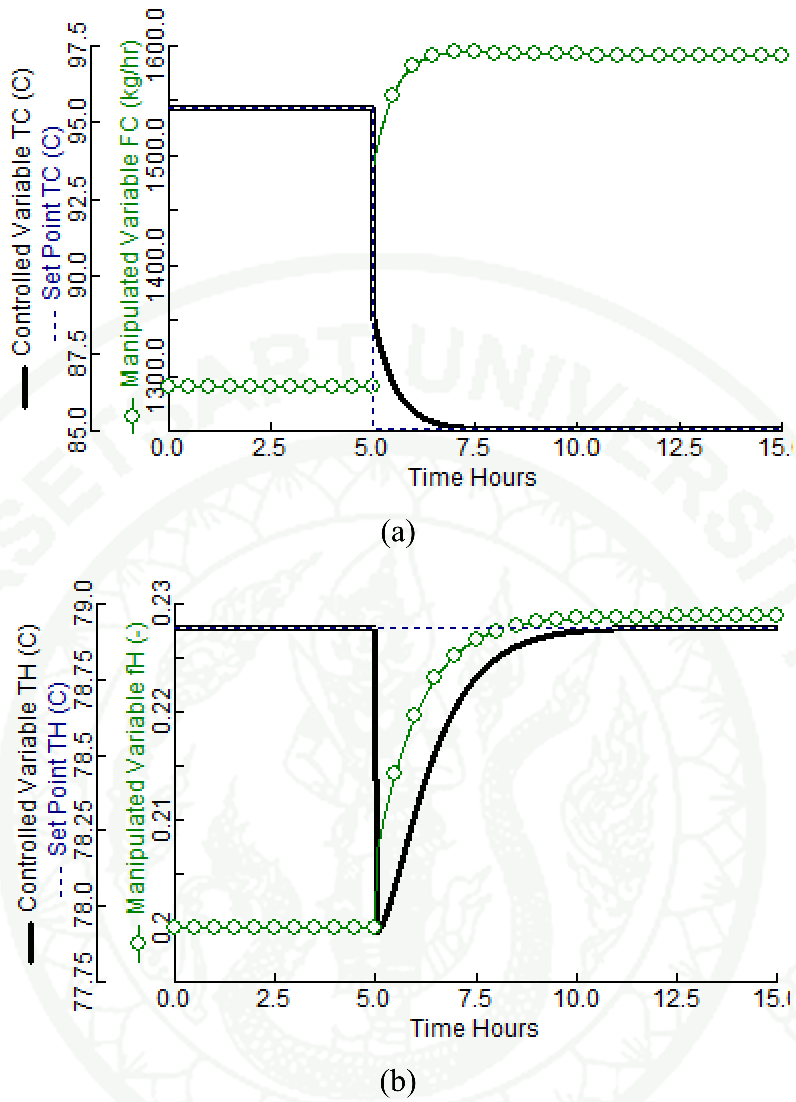

Figure 23 Responses of controllers TCC (a) and TCH (b) of -10% cold setpoint temperature at hour 5

Figure 23 shows responses of controllers TCC and TCH with default PI tuning parameters when the cold setpoint changed from 94.5 to 85.05 ºC (-10% cold setpoint temperature). When cold setpoint is changed, controller TCC manipulates cold flowrate by increasing its flowrate in order to reach the new setpoint which takes the time approximately 2.5 hours. Increasing cold flowrate also affects the lower hot temperature, thus, controller TCH manipulates bypass fraction increased to obtain the target hot temperature.

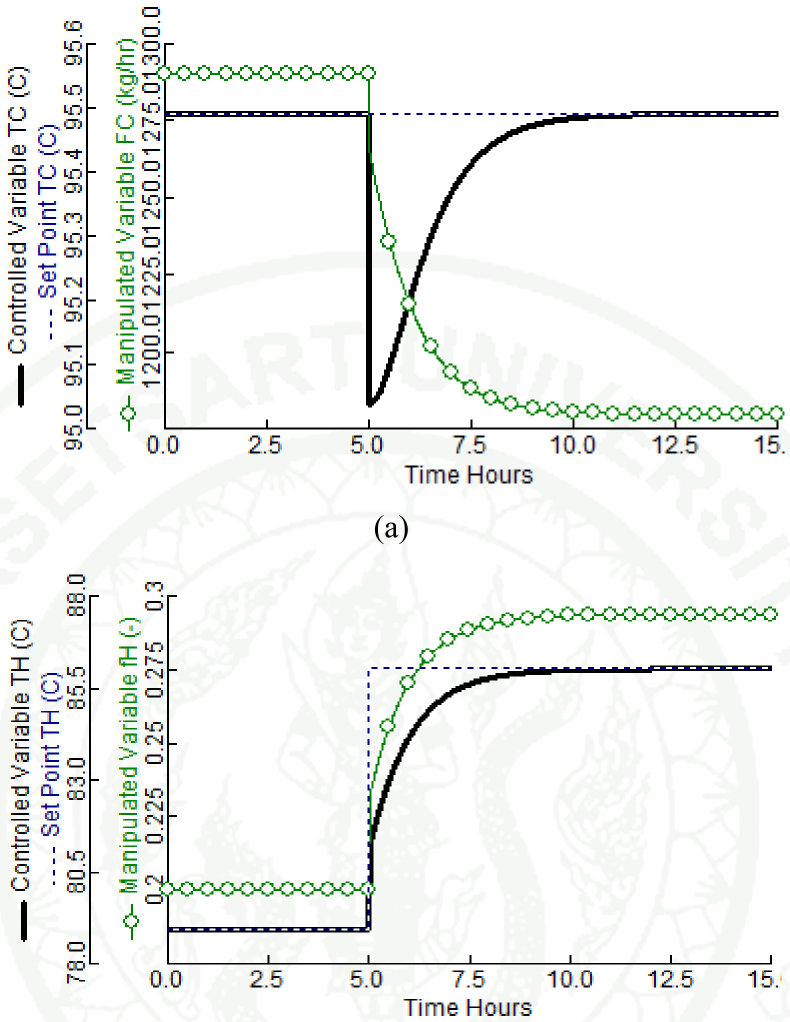

(b)

Figure 24 Responses of controllers TCC (a) and TCH (b) of +10% hot setpoint temperature at hour 5

Figure 24 shows responses of controllers TCC and TCH with default PI tuning parameters when the hot setpoint changed from 78.2 to 86.02 ºC (+10% hot setpoint temperature). When hot setpoint is changed, controller TCH manipulates bypass fraction of hot stream by increasing its bypass fraction in order to reach the new setpoint which takes the time approximately 5 hours. Changing the hot setpoint temperature affects the controller TCC since when bypass fraction is increased, hot stream entering the heat exchanger exchanges less heat with cold stream. Therefore, controller TCC reduces cold flowrate in order that cold stream temperature maintains its original setpoint.

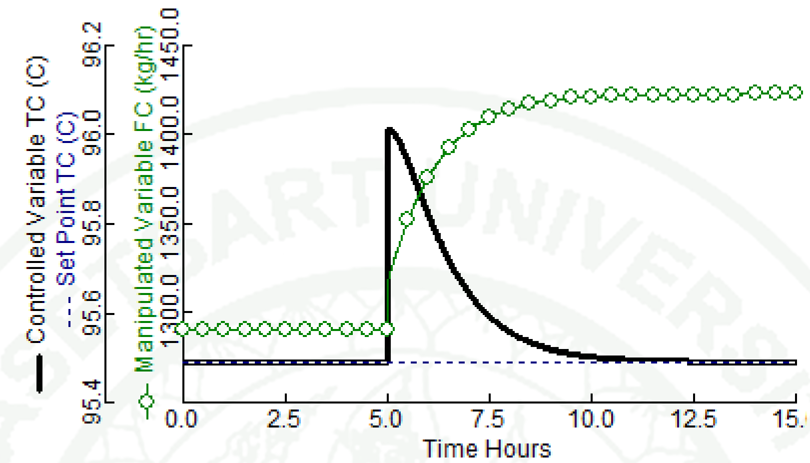

(a)

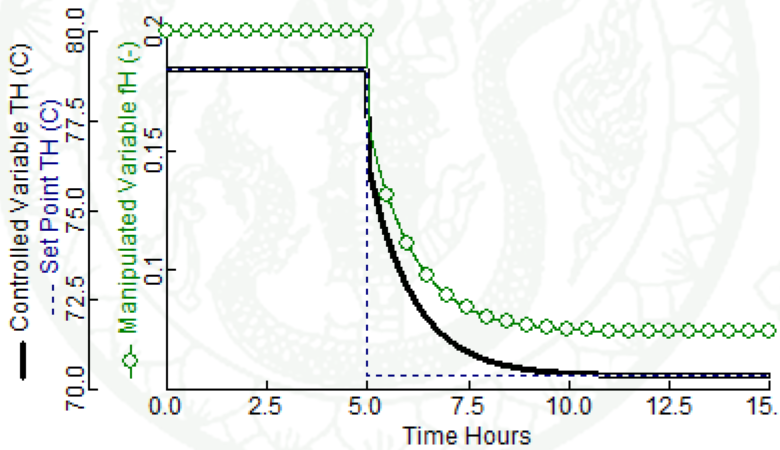

(b)

Figure 25 Response of controllers TCC (a) and TCH (b) of -10% hot setpoint temperature at hour 5

Figure 25 shows responses of controllers TCC and TCH with default PI tuning parameters when the hot setpoint changed from 78.2 to 70.38 ºC (-10% hot setpoint temperature). When hot setpoint is changed, controller TCH manipulates bypass fraction of hot stream by decreasing its bypass fraction in order to reach the new setpoint which takes the time approximately 5 hours. Changing the hot setpoint temperature also affects the controller TCC since when bypass fraction is decreased, hot stream entering the heat exchanger exchanges more heat with cold stream. Therefore, controller TCC increases cold flowrate in order that cold stream temperature maintains its original setpoint.

Figures 26 and 27 show responses of controllers TCC and TCH when a single bypass heat exchanger system is disturbed by +10% and -10% of inlet hot flowrates, respectively.

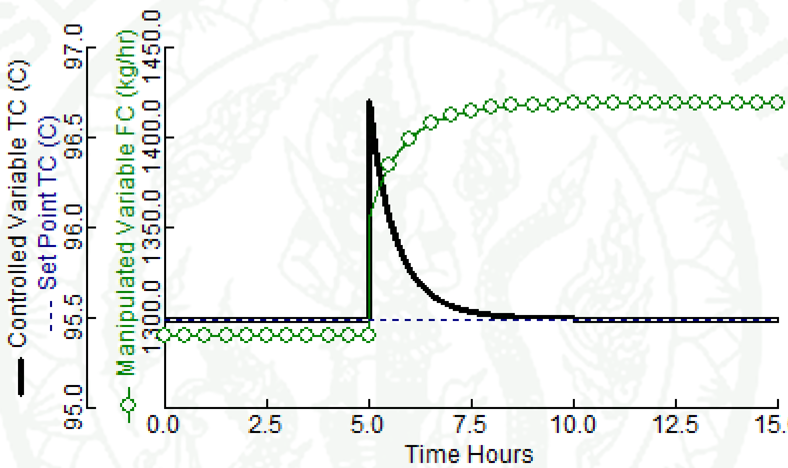

(a)

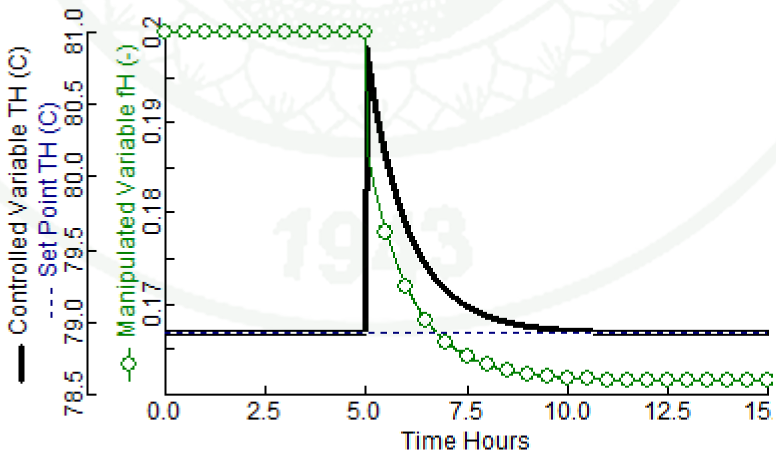

(b)

Figure 26 Responses of controllers TCC (a) and TCH (b) of +10% inlet hot flowrate disturbance at hour 5

Figure 26 shows responses of controllers TCC and TCH with default PI tuning parameters when the inlet hot flowrate of a single bypass heat exchanger is changed from 860 to 946 kg/hr (+10% inlet hot flowrate). When hot flowrate is increased, the final hot temperature increases. Therefore, in order to get the target hot temperature, controller TCH manipulates bypass fraction of hot stream by decreasing its bypass fraction which takes the time approximately 5 hours. Adjusting bypass fraction of hot stream affects the controller TCC since when bypass fraction is decreased, hot stream entering the heat exchanger exchanges more heat with cold stream. Therefore, controller TCC increases cold flowrate in order that cold stream temperature maintains its original setpoint.

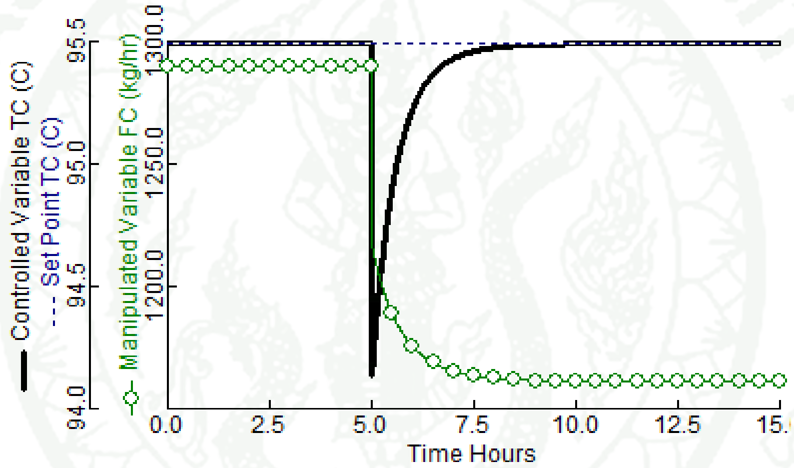

(a)

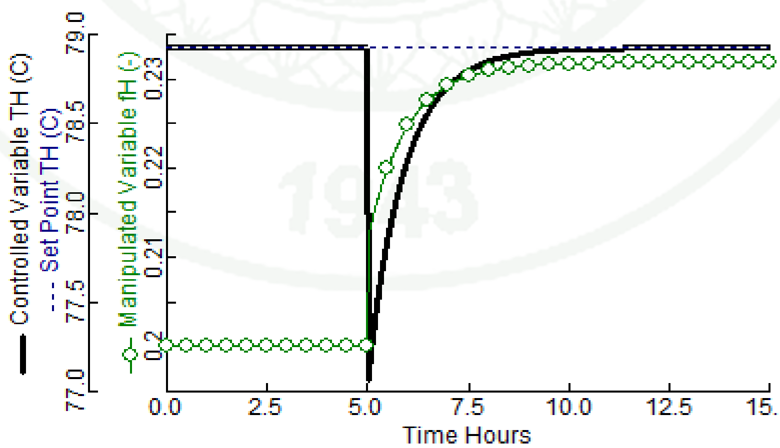

(b)

Figure 27 Responses of controllers TCC (a) and TCH (b) of -10% inlet hot flowrate disturbance at hour 5

Figure 27 shows responses of controllers TCC and TCH with default PI tuning parameters when the inlet hot flowrate of a single bypass heat exchanger is changed from 860 to 774 kg/hr (-10% inlet hot flowrate). When hot flowrate is decreased, the final hot temperature decreases. Therefore, in order to get the target hot temperature, controller TCH manipulates bypass fraction of hot stream by increasing its bypass fraction which takes approximately 5 hours. Adjusting bypass fraction of hot stream affects the controller TCC since when bypass fraction is increased, hot stream entering the heat exchanger exchanges less heat with cold stream. Therefore, controller TCC decreases cold flowrate in order that cold stream temperature maintains its original setpoint.

Figures 28 to 33 show responses of controllers TCC and TCH with passivity based PI tuning parameters when the heat exchanger system with control loops is changed its setpoint and disturbed by inlet hot flowrate disturbances, respectively.

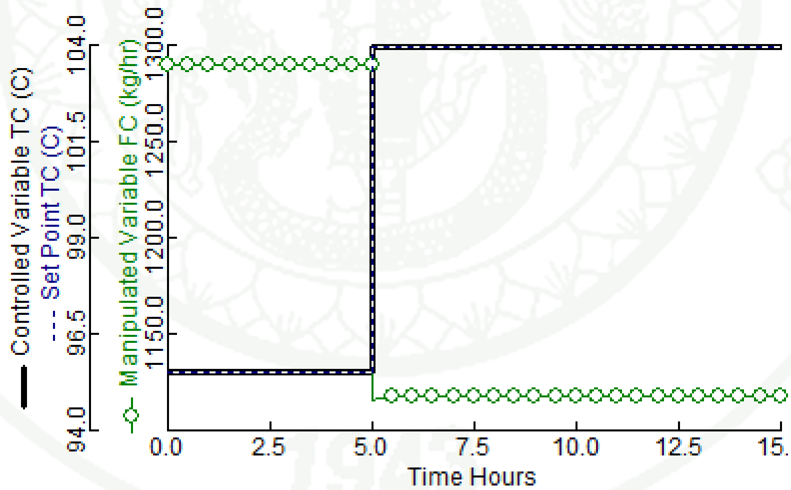

(a)

Figure 28 Responses from passivity based PI tuning of controllers TCC (a) and TCH (b) of +10% cold setpoint temperature at hour 5

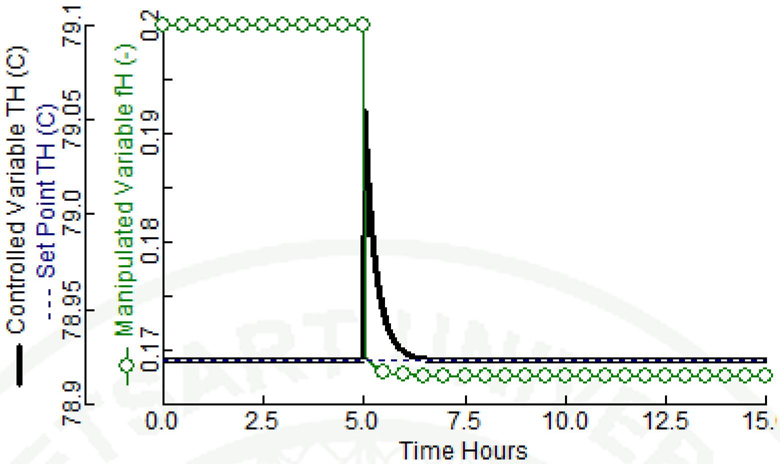

(b)

Figure 28 (Continued)

Figure 28 shows responses of controllers TCC and TCH with passivity based PI tuning parameters when the cold setpoint changed from 94.5 to 103.95 ºC (+10% cold setpoint temperature). When cold setpoint is changed, controller TCC immediately adjusts cold flowrate by decreasing its flowrate in order to reach the new setpoint in a few minutes. Decreasing cold flowrate also affects the higher hot temperature; therefore controller TCH manipulates bypass fraction decreased to obtain the target hot temperature. Compared Figures 22 and 28, the time to reach the new setpoint of the system with passivity based PI controllers is much less than that with default PI controllers.

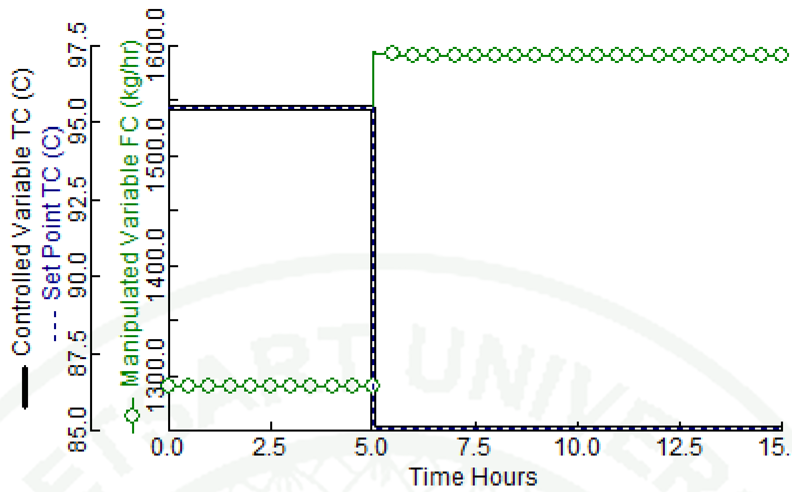

(a)

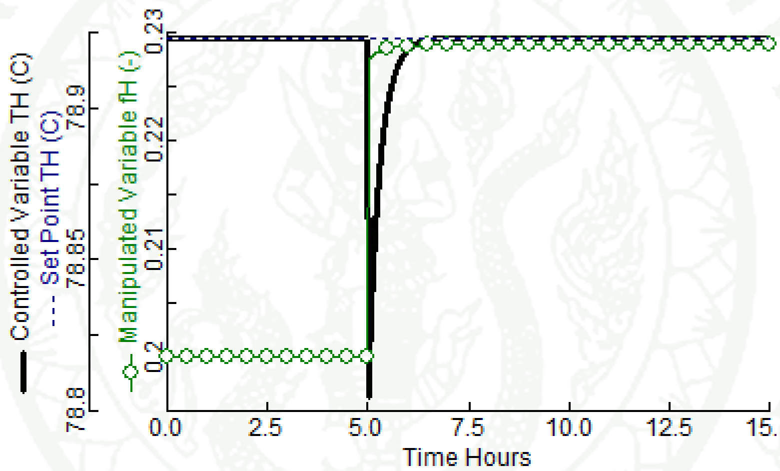

(b)

Figure 29 Responses from passivity based PI tuning of controllers TCC (a) and TCH (b) of -10% cold setpoint temperature at hour 5

Figure 29 shows responses of controllers TCC and TCH with passivity based PI tuning parameters when the cold setpoint changed from 94.5 to 85.05 ºC (-10% cold setpoint temperature). When cold setpoint is changed, controller TCC immediately adjusts cold flowrate by increasing its flowrate in order to reach the new setpoint in a few minutes. Increasing cold flowrate affects the lower hot temperature; therefore, controller TCH manipulates bypass fraction increased to maintain the target hot temperature. Compared Figures 23 and 29, the time to reach the new setpoint of the system with passivity based PI controllers is much less than that with default PI controllers.

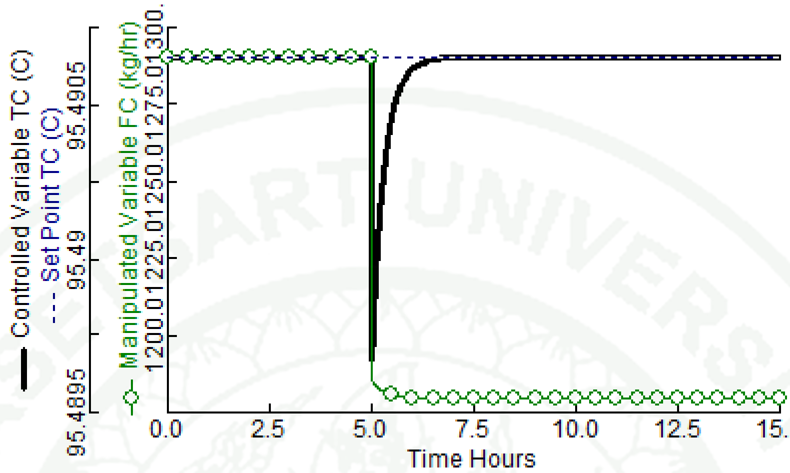

(a)

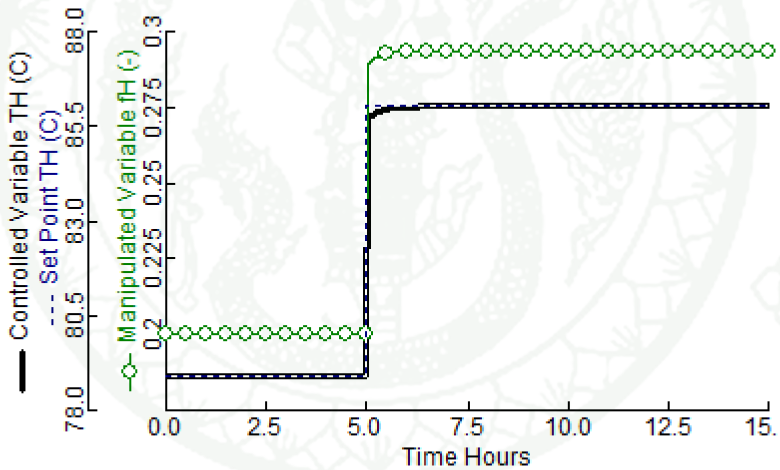

(b)

Figure 30 Responses from passivity based PI tuning of controllers TCC (a) and TCH (b) of +10% hot setpoint temperature at hour 5

Figure 30 shows responses of controllers TCC and TCH with passivity based PI tuning parameters when the hot setpoint changed from 78.2 to 86.02 ºC (+10% hot setpoint temperature). When hot setpoint is changed, controller TCH immediately adjusts bypass fraction of hot stream by increasing its fraction in order to reach the new setpoint in a few minutes. Increasing bypass fraction also affects the lower cold temperature, thus, controller TCC manipulates cold flowrate decreased to obtain the target cold temperature. Compared Figures 24 and 30, the time to reach the new setpoint of the system with passivity based PI controllers is much less than that with default PI controllers.

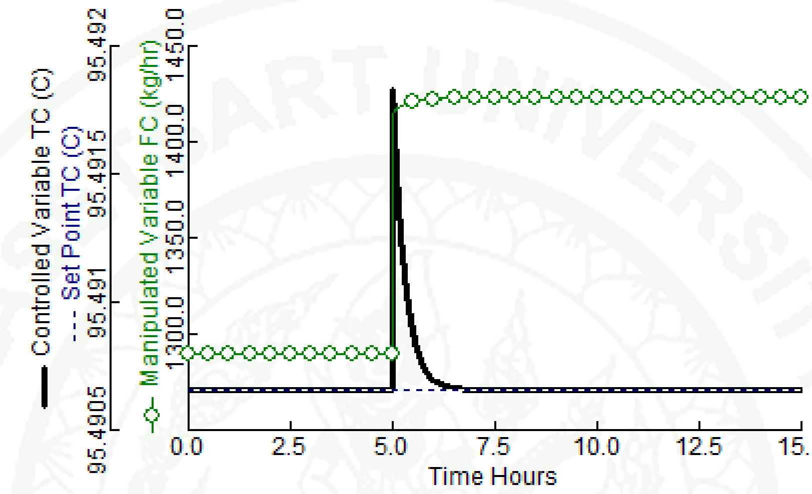

(a)

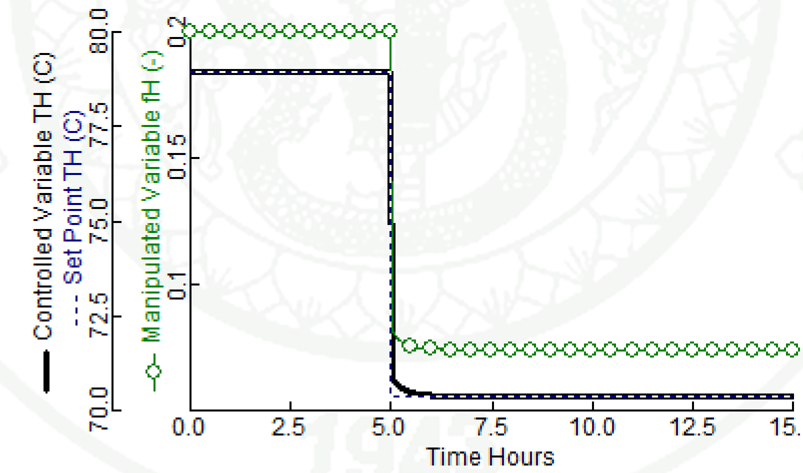

(b)

Figure 31 Responses from passivity based PI tuning of controllers TCC (a) and TCH (b) of -10% hot setpoint temperature at hour 5

Figure 31 shows responses of controllers TCC and TCH with passivity based PI tuning parameters when the hot setpoint changed from 78.2 to 70.38 ºC (-10% hot setpoint temperature). When hot setpoint is changed, controller TCH immediately adjusts bypass fraction of hot stream by decreasing its fraction in order to reach the new setpoint in a few hours. Decreasing bypass fraction also affects the higher cold temperature, thus, controller TCC manipulates cold flowrate increased to obtain the target cold temperature. Compared Figures 25 and 31, the time to reach the new setpoint of the system with passivity based PI controllers is much less than that with default PI controllers.

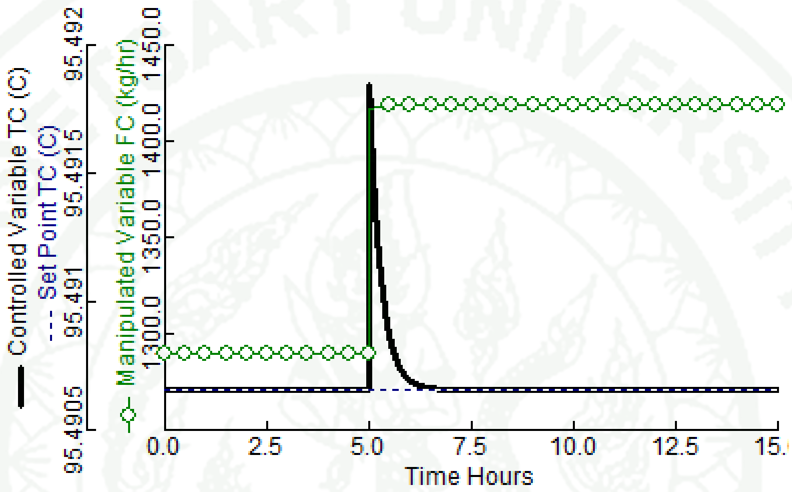

(a)

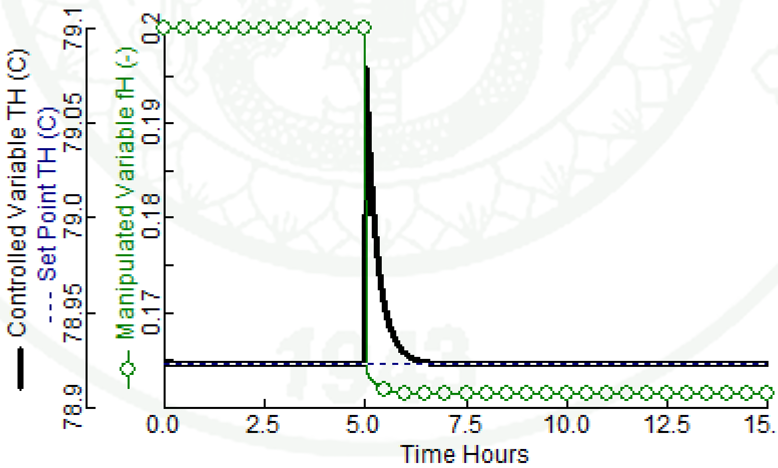

(b)

Figure 32 Responses from passivity based PI tuning of controllers TCC (a) and TCH (b) from +10% inlet hot flowrate disturbance at hour 5

Figure 32 shows responses of controllers TCC and TCH with passivity based PI tuning parameters when the inlet hot flowrate of the single bypass heat exchanger is increased from 860 to 946 kg/hr (+10% inlet hot flowrate). When hot flowrate is increased, the final hot temperature is increased. Then controller TCH manipulates bypass fraction of hot stream by decreasing its bypass fraction which takes a few hours. Adjusting bypass fraction of hot stream affects the controller TCC since when bypass fraction is decreased, hot stream entering the heat exchanger exchanges more heat with cold stream. Therefore, controller TCC manipulates cold flowrate increased in order that cold stream temperature maintains its original setpoint. Compared Figures 26 and 32, the time to reach the new setpoint of the system with passivity based PI controllers is much less than that with default PI controllers.

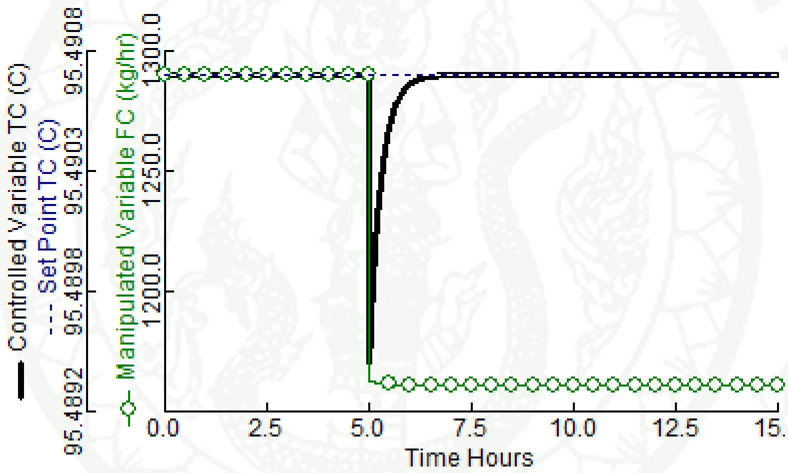

(a)

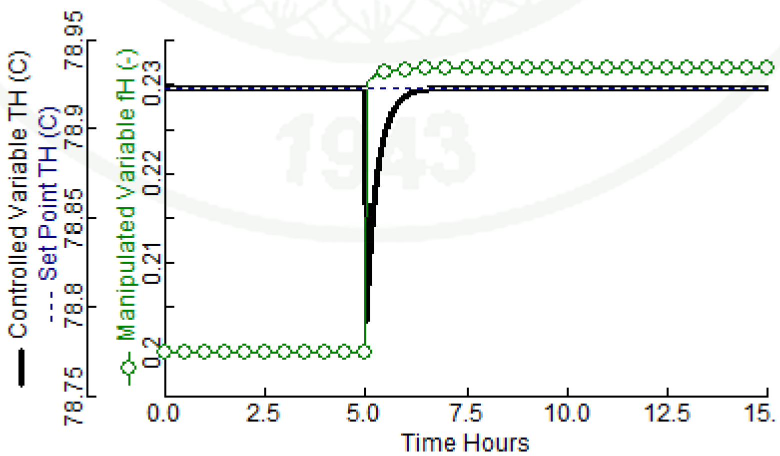

(b)

Figure 33 Responses from passivity based PI tuning of controllers TCC (a) and TCH (b) from -10% inlet hot flowrate disturbance at hour 5

Figure 33 shows responses of controllers TCC and TCH with passivity based PI tuning parameters when the inlet hot flowrate of the single bypass heat exchanger is decreased from 860 to 774 kg/hr (-10% inlet hot flowrate). When hot flowrate is increased, the final hot temperature is decreased. Then controller TCH manipulates bypass fraction of hot stream by increasing its bypass fraction which takes a few hours. Adjusting bypass fraction of hot stream affects the controller TCC since when bypass fraction is increased, hot stream entering the heat exchanger exchanges less heat with cold stream. Therefore, controller TCC manipulates cold flowrate decreased in order that cold stream temperature maintains its original setpoint. Compared Figures 27 and 33, the time to reach the new setpoint of the system with passivity based PI controllers is much less than that with default PI controllers.

2. Heat Exchanger Networks Applied with the Passivity Theorem

This section extends a single heat exchanger to a HEN which is widely used in most industries. Similarly, the HEN is also applied with the passivity theorem as the same as the heat exchanger.

2.1 Heat exchanger network model

As shown in Equations (102) and (103), the state space equation of a single heat exchanger with a single bypass is developed for a heat exchanger with a bypass on hot side. Equivalently, if a heat exchanger has a bypass on cold side exhibited in Figure 34, the state space equation for this system is presented in Equations (118) to (121).

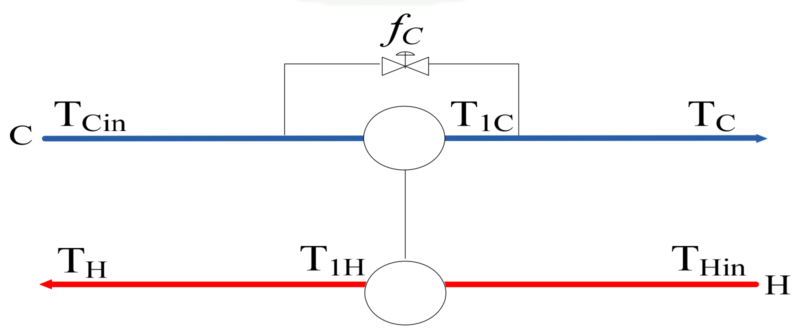

Figure 34 A grid diagram of a single heat exchanger with bypass on cold side

$$\frac{dT_{1C}}{dt}=\left(\frac{-UA+\tau_C F_C \bar{f}_C-\tau_C F_C}{\xi_C}\right)T_{1C}+\frac{UA}{\xi_C}T_{1H}+\left(\frac{\tau_C F_C \bar{T}_{1C}-\tau_C F_C T_{Cin}}{\xi_C}\right)f_C \tag{118}$$

$$\frac{dT_{1H}}{dt}=\frac{UA}{\xi_H}T_{1C}+\left(\frac{-UA-\tau_H \bar{F}_H}{\xi_H}\right)T_{1H}+\left(\frac{\tau_H T_{Hin}-\tau_H \bar{T}_{1H}}{\xi_H}\right)F_H \tag{119}$$

$$T_C=(1-\bar{f}_C)T_{1C}+(T_{Cin}-\bar{T}_{1C})f_C \tag{120}$$

$$T_H=T_{1H} \tag{121}$$

where $\tau_i=\rho_i C_{Pi}$ and $\xi_i=\rho_i V_i C_{Pi}$

Note: The full derivation of these equations is shown in Appendix C.

Therefore, the developed equations of a single heat exchanger with a single bypass on cold side are compactly summarized in the state space form in Equations (122) and (123).

$$\begin{bmatrix}\dot{T}_{1C}\\ \dot{T}_{1H}\end{bmatrix}=\begin{bmatrix}\frac{-UA+\tau_C F_C \bar{f}_C-\tau_C F_C}{\xi_C} & \frac{UA}{\xi_C}\\ \frac{UA}{\xi_H} & \frac{-UA-\tau_H \bar{F}_H}{\xi_H}\end{bmatrix}\begin{bmatrix}T_{1C}\\ T_{1H}\end{bmatrix}+\begin{bmatrix}\frac{\tau_C F_C \bar{T}_{1C}-\tau_C F_C T_{Cin}}{\xi_C} & 0\\ 0 & \frac{\tau_H T_{Hin}-\tau_H \bar{T}_{1H}}{\xi_H}\end{bmatrix}\begin{bmatrix}f_C\\ F_H\end{bmatrix} \tag{122}$$

$$\begin{bmatrix}T_C\\ T_H\end{bmatrix}=\begin{bmatrix}1-\bar{f}_C & 0\\ 0 & 1\end{bmatrix}\begin{bmatrix}T_{1C}\\ T_{1H}\end{bmatrix}+\begin{bmatrix}T_{Cin}-\bar{T}_{1C} & 0\\ 0 & 0\end{bmatrix}\begin{bmatrix}f_C\\ F_H\end{bmatrix} \tag{123}$$

where $\tau_i=\rho_i C_{Pi}$ and $\xi_i=\rho_i V_i C_{Pi}$

The HEN example used in this work is referred from Glemmestad *et al*. (1996) and presented in the following figure which the data for this network is available.

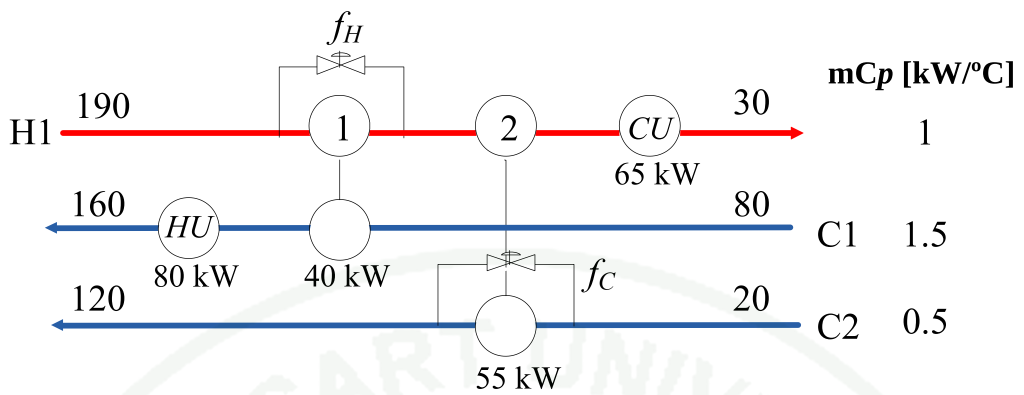

Figure 35 A grid diagram of heat exchanger networks from Glemmestad *et al*. (1996)

This network contains two heat exchangers and two utilities which already designed by pinch method, based on a minimum heat recovery approach temperature of 20 ºC. If this network is considered carefully, it can be divided into two cases. The first case is two heat exchangers with bypasses which have already tested to be non-passive, and the second case is two utilities assumed to be a heat exchanger type which have already reported by Bao and Lee (2007) to be passive. After this point, these two cases is followed the passivity based decentralized controller synthesis procedure as displayed in Figure 17.

2.2 Two heat exchangers of a heat exchanger network

2.2.1 Heat exchanger models

The state space for these two heat exchangers, which one has a single bypass on hot side and another has a single bypass on cold side, are shown in Equations (124) and (125).

$$\dot{x} = \begin{bmatrix} A_{11} & 0 \\ 0 & A_{22} \end{bmatrix} x + \begin{bmatrix} B_{11} & 0 \\ 0 & B_{22} \end{bmatrix} u \tag{124}$$

$$y = \begin{bmatrix} C_{11} & 0 \\ 0 & C_{22} \end{bmatrix} x + \begin{bmatrix} D_{11} & 0 \\ 0 & D_{22} \end{bmatrix} u \tag{125}$$

where $x = \left[T_{1C}\ T_{1H}\ T_{2C}\ T_{2H} \right]^T$, $u = \left[F_{C1}\ f_{H1}\ f_{C2}\ F_{H2} \right]^T$ $y = \left[T_{1C1}\ T_{1H1}\ T_{2C2}\ T_{2H2} \right]^T$ and partitioned matrices

$$A_{11} \text{ represents } \begin{bmatrix} \dfrac{-U_1A_1 - \tau_{C1}\bar{F}_{C1}}{\xi_{C1}} & \dfrac{U_1A_1}{\xi_{C1}} \\ \dfrac{U_1A_1}{\xi_{H1}} & \dfrac{-U_1A_1 + \tau_{H1}F_{H1}\bar{f}_{H1} - \tau_{H1}F_{H1}}{\xi_{H1}} \end{bmatrix} \tag{126}$$

$$A_{22} \text{ represents } \begin{bmatrix} \dfrac{-U_2A_2 + \tau_{C2}F_{C2}\bar{f}_{C2} - \tau_{C2}F_{C2}}{\xi_{C2}} & \dfrac{U_2A_2}{\xi_{C2}} \\ \dfrac{U_2A_2}{\xi_{H2}} & \dfrac{-U_2A_2 - \tau_{H2}\bar{F}_{H2}}{\xi_{H2}} \end{bmatrix} \tag{127}$$

$$B_{11} \text{ represents } \begin{bmatrix} \dfrac{\tau_{C1}T_{Cin1} - \tau_{C1}\bar{T}_{1C1}}{\xi_{C1}} & 0 \\ 0 & \dfrac{\tau_{H1}F_{H1}\bar{T}_{1H1} - \tau_{H1}F_{H1}T_{Hin1}}{\xi_{H1}} \end{bmatrix} \tag{128}$$

$$B_{22} \text{ represents } \begin{bmatrix} \dfrac{\tau_{C2}F_{C2}\bar{T}_{1C2} - \tau_{C2}F_{C2}T_{Cin2}}{\xi_{C2}} & 0 \\ 0 & \dfrac{\tau_{H2}T_{Hin2} - \tau_{H2}\bar{T}_{1H2}}{\xi_{H2}} \end{bmatrix} \tag{129}$$

$$C_{11} \text{ represents } \begin{bmatrix} 1 & 0 \\ 0 & 1-\bar{f}_H \end{bmatrix} \tag{130}$$

$$C_{22} \text{ represents } \begin{bmatrix} 1-\bar{f}_C & 0 \\ 0 & 1 \end{bmatrix} \tag{131}$$

$$D_{11} \text{ represents } \begin{bmatrix} 0 & 0 \\ 0 & T_{Hin} - \bar{T}_{1H} \end{bmatrix} \tag{132}$$

$$D_{22} \text{ represents } \begin{bmatrix} T_{Cin} - \bar{T}_{1C} & 0 \\ 0 & 0 \end{bmatrix} \tag{133}$$

This system is simulated by Aspen Plus to determine the necessary variables in the state space equation shown above (Equations (124) and (125)). The simulation conditions are shown in Table 7.

Table 7 Numerical values for a simulation of heat exchanger networks

Parameter	Unit	Value
Inlet temperature for hot stream	ºC	190
Inlet temperature for cold stream 1	ºC	80
Inlet temperature for cold stream 2	ºC	20
Target temperature for hot stream	ºC	30
Target temperature for cold stream 1	ºC	160
Target temperature for cold stream 2	ºC	120
Hot mass capacity flowrate	kW/ ºC	1
Cold mass capacity flowrate for stream 1	kW/ ºC	1.5
Cold mass capacity flowrate for stream 2	kW/ ºC	0.5
Heat duty for a heat exchanger 1	kW	40
Heat duty for a heat exchanger 2	kW	55
Heat duty for a cold utility	kW	65
Heat duty for a hot utility	kW	80

Source: Glemmestad *et al*. (1996)

After simulation, the results are presented in Figure 36 and Table 8.

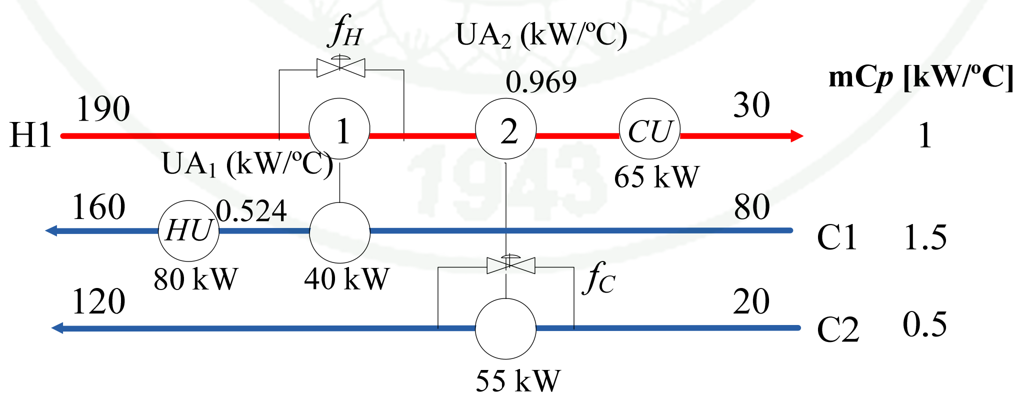

Figure 36 A grid diagram of a heat exchanger network from Glemmestad *et al*. (1996) after simulation

Table 8 Simulation results of a heat exchanger network from Glemmestad *et al*. (1996)

Parameter	Unit	Value
Output hot temperature of HE 1	ºC	155.9
Output hot temperature of HE 2	ºC	106.9
Output cold temperature of HE 1	ºC	104.4
Heat exchanger area of HE 1	m^2	0.617
Heat exchanger area of HE 2	m^2	1.14
Overall heat transfer coefficient of HE 1	$kW/m^2.ºC$	0.85
Overall heat transfer coefficient of HE 2	$kW/m^2.ºC$	0.85

When all numerical values in Equations (124) and (125) are available, they are substituted into those equations. Then Equations (124) and (125) become as follows.

$$\begin{bmatrix} \dot{T}_{1C} \\ \dot{T}_{1H} \\ \dot{T}_{2C} \\ \dot{T}_{2H} \end{bmatrix} = \begin{bmatrix} -5.31 & 2.87 & 0 & 0 \\ 0.78 & -2.27 & 0 & 0 \\ 0 & 0 & -8.02 & 5.30 \\ 0 & 0 & 1.45 & -2.94 \end{bmatrix} \begin{bmatrix} T_{1C} \\ T_{1H} \\ T_{2C} \\ T_{2H} \end{bmatrix} + \begin{bmatrix} -154.72 & 0 & 0 & 0 \\ 0 & -50.77 & 0 & 0 \\ 0 & 0 & 275.67 & 0 \\ 0 & 0 & 0 & 84.83 \end{bmatrix} \begin{bmatrix} F_{C1} \\ f_{H1} \\ f_{C2} \\ F_{H2} \end{bmatrix} \tag{134}$$

$$\begin{bmatrix} T_{1C1} \\ T_{1H1} \\ T_{2C2} \\ T_{2H2} \end{bmatrix} = \begin{bmatrix} 1 & 0 & 0 & 0 \\ 0 & 0.999 & 0 & 0 \\ 0 & 0 & 0.999 & 0 \\ 0 & 0 & 0 & 1 \end{bmatrix} \begin{bmatrix} T_{1C} \\ T_{1H} \\ T_{2C} \\ T_{2H} \end{bmatrix} + \begin{bmatrix} 0 & 0 & 0 & 0 \\ 0 & 34.1 & 0 & 0 \\ 0 & 0 & -101.1 & 0 \\ 0 & 0 & 0 & 0 \end{bmatrix} \begin{bmatrix} F_{C1} \\ f_{H1} \\ f_{C2} \\ F_{H2} \end{bmatrix} \tag{135}$$

These equations can be transformed into transfer function as Equation (136).

$$G(s)=\begin{bmatrix} \frac{-154.7s-351.2}{s^2+7.58s+9.815} & \frac{-145.7}{s^2+7.58s+9.815} & 0 & 0 \\ \frac{-120.6}{s^2+7.58s+9.815} & \frac{34.1s^2+207.8s+65.38}{s^2+7.58s+9.815} & 0 & 0 \\ 0 & 0 & \frac{-101.1s^2-832.7s-797.2}{s^2+10.96s+15.89} & \frac{449.1}{s^2+10.96s+15.89} \\ 0 & 0 & \frac{399.7}{s^2+10.96s+15.89} & \frac{84.83s+680.3}{s^2+10.96s+15.89} \end{bmatrix} \tag{136}$$

2.2.2 Passivity based pairing of two heat exchangers

This section finds the best controlled-manipulated variable pairing of heat exchangers following the procedure of passivity based pairing proposed by Bao and Lee (2007).

2.2.2.1 Determine the transfer function *G*(s) for each possible pairing scheme

Equations (134) and (135), which are the state space equation of two heat exchangers in the HEN example, have a transfer function of four-by-four matrix which has four possible pairing schemes as classified in Table 9. From Table 9, each possible pairing scheme for this network can be easily understood by the following explanation. For example, the pairing scheme 1 of 1-1/2-2/3-3/4-4 means this network uses that cold flowrate F_{C1} controls the output cold temperature T_{1C1} on a heat exchanger 1; bypass fraction on hot side f_{H1} controls the output hot temperature T_{1H1} on a heat exchanger 1; bypass fraction on cold side f_{C2} controls the output cold temperature T_{2C2}.on a heat exchanger 2; hot flowrate F_{H2} controls the output hot temperature T_{2H2} on a heat exchanger 2, respectively.

Table 9 Possible pairing schemes of two heat exchangers in the heat exchanger network example

Pairing scheme	Pairing	Manipulated Variable (MV)	Controlled Variable (CV)
(1) 1-1/2-2/3-3/4-4	1-1	F_{C1}	T_{1C1}
	2-2	f_{H1}	T_{1H1}
	3-3	f_{C2}	T_{2C2}
	4-4	F_{H2}	T_{2H2}
(2) 1-2/2-1/3-3/4-4	1-2	F_{C1}	T_{1H1}
	2-1	f_{H1}	T_{1C1}
	3-3	f_{C2}	T_{2C2}
	4-4	F_{H2}	T_{2H2}
(3) 1-1/2-2/3-4/4-3	1-1	F_{C1}	T_{1C1}
	2-2	f_{H1}	T_{1H1}
	3-4	f_{C2}	T_{2H2}
	4-3	F_{H2}	T_{2C2}
(4) 1-2/2-1/3-4/4-3	1-2	F_{C1}	T_{1H1}
	2-1	f_{H1}	T_{1C1}
	3-4	f_{C2}	T_{2H2}
	4-3	F_{H2}	T_{2C2}

2.2.2.2 Screen out the non-DIC pairing schemes by using the necessary DIC condition given in Theorem 5.

For the steady state of pairing scheme 1 (1-1/2-2/3-3/4-4), G(0) of this system is shown in Equation (137).

$$G(0) = \begin{bmatrix} -35.78 & -14.84 & 0 & 0 \\ -12.29 & 6.66 & 0 & 0 \\ 0 & 0 & -50.17 & 28.26 \\ 0 & 0 & 25.15 & 42.81 \end{bmatrix} \tag{137}$$

The relative gain array at steady state ($\Lambda(G(0))$) for pairing scheme 1 (1-1/2-2/3-3/4-4) is calculated and shown in Equation (138).

$$\Lambda(G(0)) = \begin{bmatrix} 0.5665 & 0.4335 & 0 & 0 \\ 0.4335 & 0.5665 & 0 & 0 \\ 0 & 0 & 0.7514 & 0.2486 \\ 0 & 0 & 0.2486 & 0.7514 \end{bmatrix} \tag{138}$$

The relative gain array at steady state ($\Lambda(G(0))$) for pairing scheme 2 (1-2/2-1/3-3/4-4) is calculated and shown in Equation (139).

$$\Lambda(G(0)) = \begin{bmatrix} 0.4335 & 0.5665 & 0 & 0 \\ 0.5665 & 0.4335 & 0 & 0 \\ 0 & 0 & 0.7514 & 0.2486 \\ 0 & 0 & 0.2486 & 0.7514 \end{bmatrix} \tag{139}$$

The relative gain array at steady state ($\Lambda(G(0))$) for pairing scheme 3 (1-1/2-2/3-4/4-3) is calculated and shown in Equation (140).

$$\Lambda(G(0)) = \begin{bmatrix} 0.5665 & 0.4335 & 0 & 0 \\ 0.4335 & 0.5665 & 0 & 0 \\ 0 & 0 & 0.2486 & 0.7514 \\ 0 & 0 & 0.7514 & 0.2486 \end{bmatrix} \tag{140}$$

The relative gain array at steady state ($\Lambda(G(0))$) for pairing scheme 4 (1-2/2-1/3-4/4-3) is calculated and shown in Equation (141).

$$\Lambda(G(0)) = \begin{bmatrix} 0.4335 & 0.5665 & 0 & 0 \\ 0.5665 & 0.4335 & 0 & 0 \\ 0 & 0 & 0.2486 & 0.7514 \\ 0 & 0 & 0.7514 & 0.2486 \end{bmatrix} \tag{141}$$

Relative gain arrays at steady state along the diagonal of all pairing schemes are much more than zero, thus, these pairing schemes are DIC.

2.2.2.3 Find the sign matrix U and obtain G^{+}(s) such that $G_{ii}^{+}\left(0\right)>0\ (i=1,...,m)$

From subsection 2.2.2.2, the possible pairing schemes still remain four pairing types. This section determines matrix U defined in the following equation.

$$U = diag\{U_{ii}\}, \quad i=1,...,m \tag{142}$$

where U is a diagonal matrix with either 1 or -1 along the diagonal.

Therefore, U for pairing scheme 1 of 1-1/2-2/3-3/4-4 is in Equation (143) in order that $G_{ii}^{+}\left(0\right)>0\ (i=1,...,m)$ where $G^{+}\left(s\right)=G(s)U$.

$$U=\begin{bmatrix} -1 & 0 & 0 & 0 \\ 0 & 1 & 0 & 0 \\ 0 & 0 & -1 & 0 \\ 0 & 0 & 0 & 1 \end{bmatrix} \tag{143}$$

U for pairing scheme 2 of 1-2/2-1/3-3/4-4 is presented in Equation (144).

$$U=\begin{bmatrix} -1 & 0 & 0 & 0 \\ 0 & -1 & 0 & 0 \\ 0 & 0 & -1 & 0 \\ 0 & 0 & 0 & 1 \end{bmatrix} \tag{144}$$

U for pairing scheme 3 of 1-1/2-2/3-4/4-3 is presented in Equation (145).

$$U=\begin{bmatrix} -1 & 0 & 0 & 0 \\ 0 & 1 & 0 & 0 \\ 0 & 0 & 1 & 0 \\ 0 & 0 & 0 & 1 \end{bmatrix} \tag{145}$$

U for pairing scheme 4 of 1-2/2-1/3-4/4-3 is presented in Equation (146).

$$U = \begin{bmatrix} -1 & 0 & 0 & 0 \\ 0 & -1 & 0 & 0 \\ 0 & 0 & 1 & 0 \\ 0 & 0 & 0 & 1 \end{bmatrix} \tag{146}$$

2.2.2.4 Calculate the diagonally scaled passivity index $\nu_s(G^+(s),\omega)$ at a number of frequency points.

In this step, the diagonally scaled passivity index of each pairing scheme is determined from Equation (87). The passivity index of these four pairing schemes of this system is depicted in Figures 37 to 40, respectively.

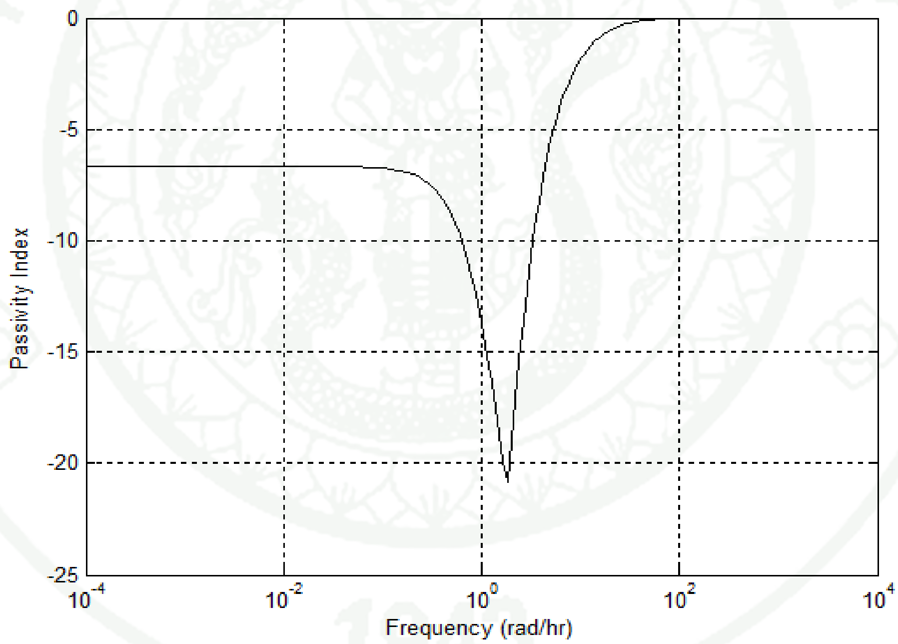

Figure 37 Passivity index of pairing scheme 1 (1-1/2-2/3-3/4-4) of heat exchangers

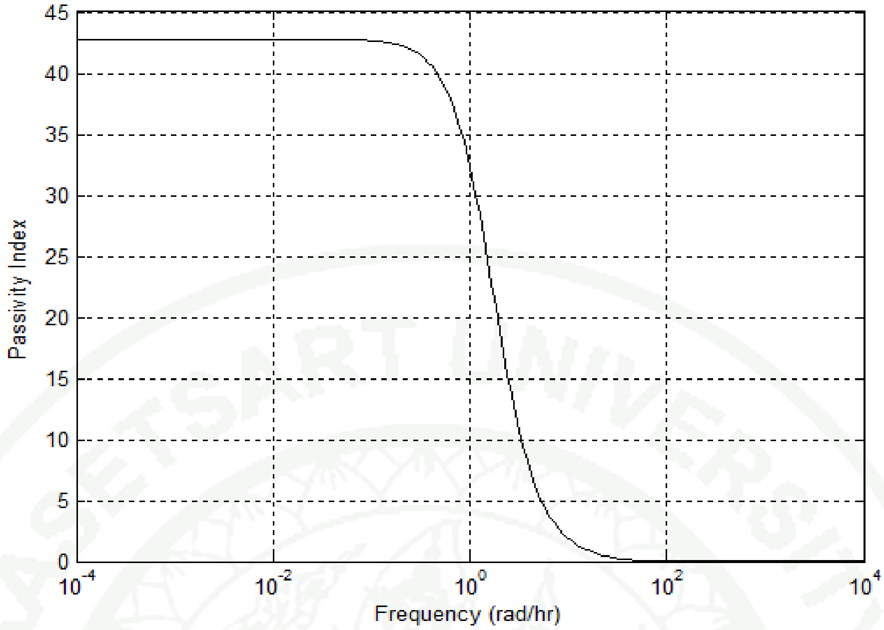

Figure 38 Passivity index of pairing scheme 2 (1-2/2-1/3-3/4-4) of heat exchangers

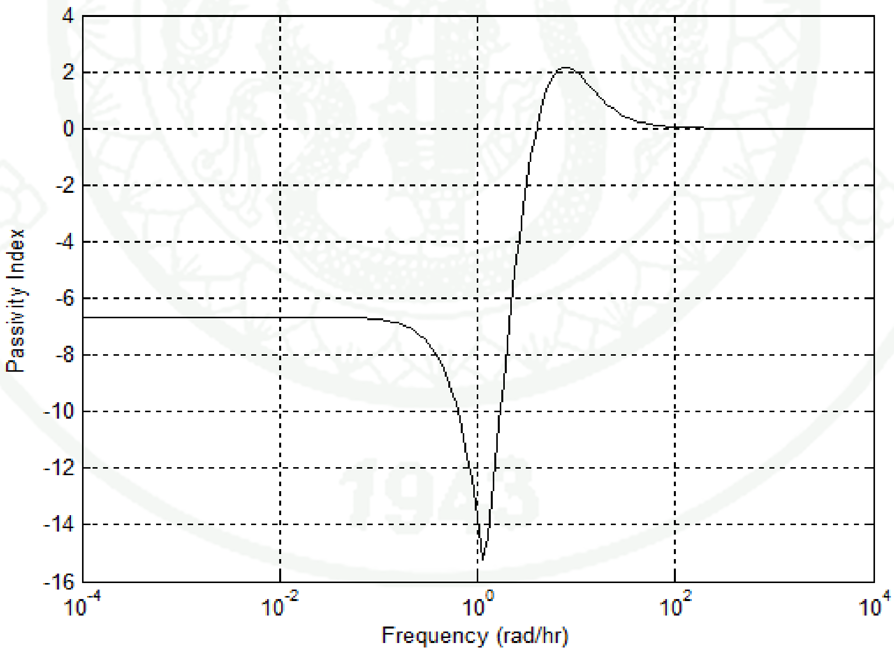

Figure 39 Passivity index of pairing scheme 3 (1-1/2-2/3-4/4-3) of heat exchangers

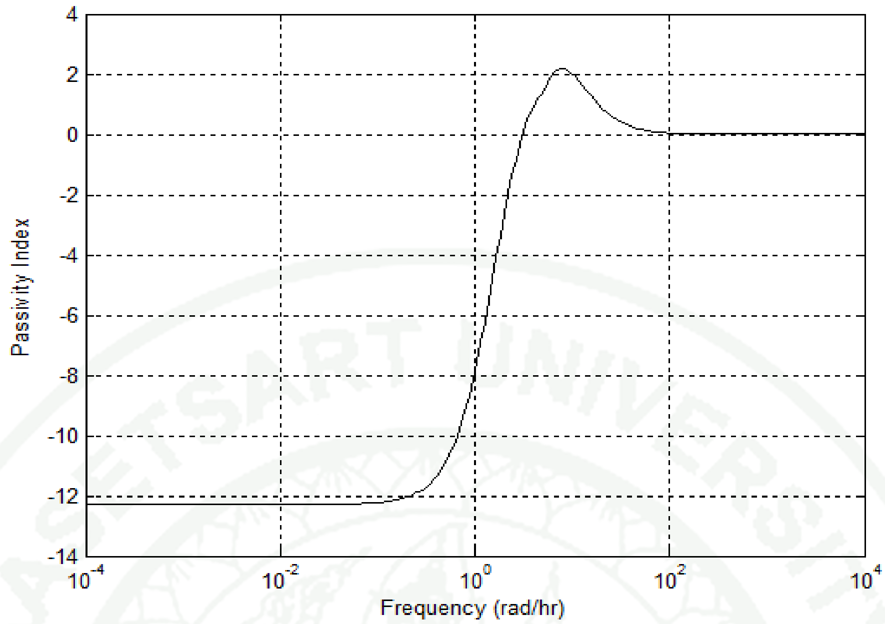

Figure 40 Passivity index of pairing scheme 4 (1-2/2-1/3-4/4-3) of heat exchangers

2.2.2.5 Compare the passivity index profiles of different pairings. The best pairing should correspond to the one with the largest frequency bandwidth ω_b such that $\nu_s\left(G^+(s),\omega\right) \le 0$ for any $\omega \in [0,\omega_b]$. This pairing scheme would allow using controllers with integral action and the fastest dynamic response.

In this step, only one pairing scheme is chosen after finding the passivity index of each pairing scheme. Compared the passivity index of four pairings illustrating in Figure 41, the pairing scheme 1 is the more passive than other pairing schemes since this one has the frequency bandwidth which passivity index is less than zero than the others. Hence, the pairing scheme 1 of 1-1/2-2/3-3/4-4, in which cold flowrate F_{C1} controls the output cold temperature T_{1C1} on a heat exchanger 1; bypass fraction on hot side f_{H1} controls the output hot temperature T_{1H1} on a heat exchanger 1; bypass fraction on cold side f_{C2} controls the output cold temperature T_{2C2} .on a heat exchanger 2; hot flowrate F_{H2} controls the output hot temperature T_{2H2} on a heat exchanger 2, respectively, is the best pairing scheme for these two heat exchangers in the HEN.

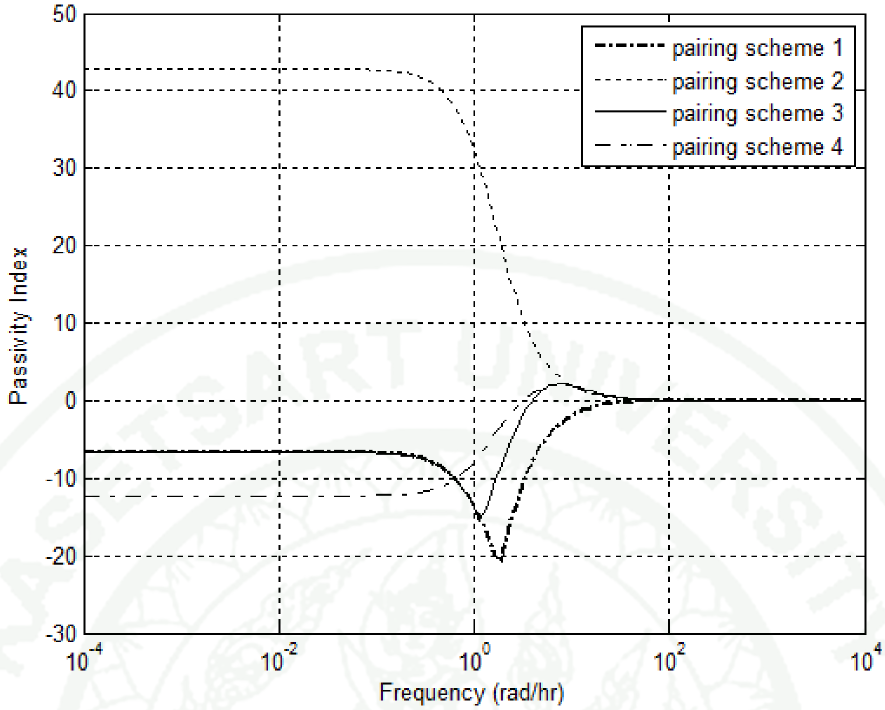

Figure 41 Passivity indices of four pairing schemes of two heat exchangers

Although the two heat exchangers in HEN have already shown the non-passivity behavior, the result from the passivity based pairing step shows that the best pairing is 1-1/2-2/3-3/4-4 pairing which is passive along the frequency range. Therefore, from Figure 17, the DUS PI controllers can be designed directly without concerning the weighting function.

2.2.3 Multi-loop PI controller design

This section shows the procedure to design multi-loop PI controller following the work of Bao *et al*. (2002a).

2.2.3.1. Determine the pairing scheme for controlled and manipulated variables according to the procedure to find the best pairing of the system.

For this step, the best pairing scheme is chosen from section 2.2.2. That pairing scheme is 1-1/2-2/3-3/4-4, in which cold flowrate F_{C1} controls the output cold temperature T_{1C1} on a heat exchanger 1; bypass fraction on hot side f_{H1} controls the output hot temperature T_{1H1} on a heat exchanger 1; bypass fraction on cold side f_{C2} controls the output cold temperature T_{2C2}.on a heat exchanger 2; hot flowrate F_{H2} controls the output hot temperature T_{2H2} on a heat exchanger 2, respectively.

2.2.3.2. For each subsystem $G_{ii}^{+}(s)$ (i = 1,…,m), solve Problem 4 for the PI controller parameters $k_{c,i}^{+}$ and $\tau_{I,i}$

This step has to find PI tuning parameters for each loop of two heat exchangers in a HEN by solving Problem 4. When this problem is solved, PI tuning parameters are presented in Table 10.

Table 10 PI tuning parameters for two heat exchangers of a HEN

PI Tuning Parameter	Loop 1[a]	Loop 2[b]	Loop 3[c]	Loop 4[d]
k_c^{+}	606.38	38.45	35.43	270.62
τ_I	10.83	15	15	14.3

Remark: [a]: 1-1 pairing/ [b]: 2-2 pairing/ [c]: 3-3 pairing/ [d]: 4-4 pairing

2.2.3.3. Adjust the sign of the final subcontroller gain $k_{c,i} = k_{c,i}^{+}U_{ii}$ to obtain the final multi-loop controller as Equation (147).

$$K(s) = diag\{k_i(s)\} = diag\left\{k_{c,i}(1+\frac{1}{\tau_{I,i}s})\right\} \tag{147}$$

When PI tuning parameters for each loop have already been determined, the final multi-loop controller as the same form in Equation (147) is shown in the following equation.

$$K(s)=\begin{bmatrix} -606.38(1+\frac{1}{10.83s}) & 0 & 0 & 0 \\ 0 & 38.45(1+\frac{1}{15s}) & 0 & 0 \\ 0 & 0 & -35.43(1+\frac{1}{15s}) & 0 \\ 0 & 0 & 0 & 270.62(1+\frac{1}{14.3s}) \end{bmatrix} \tag{148}$$

2.3 Two utilities of a heat exchanger network

2.3.1 Utility models

The state space for these two utilities which are assumed to be a heat exchanger units are shown in Equations (149) and (150).

$$\dot{x}=\begin{bmatrix} A_{33} & 0 \\ 0 & A_{44} \end{bmatrix}x+\begin{bmatrix} B_{33} & 0 \\ 0 & B_{44} \end{bmatrix}u \tag{149}$$

$$y=\begin{bmatrix} C_{33} & 0 \\ 0 & C_{44} \end{bmatrix}x+\begin{bmatrix} D_{33} & 0 \\ 0 & D_{44} \end{bmatrix}u \tag{150}$$

where $x=\left[T_{3C}\ T_{3H}\ T_{4C}\ T_{4H}\right]^T$, $u=\left[F_{3C}\ F_{3H}\ F_{4C}\ F_{4H}\right]^T$ $y=\left[T_{3C3}\ T_{3H3}\ T_{4C4}\ T_{4H4}\right]^T$ and partitioned matrices

$$A_{33} \text{ represents } \begin{bmatrix} \frac{-U_3A_3-\tau_{C3}\bar{F}_{C3}}{\xi_{C3}} & \frac{U_3A_3}{\xi_{C3}} \\ \frac{U_3A_3}{\xi_{H3}} & \frac{-U_3A_3-\tau_{H3}\bar{F}_{H3}}{\xi_{H3}} \end{bmatrix} \tag{151}$$

$$A_{44} \text{ represents } \begin{bmatrix} \dfrac{-U_4A_4-\tau_{C4}\overline{F}_{C4}}{\xi_{C4}} & \dfrac{U_4A_4}{\xi_{C4}} \\ \dfrac{U_4A_4}{\xi_{H4}} & \dfrac{-U_4A_4-\tau_{H4}\overline{F}_{H4}}{\xi_{H4}} \end{bmatrix} \tag{152}$$

$$B_{33} \text{ represents } \begin{bmatrix} \dfrac{\tau_{C3}T_{Cin3}-\tau_{C3}\overline{T}_{1C3}}{\xi_{C3}} & 0 \\ 0 & \dfrac{\tau_{H3}T_{Hin3}-\tau_{H3}\overline{T}_{1H3}}{\xi_{H3}} \end{bmatrix} \tag{153}$$

$$B_{44} \text{ represents } \begin{bmatrix} \dfrac{\tau_{C4}T_{Cin4}-\tau_{C4}\overline{T}_{1C4}}{\xi_{C4}} & 0 \\ 0 & \dfrac{\tau_{H4}T_{Hin4}-\tau_{H4}\overline{T}_{1H4}}{\xi_{H4}} \end{bmatrix} \tag{154}$$

$$C_{33} \text{ represents } \begin{bmatrix} 1 & 0 \\ 0 & 1 \end{bmatrix} \tag{155}$$

$$C_{44} \text{ represents } \begin{bmatrix} 1 & 0 \\ 0 & 1 \end{bmatrix} \tag{156}$$

$$D_{33} \text{ represents } \begin{bmatrix} 0 & 0 \\ 0 & 0 \end{bmatrix} \tag{157}$$

$$D_{44} \text{ represents } \begin{bmatrix} 0 & 0 \\ 0 & 0 \end{bmatrix} \tag{158}$$

When all numerical values in Table 8 are substituted in Equations (149) and (150), these equations become as follows.

$$\begin{bmatrix} \dot{T}_{3C} \\ \dot{T}_{3H} \\ \dot{T}_{4C} \\ \dot{T}_{4H} \end{bmatrix} = \begin{bmatrix} -50.14 & 8.93 & 0 & 0 \\ 2.44 & -3.93 & 0 & 0 \\ 0 & 0 & -11.46 & 3.29 \\ 0 & 0 & 0.90 & -11.29 \end{bmatrix} \begin{bmatrix} T_{3C} \\ T_{3H} \\ T_{4C} \\ T_{4H} \end{bmatrix} + \begin{bmatrix} -64.68 & 0 & 0 & 0 \\ 0 & 133.14 & 0 & 0 \\ 0 & 0 & -352.57 & 0 \\ 0 & 0 & 0 & 33.93 \end{bmatrix} \begin{bmatrix} F_{C3} \\ F_{H3} \\ F_{C4} \\ F_{H4} \end{bmatrix} \tag{159}$$

$$\begin{bmatrix} T_{3C3} \\ T_{3H3} \\ T_{4C4} \\ T_{4H4} \end{bmatrix} = \begin{bmatrix} 1 & 0 & 0 & 0 \\ 0 & 1 & 0 & 0 \\ 0 & 0 & 1 & 0 \\ 0 & 0 & 0 & 1 \end{bmatrix} \begin{bmatrix} T_{3C} \\ T_{3H} \\ T_{4C} \\ T_{4H} \end{bmatrix} + \begin{bmatrix} 0 & 0 & 0 & 0 \\ 0 & 0 & 0 & 0 \\ 0 & 0 & 0 & 0 \\ 0 & 0 & 0 & 0 \end{bmatrix} \begin{bmatrix} F_{C3} \\ F_{H3} \\ F_{C4} \\ F_{H4} \end{bmatrix} \tag{160}$$

These equations can be transformed into transfer function as Equation (161).

$$G(s) = \begin{bmatrix} \dfrac{-64.68s-254.2}{s^2+54.07s+175.3} & \dfrac{1189}{s^2+54.07s+175.3} & 0 & 0 \\ \dfrac{-57.8}{s^2+54.07s+175.3} & \dfrac{133.1s+6676}{s^2+54.07s+175.3} & 0 & 0 \\ 0 & 0 & \dfrac{-352.6s-3981}{s^2+22.75s+126.4} & \dfrac{111.6}{s^2+22.75s+126.4} \\ 0 & 0 & \dfrac{-317.3}{s^2+22.75s+126.4} & \dfrac{33.93s+388.8}{s^2+22.75s+126.4} \end{bmatrix} \tag{161}$$

2.3.2 Passivity based pairing of two utilities

This section finds the best controlled-manipulated variable pairing of utility units following the procedure of passivity based pairing proposed by Bao and Lee (2007).

2.3.2.1 Determine the transfer function G(s) for each possible pairing scheme

Equations (159) and (160), which are the state space equation of two utility units in the HEN example, have a transfer function of four-by-four matrix which has four pairing schemes as categorized in Table 11.

From Table 11, each possible pairing scheme for this network can be easily comprehended by the following description. For example, the pairing scheme 1 of 1-1/2-2/3-3/4-4 means this network uses that cold flowrate F_{C3} controls the output cold temperature T_{3C3} on a cold utility unit; hot flowrate F_{H3} controls the output hot temperature T_{3H3} on a cold utility unit; cold flowrate F_{C4} controls the output cold temperature T_{4C4} on a hot utility unit; hot flowrate F_{H4} controls the output hot temperature T_{4H4} on a hot utility unit, respectively. Although there are four pairing schemes for these two utility models, there is only one possible pairing scheme in this system since the main goal of using utility in a heat exchanger system is to take the stream which does not reach the target temperature to that target. For example, if a hot stream temperature does not reach the target temperature after exchanging heat from a heat exchanger unit, a cold utility will be available to take that stream temperature to its target by manipulating cold utility flowrate. Therefore, the pairing scheme 4 of 1-2/2-1/3-4/4-3 is the only one possible pairing scheme for this utilities system.

Table 11 Pairing schemes of two utility units in the heat exchanger network example

Pairing scheme	Pairing	Manipulated Variable (MV)	Controlled Variable (CV)
(1) 1-1/2-2/3-3/4-4	1-1	F_{C3}	T_{3C3}
	2-2	F_{H3}	T_{3H3}
	3-3	F_{C4}	T_{4C4}
	4-4	F_{H4}	T_{4H4}
(2) 1-2/2-1/3-3/4-4	1-2	F_{C3}	T_{3H3}
	2-1	F_{H3}	T_{3C3}
	3-3	F_{C4}	T_{4C4}
	4-4	F_{H4}	T_{4H4}
(3) 1-1/2-2/3-4/4-3	1-1	F_{C3}	T_{3C3}
	2-2	F_{H3}	T_{3H3}
	3-4	F_{C4}	T_{4H4}
	4-3	F_{H4}	T_{4C4}
(4) 1-2/2-1/3-4/4-3	1-2	F_{C3}	T_{3H3}
	2-1	F_{H3}	T_{3C3}
	3-4	F_{C4}	T_{4H4}
	4-3	F_{H4}	T_{4C4}

2.3.2.2 Screen out the non-DIC pairing schemes by using the necessary DIC condition given in Theorem 5.

For the steady state of pairing scheme 4 (1-2/2-1/3-4/4-3), G(0) of this system is shown in Equation (162).

$$G(0) = \begin{bmatrix} -1.45 & 6.78 & 0 & 0 \\ -0.33 & 38.08 & 0 & 0 \\ 0 & 0 & -31.495 & 0.88 \\ 0 & 0 & -2.51 & 3.08 \end{bmatrix} \tag{162}$$

The relative gain array at steady state ($\Lambda(G(0))$) for pairing scheme 4 (1-2/2-1/3-4/4-3) is calculated and shown in Equation (163).

$$\Lambda(G(0)) = \begin{bmatrix} 1.0422 & -0.0422 & 0 & 0 \\ -0.0422 & 1.0422 & 0 & 0 \\ 0 & 0 & 1.0233 & -0.0233 \\ 0 & 0 & -0.0233 & 1.0233 \end{bmatrix} \tag{163}$$

The relative gain array at steady state of pairing scheme 4 is much more than zero which satisfy the theorem 5, thus, this pairing scheme are DIC.

2.3.2.3 Find the sign matrix U and obtain G^{+}(s) such that $G_{ii}^{+}\left(0\right) > 0 \;\; (i = 1, \ldots, m)$

From previous subsection, the possible pairing scheme remains only one pairing type. This section determines matrix U defined in the following equation.

$$U = diag\{U_{ii}\}, \quad i = 1, \ldots, m \tag{164}$$

where U is a diagonal matrix with either 1 or -1 along the diagonal.

Therefore, U for pairing scheme 4 of 1-2/2-1/3-4/4-3 is in Equation (165) in order that $G_{ii}^{+}\left(0\right)>0$ $(i=1,...,m)$ where $G^{+}\left(s\right)=G(s)U$.

$$U=\begin{bmatrix} -1 & 0 & 0 & 0 \\ 0 & 1 & 0 & 0 \\ 0 & 0 & -1 & 0 \\ 0 & 0 & 0 & 1 \end{bmatrix} \tag{165}$$

2.3.3 Multi-loop PI controller design

Since utilities are heat exchanger units which have already passive, it is not necessary to determine the weighting function. This reason comes from the procedure as shown in passivity based decentralized controller synthesis procedure (Figure 17). Therefore, this section shows the procedure to design multi-loop PI controller following the work of Bao *et al*. (2002a).

2.3.3.1. Determine the pairing scheme for controlled and manipulated variables according to the procedure to find the best pairing of the system.

For this step, the best pairing scheme is chosen from section 2.3.2. That pairing scheme is 1-2/2-1/3-4/4-3, in which cold flowrate F_{C3} controls the output hot temperature T_{3H3} on a cold utility unit; hot flowrate F_{H3} controls the output cold temperature T_{3C3} on a cold utility unit; cold flowrate F_{C4} controls the output hot temperature T_{4H4} on a hot utility unit; hot flowrate F_{H4} controls the output cold temperature T_{4C4} on a hot utility unit, respectively.

2.3.3.2. For each subsystem $G_{ii}^{+}(s)$ (i = 1,…,m), solve Problem 4 for the PI controller parameters $k_{c,i}^{+}$ and $\tau_{I,i}$

This step has to find PI tuning parameters for each loop of utilities in a HEN by solving Problem 4. When this problem is solved, PI tuning parameters are presented in Table 12.

.

Table 12 PI tuning parameters for two utility units of a HEN

PI Tuning Parameter	Loop 1[a]	Loop 2[b]	Loop 3[c]	Loop 4[d]
k_c^+	172.53	348.87	54.48	330.19
τ_I	20.95	12.47	13.13	17.36

Remark: [a]: 1-2 pairing/ [b]: 2-1 pairing/ [c]: 3-4 pairing/ [d]: 4-3 pairing

2.3.3.3. Adjust the sign of the final subcontroller gain $k_{c,i} = k_{c,i}^+ U_{ii}$ to obtain the final multi-loop controller as Equation (166).

$$K(s) = diag\{k_i(s)\} = diag\left\{k_{c,i}(1+\frac{1}{\tau_{I,i}s})\right\} \tag{166}$$

When PI tuning parameters for each loop have already been determined, the final multi-loop controller for utility units as the same form in Equation (166) is shown in the following equation.

$$K(s) = \begin{bmatrix} -172.53(1+\frac{1}{20.95s}) & 0 & 0 & 0 \\ 0 & 348.87(1+\frac{1}{12.47s}) & 0 & 0 \\ 0 & 0 & -54.48(1+\frac{1}{13.13s}) & 0 \\ 0 & 0 & 0 & 330.19(1+\frac{1}{17.36s}) \end{bmatrix} \tag{167}$$

2.4 Verification of results

When passivity based PI tuning parameters have already been designed, these values are used to verify the results with the HEN example as shown in Figure 36. The HEN accompanied with controllers is presented as follows.

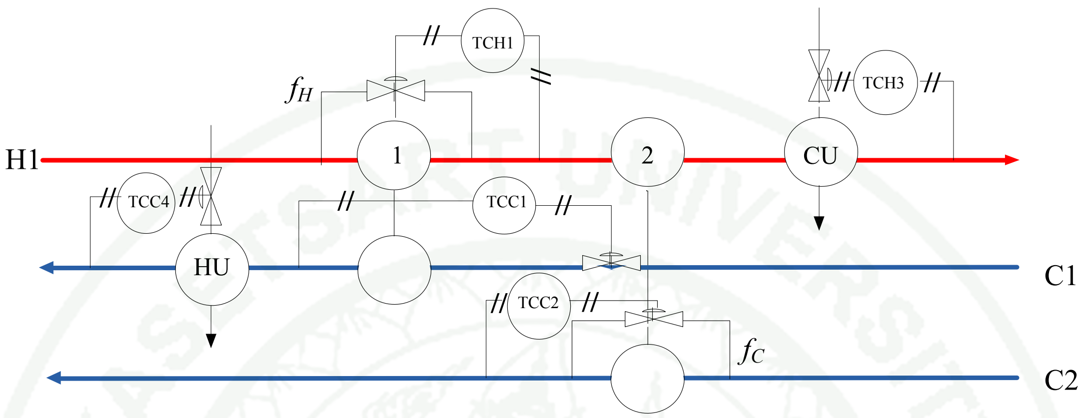

Figure 42 A heat exchanger network accompanied with controllers

This HEN system with control loops is tested with two main controller classes; controllers with default PI tuning parameters from Aspen Dynamics and controllers with passivity based PI tuning parameters from passivity concept. This system with both controller types is tested with disturbance of -1% and +1% inlet hot flowrates. Figures 43 and 44 show responses of each controller with default PI tuning parameters when the HEN with control loops is disturbed by changing inlet hot flowrate. Likewise, Figures 45 and 46 show responses of each controller with passivity based PI tuning parameters when the HEN with control loops is disturbed by changing inlet hot flowrate.

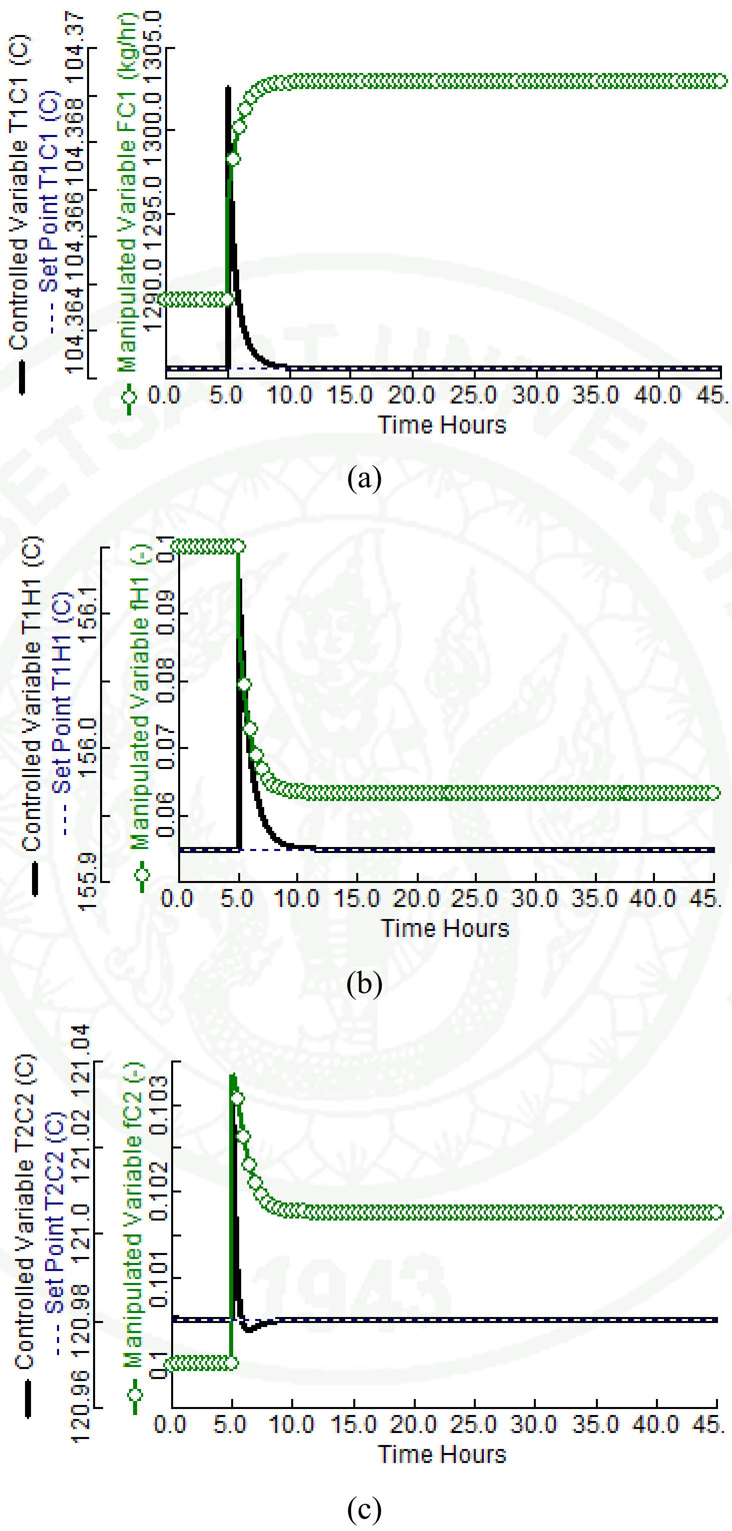

Figure 43 Responses of controllers TCC1 (a), TCH1 (b), TCC2 (c), TCH3 (d) and TCC4 (e) from +1% inlet flowrate disturbance of hot stream at hour 5

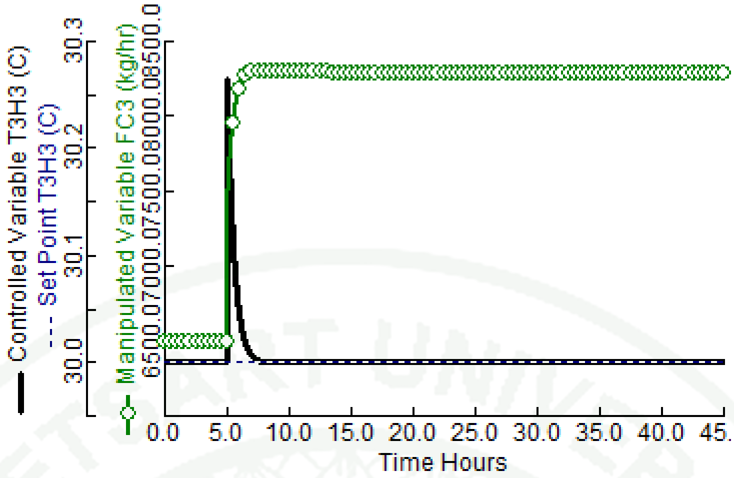

(d)

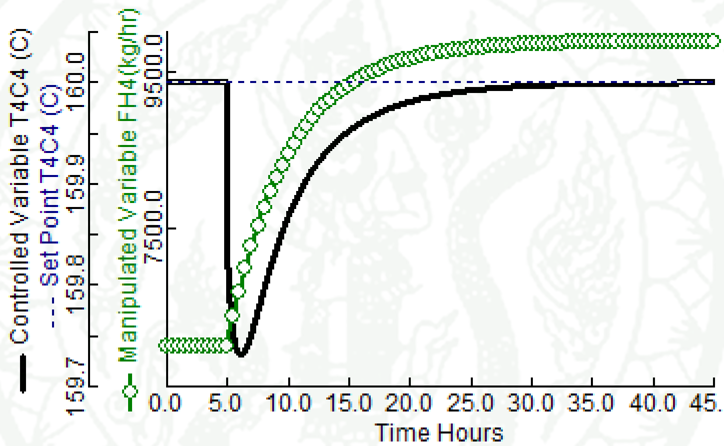

(e)

Figure 43 (Continued)

Figure 43 shows responses of each controller with default PI tuning parameters when the inlet hot flowrate changed from 860 to 868.6 kg/hr (+1% inlet hot flowrate). When inlet hot flowrate is changed, each controller try to adjust their manipulated variables in order to maintain their original setpoint temperatures. Each controller from this figure takes the times to get their setpoint temperatures 5, 5, 5, 5 and 35 hours, respectively.

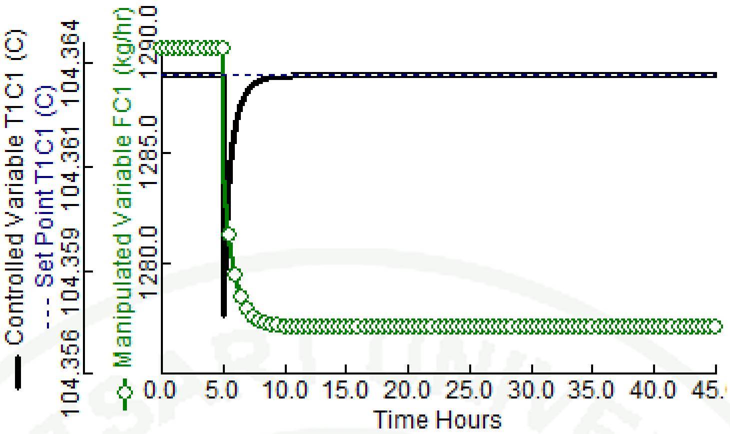

(a)

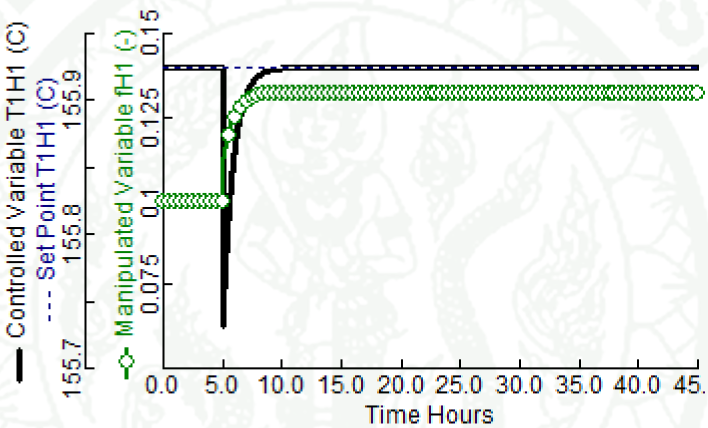

(b)

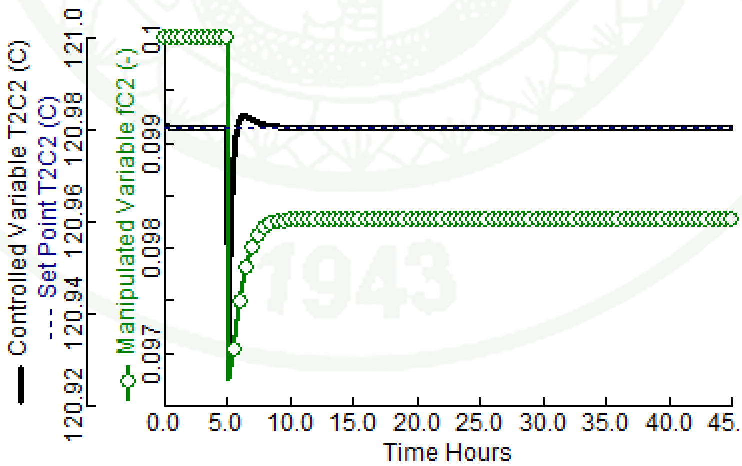

(c)

Figure 44 Responses of controllers TCC1 (a), TCH1 (b), TCC2 (c), TCH3 (d) and TCC4 (e) from -1% inlet flowrate disturbance of hot stream at hour 5

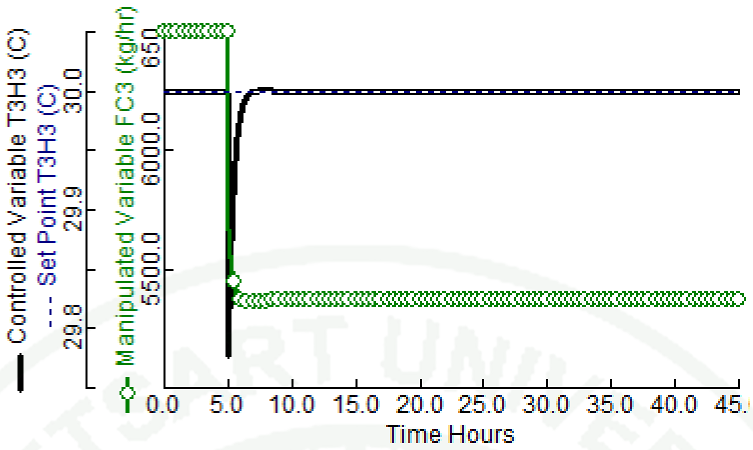

(d)

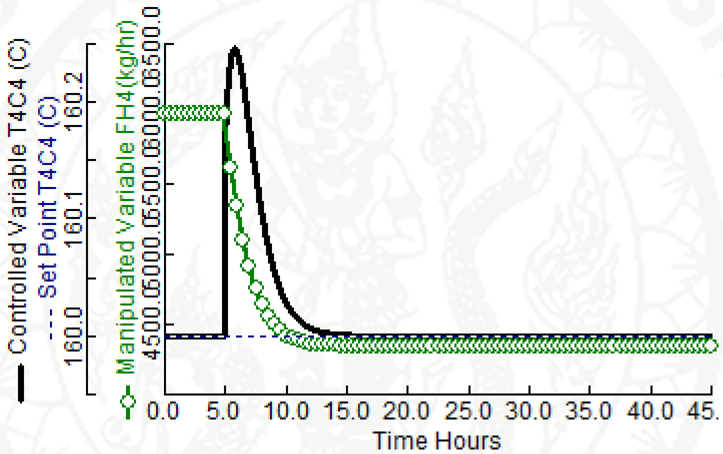

(e)

Figure 44 (Continued)

Figure 44 shows responses of each controller with default PI tuning parameters when the inlet hot flowrate changed from 860 to 851.4 kg/hr (-1% inlet hot flowrate). When inlet hot flowrate is changed, each controller try to adjust their manipulated variables in order to maintain their original setpoint temperatures. Each controller from this figure takes the times to get its setpoint temperature 5, 5, 5, 5 and 15 hours, respectively.

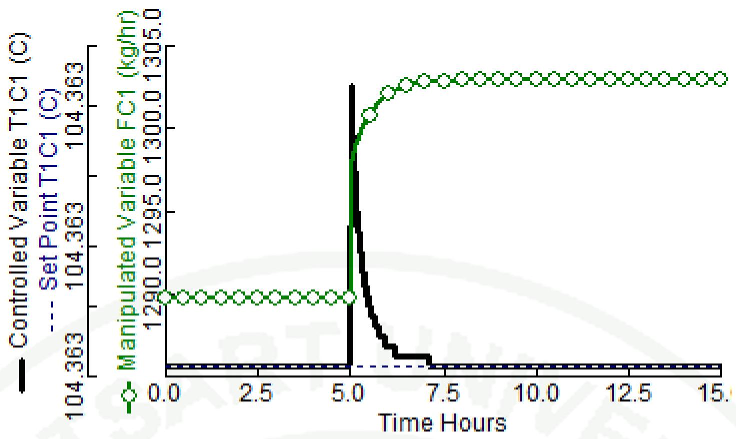

(a)

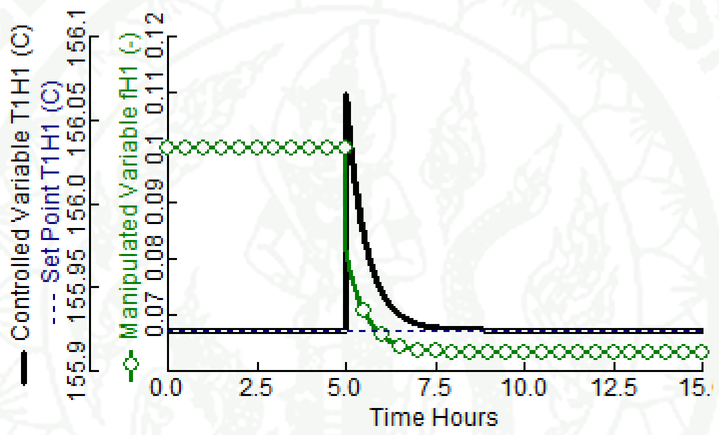

(b)

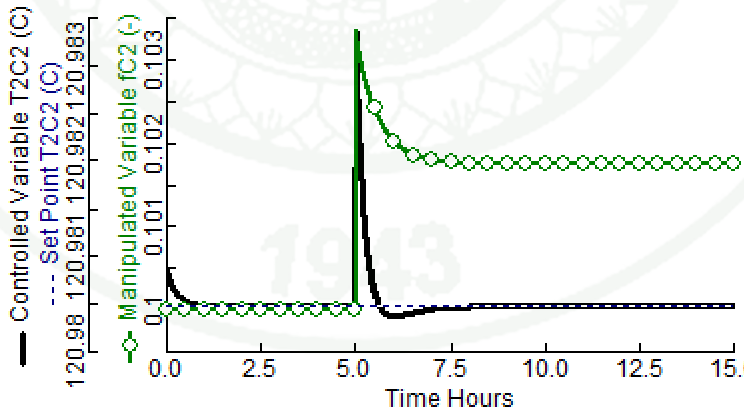

(c)

Figure 45 Responses from passivity based PI tuning of controllers TCC1 (a), TCH1 (b), TCC2 (c), TCH3 (d) and TCC4 (e) from +1% inlet hot flowrate disturbance at hour 5

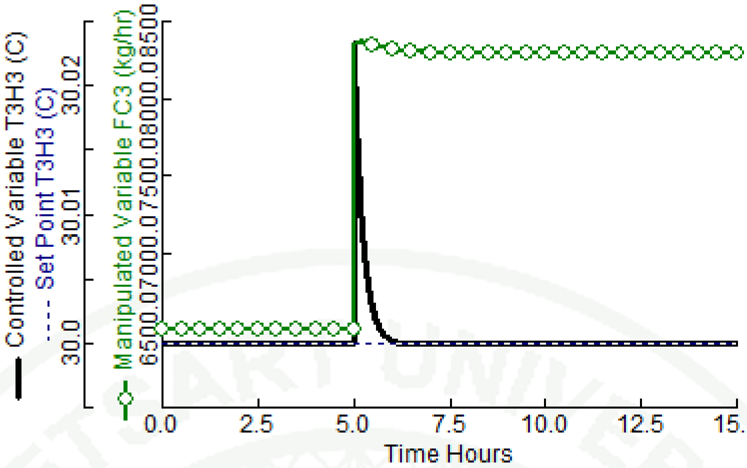

(d)

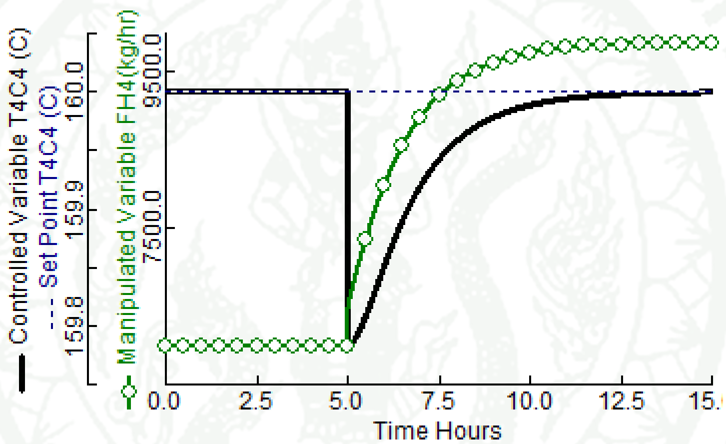

(e)

Figure 45 (Continued)

Figure 45 shows responses of each controller with passivity based PI tuning parameters when the inlet hot flowrate changed from 860 to 868.6 kg/hr (+1% inlet hot flowrate). When inlet hot flowrate is changed, each controller try to adjust their manipulated variables in order to maintain their original setpoint temperatures. Each controller from this figure takes the times to get their setpoint temperature 2.5, 2.5, 2.5, 1 and 7.5 hours, respectively. Compared Figures 43 and 45, the times to reach the new setpoint of the system with passivity based PI controllers are less than that with default PI controllers.

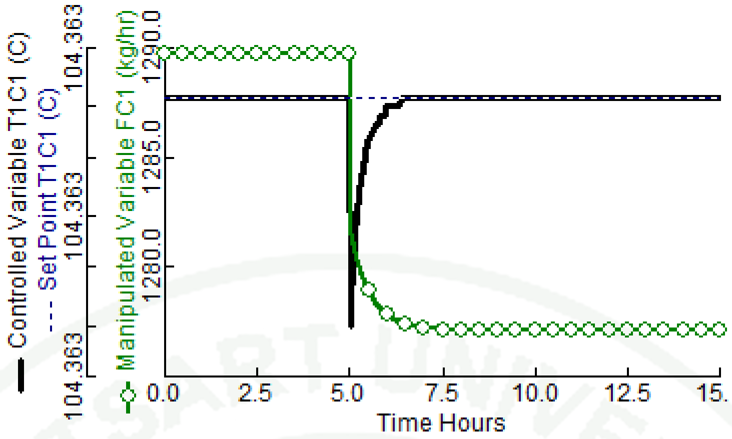

(a)

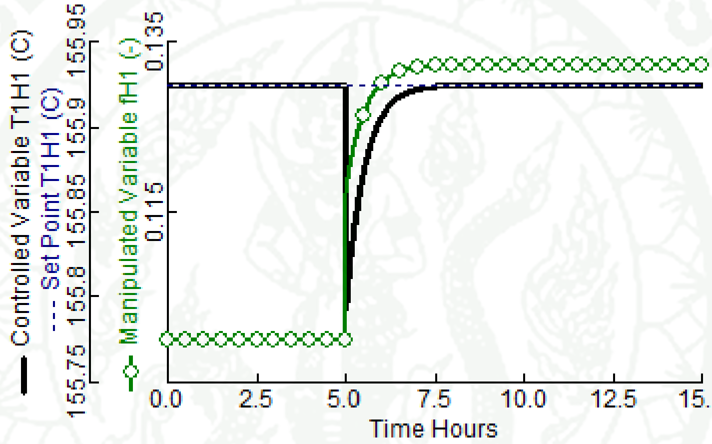

(b)

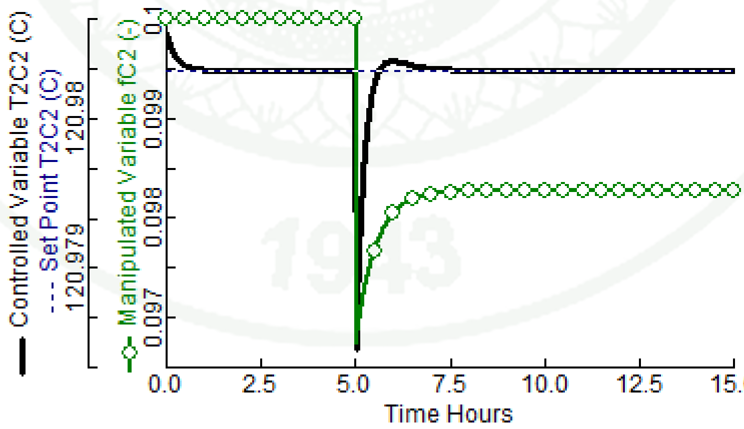

(c)

Figure 46 Responses from passivity based PI tuning of controllers TCC1 (a), TCH1 (b), TCC2 (c), TCH3 (d) and TCC4 (e) from -1% inlet hot flowrate disturbance at hour 5

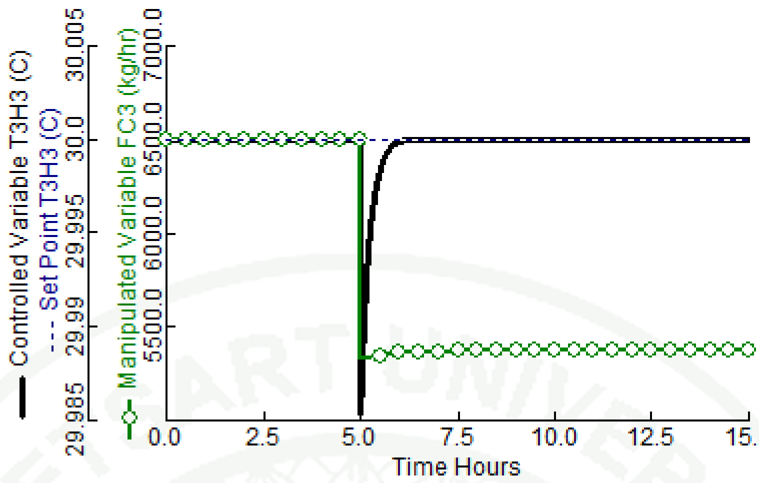

(d)

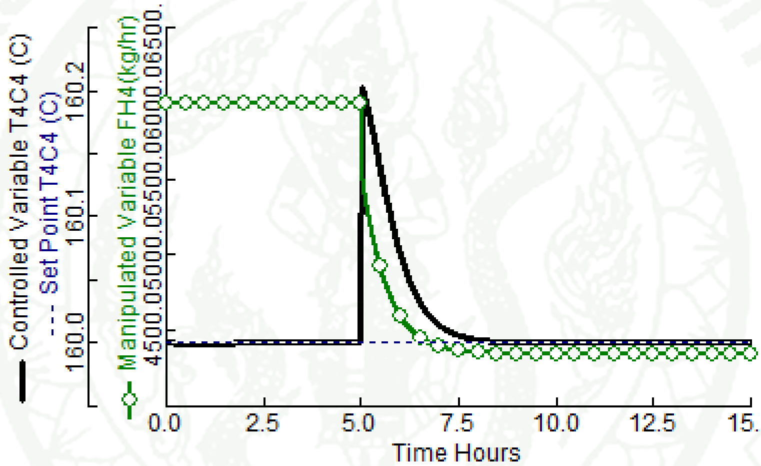

(e)

Figure 46 (Continued)

Figure 46 shows responses of each controller with passivity based PI tuning parameters when the inlet hot flowrate changed from 860 to 851.4 kg/hr (-1% inlet hot flowrate). When inlet hot flowrate is changed, each controller try to adjust their manipulated variables in order to maintain their original setpoint temperatures. Each controller from this figure takes the times to get their setpoint temperatures 2, 2, 2, 1 and 2 hours, respectively. Compared Figures 44 and 46, the times to reach the new setpoint of the system with passivity based PI controllers are less than that with default PI controllers.

After verifying the results, the HEN is tested fault-tolerant control in order to ensure that when the system and controllers are passive, they can achieve decentralized unconditional stability (DUS). These results are compared with those from the system with default PI controllers from Aspen Dynamics. This HEN system is disturbed with -1% and +1% of inlet hot flowrates when which one of controllers fails. The following figure displays a HEN with controlled variables provided that it is easily to track the responses of each controller when getting disturbances.

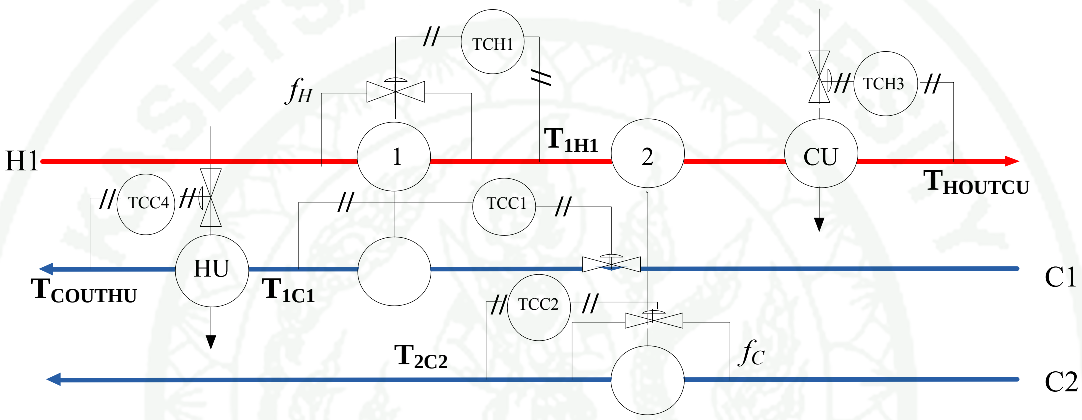

Figure 47 A heat exchanger network with controlled variables accompanied with Controllers

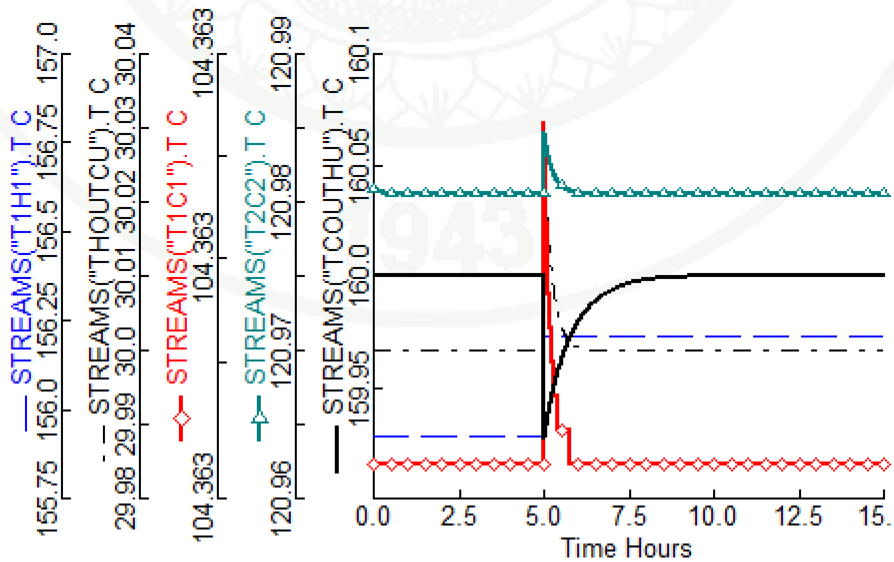

Figure 48 Temperature responses of controlled variables disturbed by +1% inlet flowrate of hot stream with failing passivity based PI controller TCH1

Figure 48 shows temperature responses of each controlled variable disturbed by +1% inlet flowrate of hot stream with failing controller TCH1. The result reports that when controller TCH1 fails, the temperature of T1H1 increases and affects the higher temperature of streams T1C1, T2C2 and THOUTCU. However, controllers TCC1, TCC2 and TCH3 adjust their manipulated variables in order to control their stream temperatures to their setpoints. Moreover, the elevated hot flowrate takes a small effect to stream TCOUTHU decreased, but it can be reached its setpoint by controller TCC4.

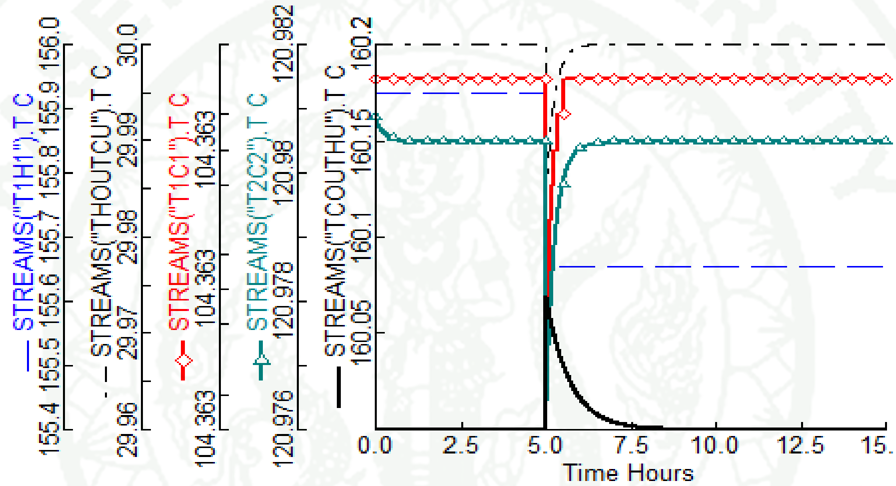

Figure 49 Temperature responses of controlled variables disturbed by -1% inlet flowrate of hot stream with failing passivity based PI controller TCH1

Figure 49 shows temperature responses of each controlled variable disturbed by -1% inlet flowrate of hot stream with failing controller TCH1. The result reports that when controller TCH1 fails, the temperature of T1H1 decreases and affects the lower temperature of streams T1C1, T2C2 and THOUTCU. However, controllers TCC1, TCC2 and TCH3 adjust their manipulated variables in order to control their stream temperatures to their setpoints. Moreover, the decreased hot flowrate takes a small effect to stream TCOUTHU increased, but it can be reached its setpoint by controller TCC4.

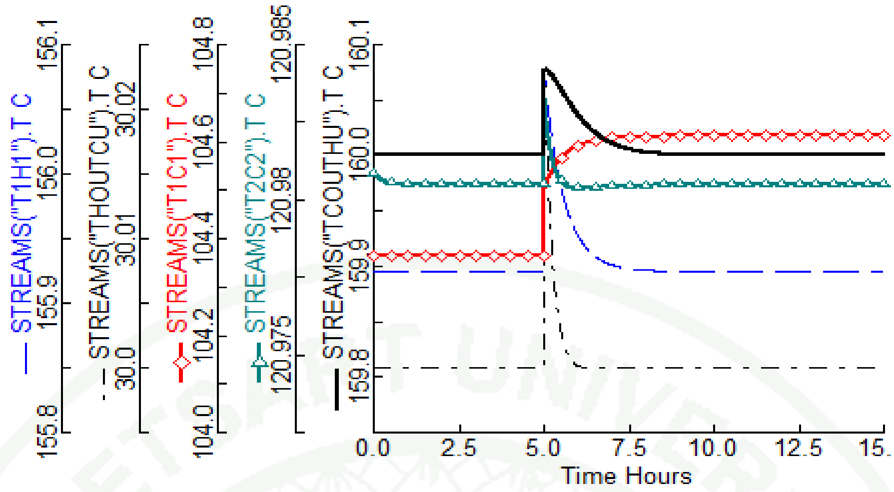

Figure 50 Temperature responses of controlled variables disturbed by +1% inlet flowrate of hot stream with failing passivity based PI controller TCC1

Figure 50 shows temperature responses of each controlled variable disturbed by +1% inlet flowrate of hot stream with failing controller TCC1. The result reports that when controller TCC1 fails, the temperature of T1C1 increases and affects the higher temperature of streams T1H1, T2C2, THOUTCU and TCOUTHU. However, controllers TCH1, TCC2, TCH3 and TCC4 adjust their manipulated variables in order to control their stream temperatures to their setpoints.

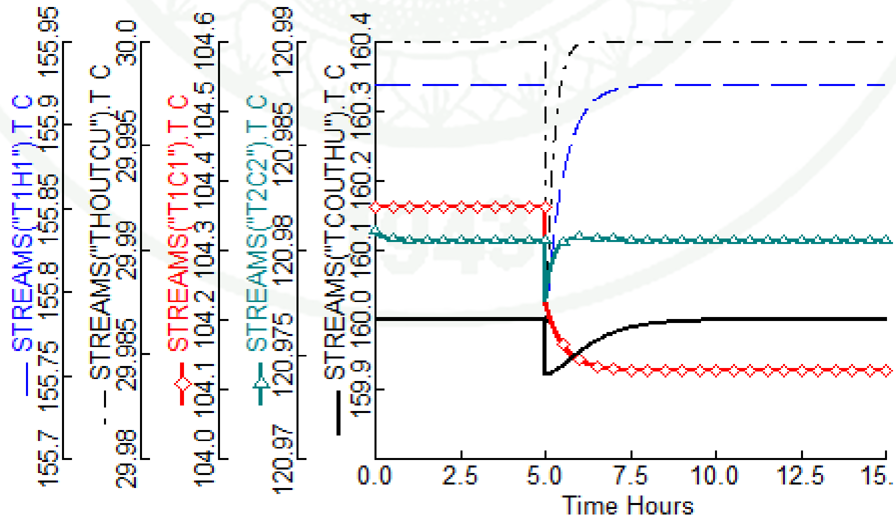

Figure 51 Temperature responses of controlled variables disturbed by -1% inlet flowrate of hot stream with failing passivity based PI controller TCC1

Figure 51 shows temperature responses of each controlled variable disturbed by -1% inlet flowrate of hot stream with failing controller TCC1. The result reports that when controller TCC1 fails, the temperature of T1C1 increases and affects the lower temperature of streams T1H1, T2C2, THOUTCU and TCOUTHU. However, controllers TCH1, TCC2, TCH3 and TCC4 adjust their manipulated variables in order to control their stream temperatures to their setpoints.

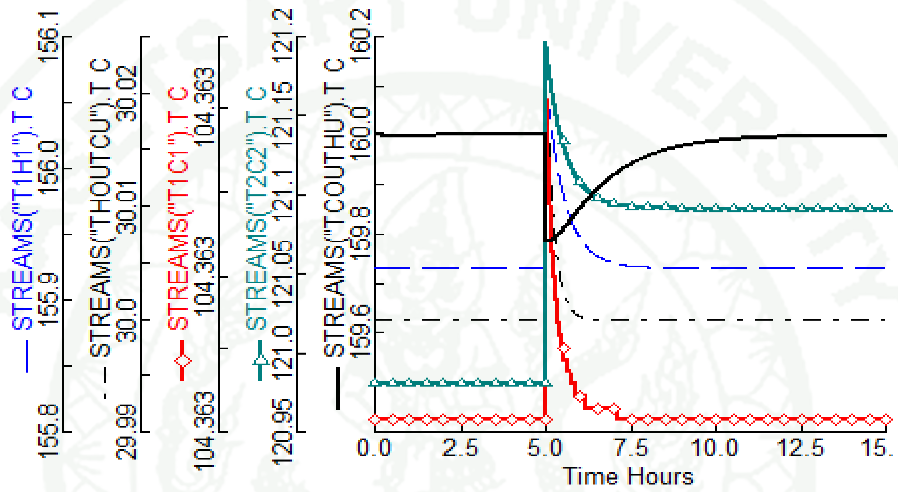

Figure 52 Temperature responses of controlled variables disturbed by +1% inlet flowrate of hot stream with failing passivity based PI controller TCC2

Figure 52 shows temperature responses of each controlled variable disturbed by +1% inlet flowrate of hot stream with failing controller TCC2. The result reports that when controller TCC2 fails, the temperature of T2C2 increases and affects the higher temperature of streams T1H1, T1C1 and THOUTCU. However, controllers TCH1, TCC1 and TCH3 adjust their manipulated variables in order to control their stream temperatures to their setpoints. The elevated hot flowrate also takes the effect to stream TCOUTHU decreased, but it can reach its setpoint by controller TCC4.

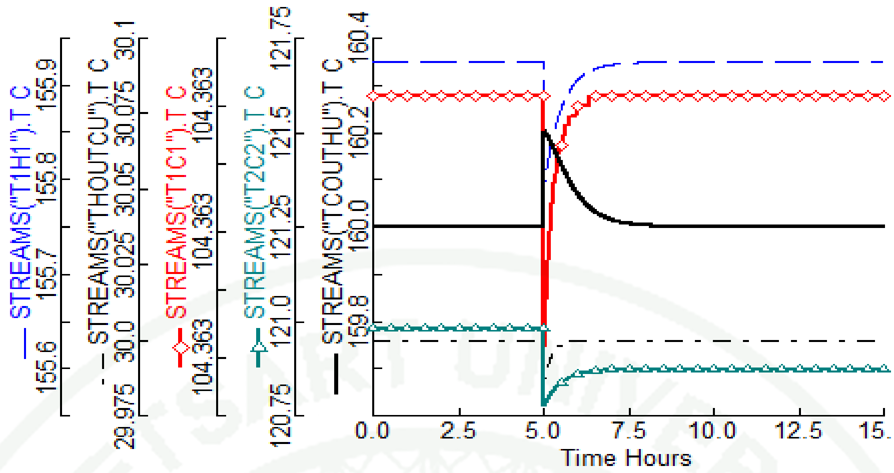

Figure 53 Temperature responses of controlled variables disturbed by -1% inlet flowrate of hot stream with failing passivity based PI controller TCC2

Figure 53 shows temperature responses of each controlled variable disturbed by -1% inlet flowrate of hot stream with failing controller TCC2. The result reports that when controller TCC2 fails, the temperature of T2C2 decreases and affects the lower temperature of streams T1H1, T1C1 and THOUTCU. However, controllers TCH1, TCC1 and TCH3 adjust their manipulated variables in order to control their stream temperatures to their setpoints. Moreover, the decreased hot flowrate takes the effect to stream TCOUTHU, but it can reach its setpoint by controller TCC4.

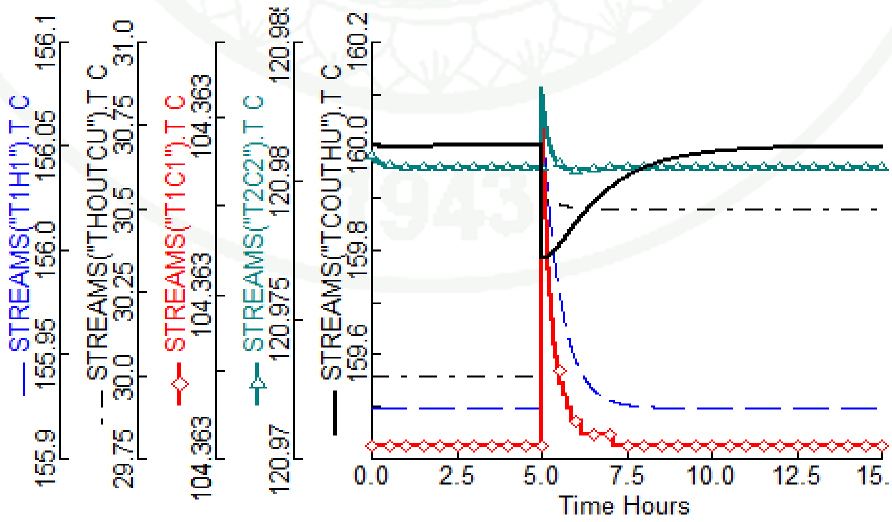

Figure 54 Temperature responses of controlled variables disturbed by +1% inlet flowrate of hot stream with failing passivity based PI controller TCH3

Figure 54 shows temperature responses of each controlled variable disturbed by +1% inlet flowrate of hot stream with failing controller TCH3. The result reports that when controller TCH3 fails, the temperature of THOUTCU increases and affects the higher temperature of streams T1H1, T1C1 and T2C2. However, controllers TCH1, TCC1 and TCC2 adjust their manipulated variables in order to control their stream temperatures to their setpoints. The elevated hot flowrate also takes the effect to stream TCOUTHU decreased, but it can reach its setpoint by controller TCC4.

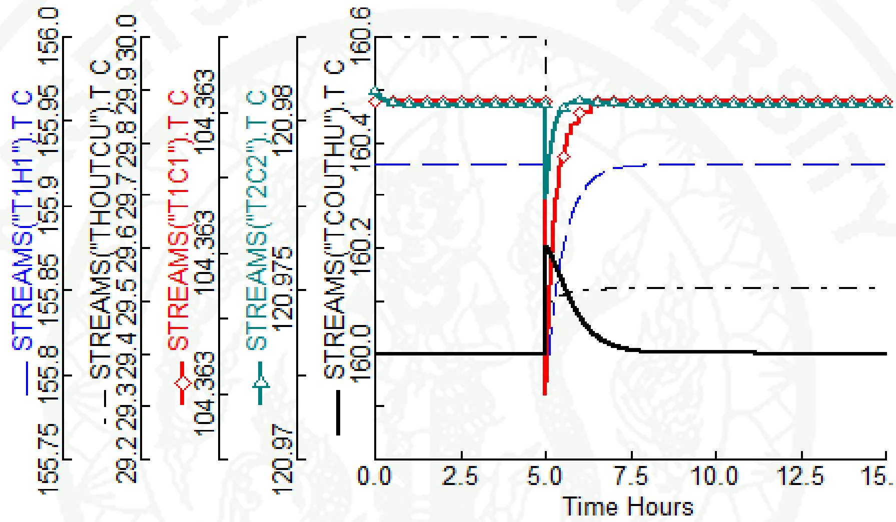

Figure 55 Temperature responses of controlled variables disturbed by -1% inlet flowrate of hot stream with failing passivity based PI controller TCH3

Figure 55 shows temperature responses of each controlled variable disturbed by -1% inlet flowrate of hot stream with failing controller TCH3. The result reports that when controller TCH3 fails, the temperature of THOUTCU decreases and affects the lower temperature of streams T1H1, T1C1 and T2C2. However, controllers TCH1, TCC1 and TCC4 adjust their manipulated variables in order to control their stream temperatures to their setpoints. Moreover, the decreased hot flowrate takes the effect to stream TCOUTHU, but it can be reached its setpoint by controller TCC4.

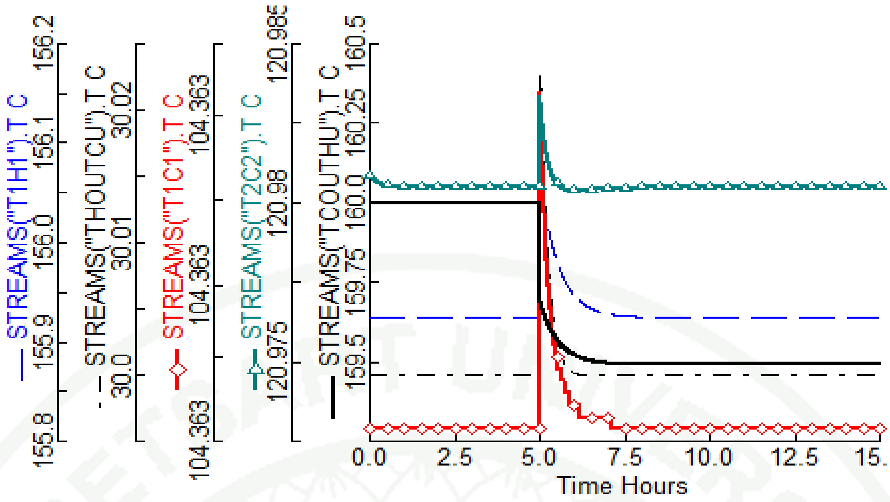

Figure 56 Temperature responses of controlled variables disturbed by +1% inlet flowrate of hot stream with failing passivity based PI controller TCC4

Figure 56 shows temperature responses of each controlled variable disturbed by +1% inlet flowrate of hot stream with failing controller TCC4. The result reports that when controller TCC4 fails, the temperature of TCOUTHU decreases and affects the higher temperature of streams T1H1, T1C1, T2C2 and THOUTCU. However, controllers TCH1, TCC1, TCC2 and TCH3 adjust their manipulated variables in order to control their stream temperatures to their setpoints.

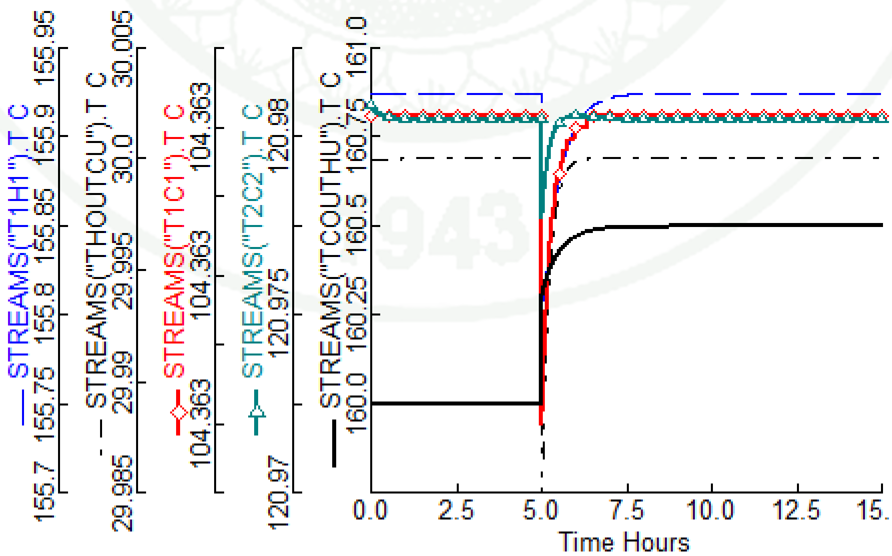

Figure 57 Temperature responses of controlled variables disturbed by -1% inlet flowrate of hot stream with failing passivity based PI controller TCC4

Figure 57 shows temperature responses of each controlled variable disturbed by -1% inlet flowrate of hot stream with failing controller TCC4. The result reports that when controller TCC4 fails, the temperature of TCOUTHU increases and affects the lower temperature of streams T1H1, T1C1, T2C2 and THOUTCU. However, controllers TCH1, TCC1, TCC2 and TCH3 adjust their manipulated variables in order to control their stream temperatures to their setpoints.

The following figures show temperature responses of each controlled variable of the system with failing default PI controller from Aspen Dynamics simulator getting the disturbance as the same as that with failing passivity based PI controller.

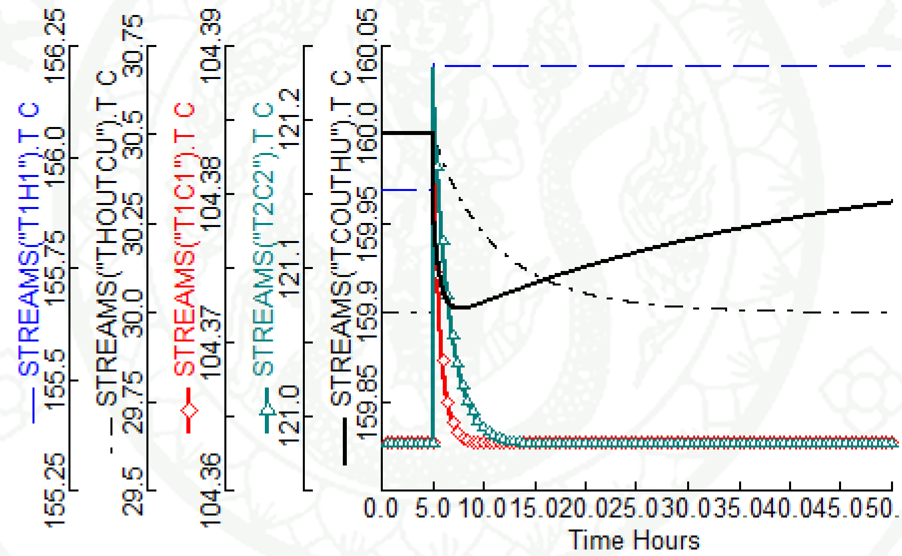

Figure 58 Temperature responses of controlled variables disturbed by +1% inlet flowrate of hot stream with failing PI controller TCH1

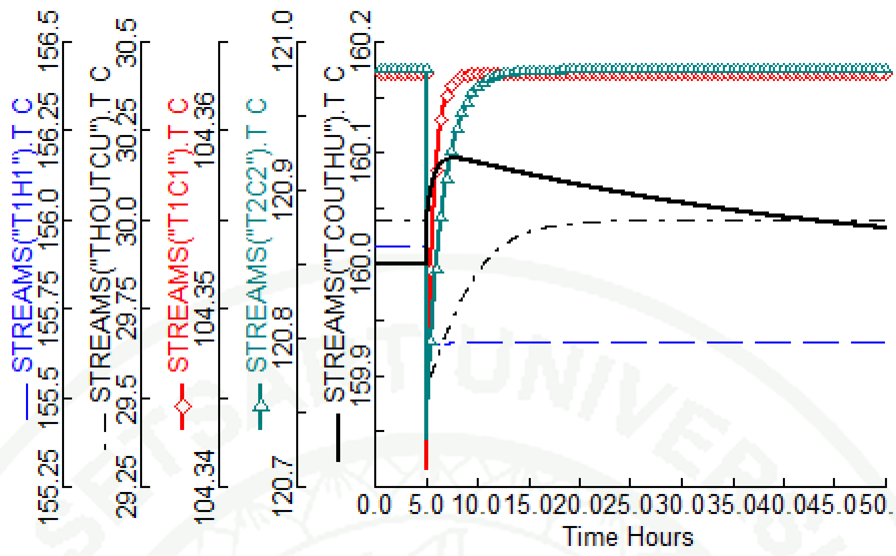

Figure 59 Temperature responses of controlled variables disturbed by -1% inlet flowrate of hot stream with failing PI controller TCH1

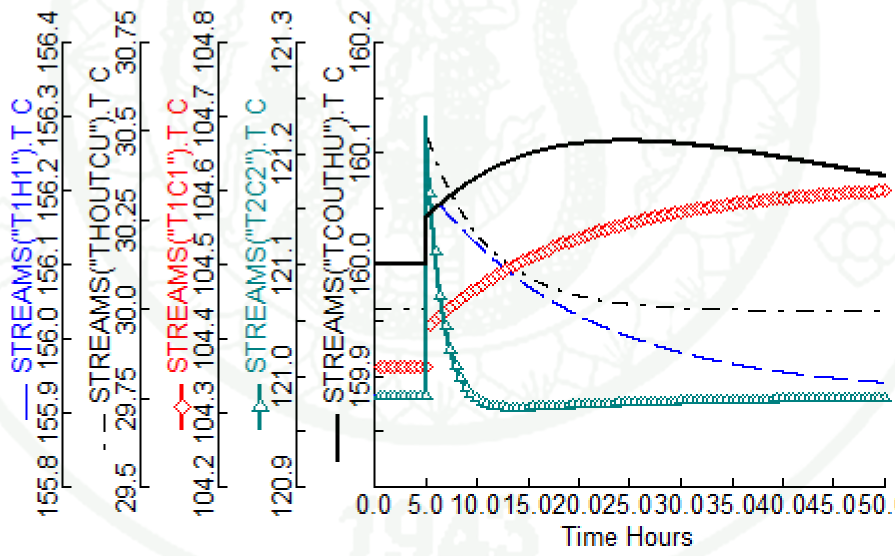

Figure 60 Temperature responses of controlled variables disturbed by +1% inlet flowrate of hot stream with failing PI controller TCC1

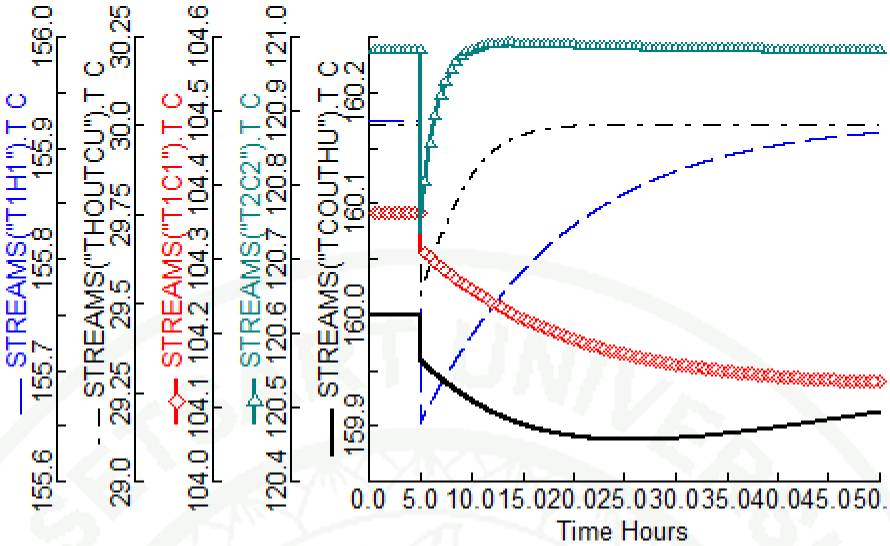

Figure 61 Temperature responses of controlled variables disturbed by -1% inlet flowrate of hot stream with failing PI controller TCC1

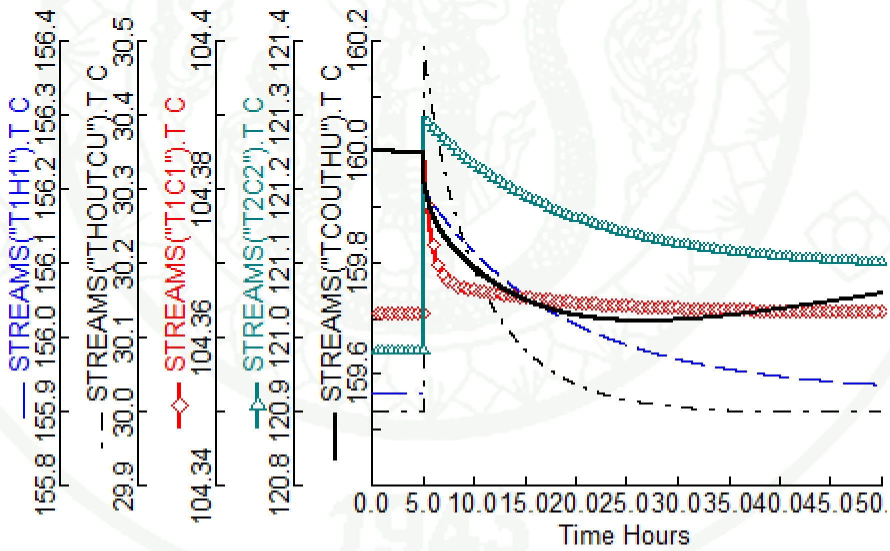

Figure 62 Temperature responses of controlled variables disturbed by +1% inlet flowrate of hot stream with failing PI controller TCC2

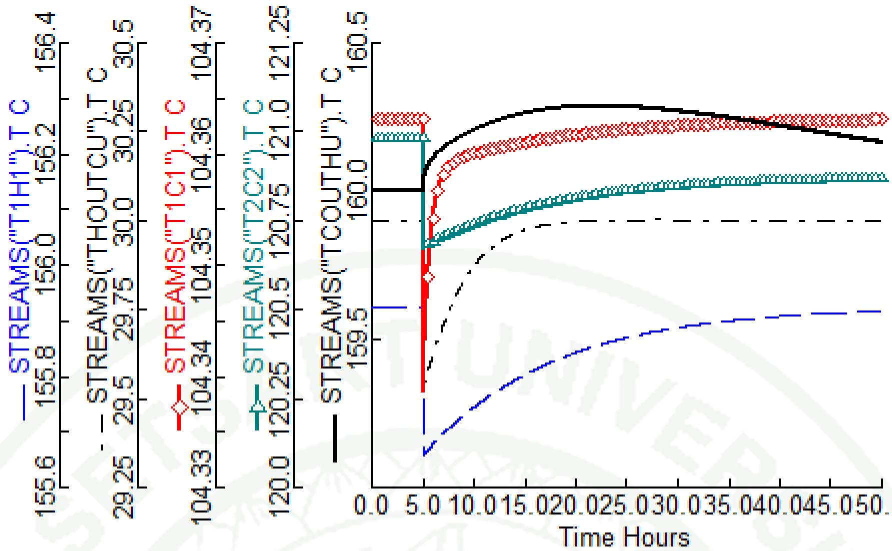

Figure 63 Temperature responses of controlled variables disturbed by -1% inlet flowrate of hot stream with failing PI controller TCC2

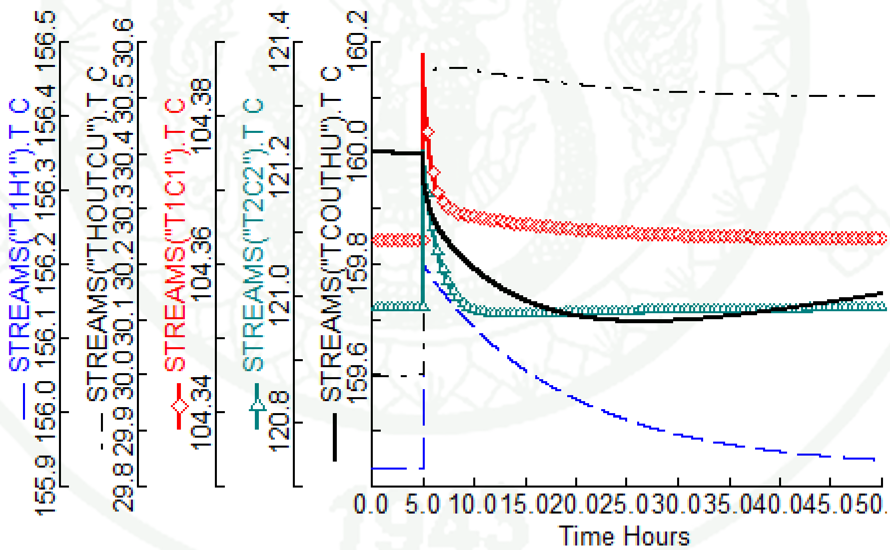

Figure 64 Temperature responses of controlled variables disturbed by +1% inlet flowrate of hot stream with failing PI controller TCH3

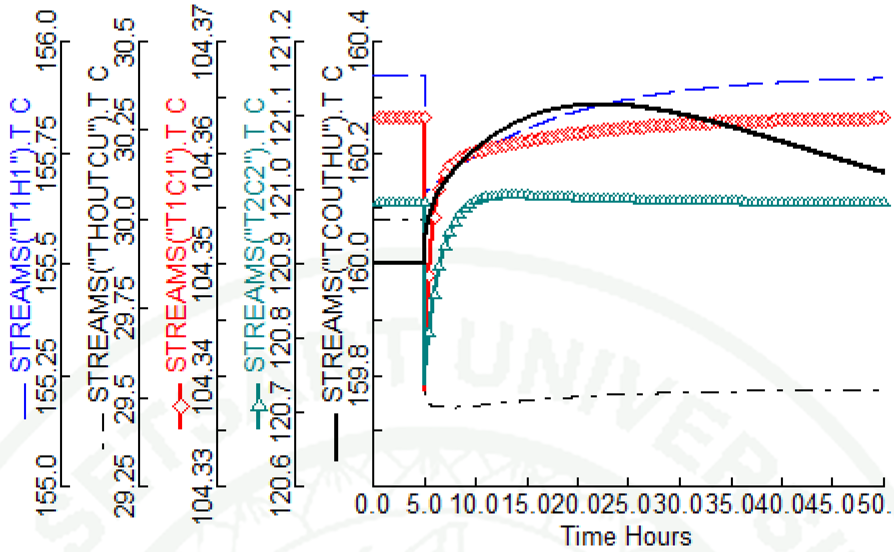

Figure 65 Temperature responses of controlled variables disturbed by -1% inlet flowrate of hot stream with failing PI controller TCH3

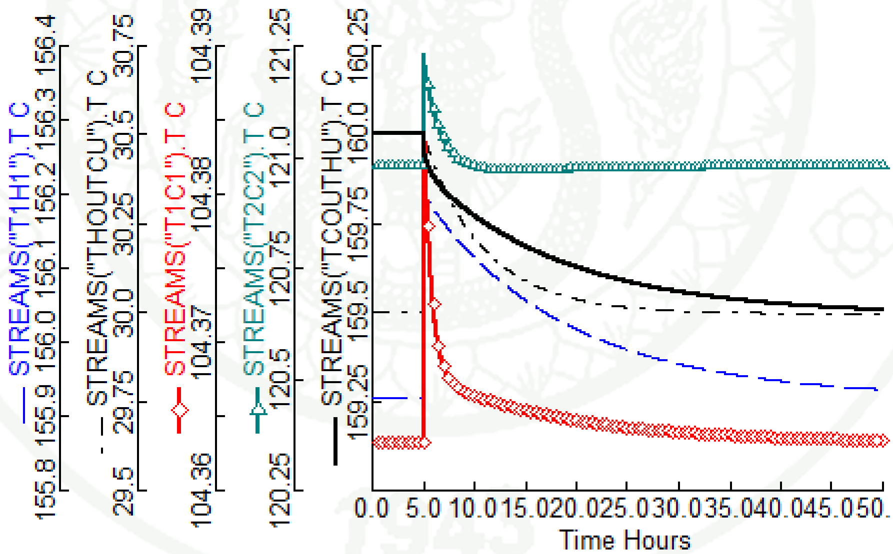

Figure 66 Temperature responses of controlled variables disturbed by +1% inlet flowrate of hot stream with failing PI controller TCC4

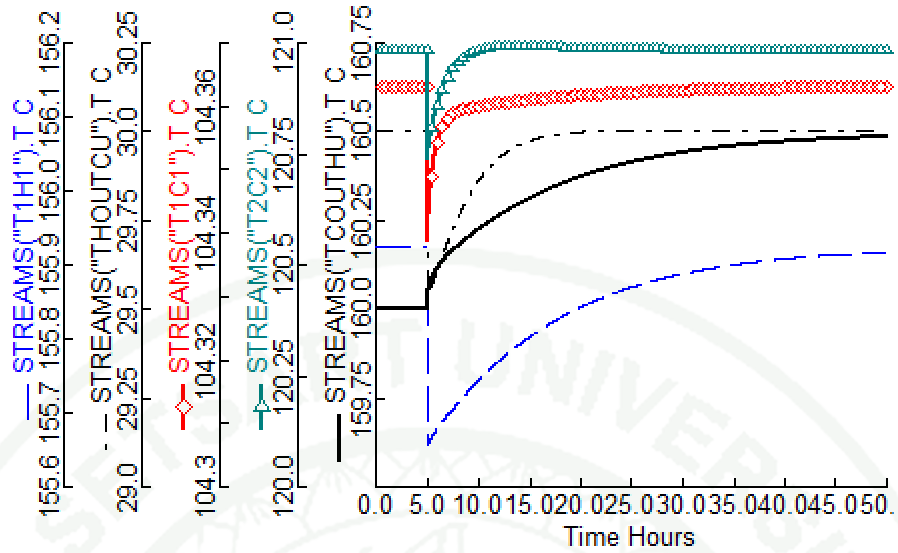

Figure 67 Temperature responses of controlled variables disturbed by -1% inlet flowrate of hot stream with failing PI controller TCC4

Figures 58 to 67 show the slow responses to get the new state resulted from a disturbance for a failing controller, or even working controllers adjust their manipulated variables slowly to reach the original setpoint. From Figures 58 to 65, when the HEN with failing PI controllers TCC1, TCH1, TCC2, TCH3 or TCC4 is disturbed by +1% and -1% inlet hot flowrates, the results show that the temperature of stream TCOUTHU cannot meet its original setpoint within 50 hours. These responses are very slow; therefore, it implies these disturbances make the controller loop of TCC4 fail. It cannot accordingly adjust the controlled temperature to its original setpoint temperature.

When compared the results from fault-tolerant control test, the results from passivity based PI controllers are better than PI controllers. Passivity based PI controller can cope with fault-tolerant control, has a fast response, and also guarantee stability. Thus, the system and controllers which are passive can achieve decentralized unconditional stability.

CONCLUSION AND RECOMMENDATION

Conclusion

This work presented that the passivity theorem as one of the cornerstones in nonlinear control theory was applied with a single bypass heat exchanger and HENs. Both applications were followed the passivity based decentralized controller synthesis procedure which was systematically combined each step from the works of Bao *et al*. (1998; 2000; 2002; 2007). The aim of this work was to design the passivity based DUS controllers for these systems to obtain the passivity based DUS control system.

Firstly, the state space model for a single bypass heat exchanger giving more practical idea was developed from that for a single heat exchanger. The example for this case used to this model was referred from Westhalen *et al*. (2003), and then its transfer function was formulated to test whether this system is passive or not by passivity index. The result from Bao and Lee (2007) reported that a single heat exchanger was inherently passive, but it was of interest to know that a single bypass heat exchanger developed in this work showed either passive or non-passive behaviors depending on its possible pairing schemes. However, the best pairing scheme which was the most passive was obtained when compared the passivity indices of each possible pairing scheme. In addition, the passivity based decentralized unconditional stability (DUS) PI controllers for this system were designed, and, finally, also verified via Aspen Dynamics simulator. This system was tested by making $\pm 10\%$ of setpoint temperatures and $\pm 10\%$ inlet hot flowrates. The results showed that the passivity approach gave better setpoint tracking than conventional PI controllers.

The passivity theorem was also extended to a HEN. The case study which has a feasible structure was referred from Glemmestad *et al*. (1996). This network comprised of two heat exchangers and two utility units. As the same as a single bypass heat exchanger, the HEN was tested by passivity index and followed the passivity based DUS PI controller synthesis procedure. However, this HEN part was divided into two parts; the first part was two heat exchangers with bypasses which were non-passive, and the second one was two utilities which were assumed to be a heat exchanger type and resulted passive behavior. In addition to verify the results by disturbing ± 1% inlet hot flowrates, this network was also tested fault-tolerant control to guarantee that when the system and controllers was passive, that system achieved DUS. The fault-tolerant control test was performed by letting one of controllers failed while the network got disturbances. The results reported HENs controlled by this approach can capably achieve fault-tolerant control while another PI controller could not achieve it.

Recommendation

1. The economic objective should be concerned with the control objective in HENs to obtain the minimum cost accompanied with the best performance.

2. This passivity theorem should be applied with a large-scale HEN to guarantee that this approach can handle with highly nonlinear and large interaction system which has not been researched yet.

3. The results from HENs applied with the passivity theorem should be compared those applied with other methods

4. The disturbances entering HENs should be over ± 1% inlet hot flowrates.

LITERATURE CITED

Amir-Moez, A. 1956. Extreme Properties of a Hermitian Transformation and Singular Values of the Sum and Product of Linear Transformation. **Duke Math. J.** (23):463-476.

Bao, J. 1998. **Robust Process Control: A Passivity Theorem Approach**. PhD. Thesis, Zhejiang University.

______, P. L. Lee, F. Y. Wang and W. B. Zhou. 1998. New Robust Stability Criterion and Robust Controller Synthesis. **Int J. Robust. Nonlinear Control**. (8):49-59.

______, ______ , ______ and ______ . 2000a. A New Approach to Decentralized Control Using Passivity and Sector Stability Conditions. **Chem. Eng. Comm**. (182):213-237.

______, W.Z. Zhang and P.L. Lee. 2000b. A Passivity-based Approach to Multi-loop PI Controller Tuning. *In* **Proceeding of Sixth International Conference on Control, Automation**, Robotics and Vision.

______, ______ and ______. 2002a. Decentralized Unconditional Stability Conditions based on the Passivity Theorem for Multi-loop Control Systems. **Comput. Chem. Eng.** (41):1569-1578.

______, ______ and ______ 2002b. Passivity-Based Decentralized Failure-Tolerant Control. **Ind. Eng. Chem. Res**. (41): 5702-5715.

______, ______ and ______ . 2002c. A New Pairing Method for Multi-loop Control Based on the Passivity Theorem. *In* **Proceeding of International of Symposium on Advanced Control of Industrial Processes**.

Bao, J. and P.L. Lee. 2007. **Process Control: The Passive Systems Approach**. Advanced in Industrial Control.

Bristol, E. H. 1966. On a New Measure of Interaction for Multivariable Process Control. **IEEE Trans on Automatic Control**. (11):133-134.

Boonkhao, B. 2004. **Controllability Study of Chemical Processes Based on the Concept of Passivity**. M.D. Thesis, Kasetsart University.

Chi-Tsong, T. 1984. **Linear System Theory & Design**. Oxford University Press, Inc.

Desoer, C. A. and M. Vidyasagar. 1975. **Feedback Systems: Input-Output Properties**. Acedamic Press, New York.

Escobar, M. and J.O. Trierweiler. 2009. Bypass Design for Control and Optimization of Heat Exchanger Networks. *In* **10th International Symposium on Process Systems Engineering - PSE2009**.

Friedland, B. 1987. **Control System Design: An Introduction to State-Space Methods**. McGraw-Hill Book Company, New York.

Furman, C.K. and N.V. Sahinidis. 2002. A Critical Review and Annotated Bibliography for Heat Exchanger Network Synthesis in the 20th Century. **Ind. Eng. Chem. Res.** (41):2335-2370.

Gahinet, P., A. Nemirovski, A.J. Laub and M. Chilali. 1995. **LMI Control Toolbox: For Use with MATLAB**. The Math Works, Inc.

Glemmestad, B., K.W. Mathisen and T. Gundersen. 1996. Optimal Operation of Heat Exchanger Networks Based on Structural Information. **Comput. Chem. Eng.** (20):823–828.

Glemmestad, B., S. Skogestad and T. Gundersen. 1999. Optimal Operation of Heat Exchanger Networks. **Comput. Chem. Eng.** (23):509–522

Gonzalez, A.H., D. Odloak, J.L. Machetti and O.A.Z. Sotomayor. 2006. Predictive Control Applied to Heat Exchanger Networks. **Chem. Eng. Prac**. (45):661-671.

Grosdidier, P., M. Morari and B. R. Holt. 1985 Closed Loop Properties from Steady State Gain Information. **Ind. Eng. Chem. Fundam.** (24):221-235.

Guillemin, E.A. 1957. **Synthesis of Passive Networks**. Wiley, New York.

Haddad, W.M. and D.S. Bernstein. 1991. Robust Stabilization with Positive Real Uncertainty: Beyond The Small-Gain theory. **Syst. Contr. Lett.** 17(3):191-208.

Hangos, K.M. and I.T. Cameron. 2001. **Process Modelling and Model Analysis**. Academic Press, London.

______, J. Bokor and G. Szederkényi. 2004. **Analysis and Control of Nonlinear Process Systems**.

Kern, D. 1950. **Process Heat Transfer**. McGraw-Hill, New York.

Lengsukchai, S. 2003. **Interaction Analysis and Controller Design for Multi-loop Control**. M.D. Thesis, King Mongkut's, University of Technology Thonburi.

Lersbamrungsuk, V., T. Srinophakun, S. Narasimhan and S. Skogestad. 2007. Control Structure Design for Optimal Operation of Heat Exchanger Networks. **AIChE J.** (52):150-162.

Lersbamrungsuk, V. 2008. **Development of Control Structure Design and Structural Controllability for Heat Exchanger Networks**. PhD. Thesis, Kasetsart University.

Luyben, L. M. and W. L. Luyben. 1997. **Essentials of Process Control**. McGraw-Hill International Editions: Chemical Engineering Series.

Mathisen, K.W. 1994. **Integrated Design and Control of Heat Exchanger Networks**. Ph.D. Thesis, University of Trondheim.

______, M. Morari and S. Skogestad. 1994. Dynamic Models for Heat Exchangers and Heat Exchanger Networks. **Comput. Chem. Eng.** (18):S459-S463.

Morari, M. and E. Zafiriou. 1989. **Robust Process Control**. Prentice-Hall, Inc., Englewood Cliffs, N.J.

Ogata, K. 1967. **State Space Analysis of Control System**. Prentice-Hall, Inc., Englewood Cliffs, N.J.

Safonov, M.G. 1982. Stability Margins of Diagonally Perturbed Multivariable Feedback Systems. **IEE Proceedings: Control & Theory Applications**. 129-D (6), 251-255.

Seborg, D.E., T.F. Edgar and D.A. Mellichamp. 2004. **Process Dynamics and Control**. 2nd Ed. New York; Wiley.

Sirisak, R. 2002. **Stability Analysis of Falling Film Evaporator with Passivity Theorem**. M.D. Thesis, King Mongkut's University of Technology Thonburi.

Van Der Schaft, A.J. 1997. **L_2-Gain and Passivity Techniques in Nonlinear Control**. Springer-Verlag, London.

Varga, E.I., K.M. Hangos and F. Szigeti. 1995. Controllability and Observability of Heat Exchanger Networks in the Time-Varying Parameter Case. **Control Eng. Prac**. 3(10):1409-1419.

Weinberg, L. 1962. **Network Analysis and Synthesis**, McGraw-Hill, New York.

Westhalen , L.D., R.B. Young and W.Y. Svrcek. 2003. A Controllability Index for Heat Exchanger Networks. **Ind. Eng. Chem. Res**. (42):4659-4667.

Willems, J. C. 1972a. Dissipative Dynamical Systems, Part I: General Theory. **Arch Rational Mech. Anal**., 45(5):321-351.

______. 1972b. Dissipative Dynamical Systems, Part II: Linear Systems with Quadratic Supply Rates. **Arch Rational Mech. Anal**. 45(5):352-393.

Wolff, E.A., K.W. Mathisen and S. Slogestad. 1991. Dynamics and Controllability of Heat Exchanger Networks. *In* **Proc. of Computer Oriented Process Engineering (COPE-91)**, (ed. L. Puigjaner and A. Espuna), 117-122.

Yee, T.F. and I.E. Grossman. 1990. Simultaneous Optimization Models for Heat Integration - II. Heat Exchanger Network Synthesis. **Comput. Chem. Eng.** (14):1165-1184.

APPENDICES

Appendix A
State space model

This section explains more information in order the reader to clearly understand concepts of a state space. The state space model can be divided into two systems. The first one is time-varying system, and the second one is time-invariant system (Friedland, 1987).

A.1 Definition of Dynamical Equation

Dynamical equation means the set of equations that describes the unique relations between the input, output, and state (Chi-Tsong, 1984). Their forms are:

$$\dot{x}(t) = h(x(t), u(t), t) \qquad \text{(state equation)} \tag{A.1}$$

$$y(t) = g(x(t), u(t), t) \qquad \text{(output equation)} \tag{A.2}$$

or more explicitly,

$$\begin{aligned} \dot{x}_1(t) &= h_1(x_1(t), x_2(t), \ldots, x_n(t), u_1(t), u_2(t), \ldots, u_m(t), t) \\ \dot{x}_2(t) &= h_2(x_1(t), x_2(t), \ldots, x_n(t), u_1(t), u_2(t), \ldots, u_m(t), t) \\ &\vdots \\ \dot{x}_n(t) &= h_n(x_1(t), x_2(t), \ldots, x_n(t), u_1(t), u_2(t), \ldots, u_m(t), t) \end{aligned} \tag{A.3}$$

$$\begin{aligned} y_1(t) &= g_1(x_1(t), x_2(t), \ldots, x_n(t), u_1(t), u_2(t), \ldots, u_m(t), t) \\ y_2(t) &= g_2(x_1(t), x_2(t), \ldots, x_n(t), u_1(t), u_2(t), \ldots, u_m(t), t) \\ &\vdots \\ y_k(t) &= g_k(x_1(t), x_2(t), \ldots, x_n(t), u_1(t), u_2(t), \ldots, u_m(t), t) \end{aligned} \tag{A.4}$$

where $x = [x_1, \ldots, x_n]^T$ is the state, $y = [y_1, \ldots, y_k]^T$ is the output, and $u = [u_1, \ldots, u_m]^T$ is the input.

A.2 State space Model for Time-Varying System

The equations used to describe the behavior of the systems depending on time are shown below (Friedland, 1987).

$$\begin{aligned}
\dot{x}_1 &= \frac{dx_1}{dt} = a_{11}(t)x_1 + \ldots + a_{1n}(t)x_n + b_{11}(t)u_1 + \ldots + b_{1m}(t)u_1 \\
\dot{x}_2 &= \frac{dx_2}{dt} = a_{21}(t)x_1 + \ldots + a_{2n}(t)x_n + b_{21}(t)u_1 + \ldots + b_{2m}(t)u_1 \\
&\vdots \\
\dot{x}_n &= \frac{dx_n}{dt} = a_{n1}(t)x_1 + \ldots + a_{nn}(t)x_n + b_{n1}(t)u_1 + \ldots + b_{nm}(t)u_1
\end{aligned} \tag{A.5}$$

Those can be written compactly into the matrix form as Equation (A.6).

$$\dot{x} = \frac{dx}{dt} = A(t)x + B(t)u \tag{A.6}$$

where A(t) and B(t) are matrices given by Equation (A.7).

$$A(t) = \begin{bmatrix} a_{11}(t)\ldots a_{1n}(t) \\ a_{21}(t)\ldots a_{2n}(t) \\ \vdots \quad \ddots \quad \vdots \\ a_{n1}(t)\ldots a_{nn}(t) \end{bmatrix} \qquad B(t) = \begin{bmatrix} b_{11}(t)\ldots b_{1m}(t) \\ b_{21}(t)\ldots b_{2m}(t) \\ \vdots \quad \ddots \quad \vdots \\ b_{n1}(t)\ldots b_{nm}(t) \end{bmatrix} \tag{A.7}$$

It is noted that the matrix A(t) is always a square (n by n) matrix, but that the matrix B(t) need not be square.

A.3 State space Model for Time-Invariant System

When none of elements in the matrices A and B depends upon time, the system is time-invariant system having the dynamic equations (Friedland, 1987).

$$\dot{x} = Ax + Bu \tag{A.8}$$

where A and B are constant matrices

For both cases, although the state of a system is fundamental, there are many situations in which one is not interested in the state directly, but only in its effect on the system *output* equation $y(t)$.

$$y(t) = \begin{bmatrix} y_1(t) \\ \vdots \\ y_k(t) \end{bmatrix} \tag{A.9}$$

for a system having k outputs. In a linear system, the output equation is assumed to be a linear combination of the state and the input.

$$y(t) = C(t)x(t) + D(t)u(t) \tag{A.10}$$

where C(t) is an k by n matrix and D(t) is an k by m matrix. If the system is time-invariant, C(t) and D(t) are constant matrices.

The presence of matrix D in equation (A.10) means that there is a direction connection between the input $u(t)$ and the output $y(t)$, without intervention of the state $x(t)$ (Friedland, 1987). The following figure shows a block diagram representation of general linear system of state space.

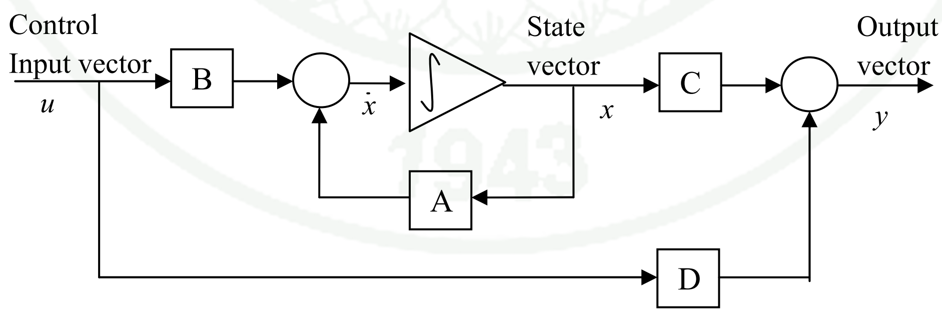

Appendix Figure A1 Block diagram representation of general linear system of a state space

Source: Friedland (1987)

Appendix B

Model construction procedure

This section shows the procedure to construct a process model, which is referred from Hangos *et al.* (2004), used in constructing a heat exchanger model as shown in the theoretical heat exchanger section.

Step 0*: System and subsystem boundary and balance volume definitions*

The outcome of this step is the set of balance volumes for mass, energy and momentum. These are the conserved extensive quantities normally considered in process systems. Moreover, the number of components is also fixed for each mass balance volume.

Step 1*: Establish the balance equations*

Here we set up conservation balances for mass, energy and momentum for each balance volume.

Step 2*: Transfer and reaction rate specifications*

The transfer rate expressions between different balance volumes in the conservation balances are specified here usually as functions of intensive quantities. The reaction rates within balance volumes are also specified

Step 3*: Property relation specifications*

Mostly algebraic relationships expressing thermodynamic knowledge, such as equations of state and the dependence of physico-chemical properties on thermodynamic state variables are considered here.

Step 4*: Balance volume relation specifications*

Equipment with a fixed physical volume is often divided into several balance volumes if multiple phases are presented. A balance volume relation describes a relation between balance volumes and physical volumes.

Step 5: *Equipment and control constraint specifications*

There is inevitably the need to define constraints on process systems. These constraints are typically in the form of equipment-operating constraints (in terms of temperatures, pressures, etc.) and in terms of control constraints, which define relations between manipulated and controlled variables in the system.

Step 6: *Selection of design variables*

The selection of design variables is highly dependent on the application area or problem and is not necessarily *process- specific*. The process itself only provides constraints on which variables are potentially relevant. The selection of design variables may greatly influence the mathematical properties of the model equations, such as the differential index.

Appendix C

Heat exchanger model development

This section shows a derivation of the heat exchanger models used in this work. It can be divided into four main parts; the first two parts present the derivations of a single heat exchanger model with a single bypass on hot side and cold side, respectively, into a state space model, the third part presents the derivation of a single heat exchanger model without bypass concerning volumetric flowrates as manipulated variables, and the last part presents another way of derivation of linearization and perturbation used in the model development in previous two parts to ensure that developed models are correct.

In order to get a state space model of a single heat exchanger with a single bypass, the state and output equation of a single heat exchanger with a single bypass have to be concerned. However, there are many variables presented in this section, all those are shown in the nomenclature section.

C.1 Derivation of a Single Heat Exchanger with a Single Bypass on Hot Side to State Space Model

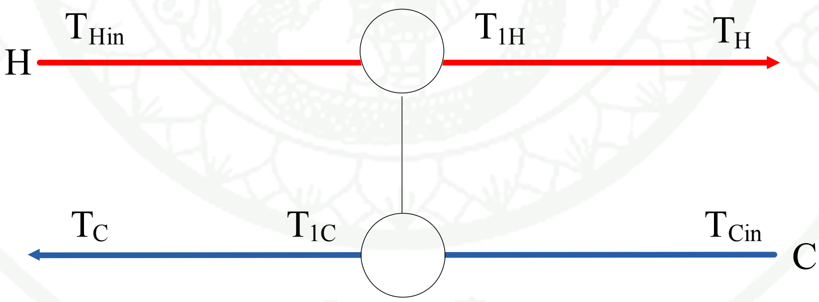

Appendix Figure C1 A single heat exchanger

Source: Hangos *et al*. (2004)

Consider a heat exchanger model without bypass mostly used first. Equations (C.1) and (C.2) are the state equation of cold and hot stream of a single heat exchanger without bypass (Hangos *et al*., 2004; Bao and Lee, 2007; Varga *et al*., 1995).

$$\rho_C V_C C_{pC} \frac{dT_{1C}}{dt} = \rho_C F_C C_{pC} (T_{Cin} - T_{1C}) + UA(T_{1H} - T_{1C}) \tag{C.1}$$

$$\rho_H V_H C_{pH} \frac{dT_{1H}}{dt} = \rho_H F_H C_{pH} (T_{Hin} - T_{1H}) + UA(T_{1C} - T_{1H}) \tag{C.2}$$

And Equations (C.3) and (C.4) are the output equation of cold and hot streams, respectively.

$$T_C = T_{1C} \tag{C.3}$$

$$T_H = T_{1H} \tag{C.4}$$

It was built under the following assumptions (Hangos *et al*., 2004; Bao and Lee, 2007):

1. A heat exchanger model is assumed to be an approximate lumped parameter system instead of a distributed parameter system.

2. Volumes of hot and cold streams in the heat exchanger (V_H and V_C) are constant.

3. Physicochemical properties, including density of the hot and cold streams (ρ_H and ρ_C) and their specific heats (C_{pH} and C_{pC}) are constant.

4. Heat transfer coefficient U and area A are constant.

5. Both hot and cold streams are well mixed and the temperatures of the hot and cold streams inside the tube are approximated by the outlet temperatures T_{1H} and T_{1C}.

This work uses above assumptions in derivation of a single heat exchanger with a single bypass.

C.1.1 State equations for hot and cold streams of a single heat exchanger with a single bypass on hot side.

Let us consider a single heat exchanger with a single bypass on hot side as shown in Appendix Figure C2.

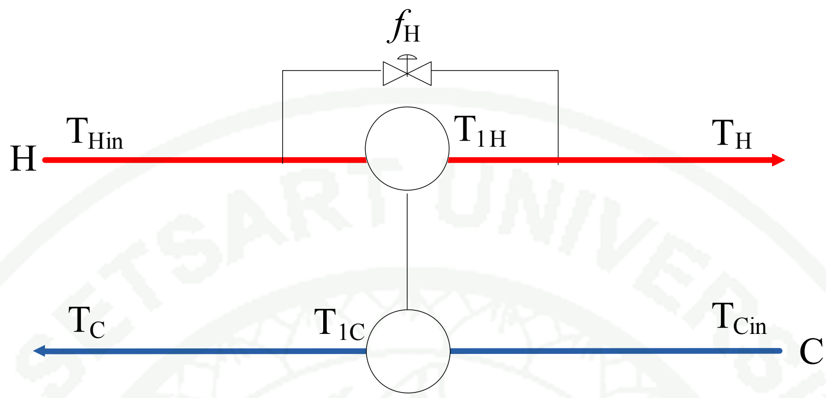

Appendix Figure C2 A single heat exchanger with a single bypass on hot side

Before deriving the equations, it is necessary to specify what state and manipulated variables of this system are. From above figure, the state variables of this system are the outlet temperature of cold and hot streams T_{1C} and T_{1H}, and the manipulated variables are cold flowrate F_C and bypass fraction f_H by assuming constant hot flowrate.

The state equations in Equations (C.5) for the hot stream and (C.6) for the cold stream

$$\rho_H V_H C_{pH} \frac{dT_{1H}}{dt} = \rho_H (1 - f_H) F_H C_{pH} (T_{Hin} - T_{1H}) + UA(T_{1C} - T_{1H}) \qquad \text{(C.5)}$$

where $\dfrac{dT_{1H}}{dt} = \lim\limits_{t \to 0} \left(\dfrac{T_{1H}^{t+1} - T_{1H}^{t}}{\Delta t} \right)$

$$\rho_C V_C C_{pC} \frac{dT_{1C}}{dt} = \rho_C F_C C_{pC} (T_{Cin} - T_{1C}) + UA(T_{1H} - T_{1C}) \qquad \text{(C.6)}$$

From Equation (C.5), the dynamic equation for hot stream is developed and changed into the state space form.

$$\rho_H V_H C_{pH} \frac{dT_{1H}}{dt} = \rho_H F_H C_{pH} (T_{Hin} - T_{1H}) - f_H \rho_H F_H C_{pH} (T_{Hin} - T_{1H}) + UA(T_{1C} - T_{1H})$$

(C.7)

Let $\tau_H = \rho_H C_{pH}$ then Equation (C.7) becomes:

$$\rho_H V_H C_{pH} \frac{dT_{1H}}{dt} = \tau_H F_H (T_{Hin} - T_{1H}) - \tau_H F_H f_H (T_{Hin} - T_{1H}) + UA(T_{1C} - T_{1H}) \tag{C.8}$$

$$\rho_H V_H C_{pH} \frac{dT_{1H}}{dt} = \tau_H F_H T_{Hin} - \tau_H F_H T_{1H} - \tau_H F_H T_{Hin} f_H - \tau_H F_H f_H T_{1H} + UAT_{1C} - UAT_{1H} \tag{C.9}$$

From Equation (C.9), although most terms on the right are linear, the forth one is nonlinear due to T_{1H} and f_H which are state and manipulated variables. Therefore, Taylor's series (Luyben *et al*., 1997) for linearization are presented.

$$f(x_1, x_2) \cong f(\overline{x_1}, \overline{x_2}) + \left(\frac{\partial f}{\partial x_1}\right)_{\overline{x_1}, \overline{x_2}} (x_1 - \overline{x_1}) + \left(\frac{\partial f}{\partial x_2}\right)_{\overline{x_1}, \overline{x_2}} (x_2 - \overline{x_2}) + \left(\frac{\partial^2 f}{\partial x_1^2}\right)_{\overline{x_1}, \overline{x_2}} \frac{(x_1 - \overline{x_1})^2}{2!} + \ldots \tag{C.10}$$

Consider only the first order term, thus, Equation (C.10) becomes

$$f(x_1, x_2) \cong f(\overline{x_1}, \overline{x_2}) + \left(\frac{\partial f}{\partial x_1}\right)_{\overline{x_1}, \overline{x_2}} (x_1 - \overline{x_1}) + \left(\frac{\partial f}{\partial x_2}\right)_{\overline{x_1}, \overline{x_2}} (x_2 - \overline{x_2}) \tag{C.11}$$

Using Taylor's series with the forth term in Equation (C.9), its derivation is presented as follows.

$$\begin{aligned} \tau_H F_H f_H T_{1H} = {} & \tau_H F_H \overline{f}_H \overline{T}_{1H} + \frac{\partial}{\partial f_H}\left(\tau_H F_H f_H T_{1H}\right)_{\overline{f}_H, \overline{T}_{1H}} (f_H - \overline{f}_H) \\ & + \frac{\partial}{\partial T_{1H}}\left(\tau_H F_H f_H T_{1H}\right)_{\overline{f}_H, \overline{T}_{1H}} (T_{1H} - \overline{T}_{1H}) \end{aligned} \tag{C.12}$$

At steady state, $\tau_H F_H \overline{f}_H \overline{T}_{1H}$ is usually zero (Seborg *et al*., 2004), thus, Equation (C.12) is reduced into Equation (C.13).

$$\tau_H F_H f_H T_{1H} = \tau_H F_H \overline{T}_{1H} (f_H - \overline{f}_H) + \tau_H F_H \overline{f}_H (T_{1H} - \overline{T}_{1H}) \tag{C.13}$$

After linearization by using Taylor's series, Equation (C.9) becomes:

$$\rho_H V_H C_{pH} \frac{dT_{1H}}{dt} = \tau_H F_H T_{Hin} - \tau_H F_H T_{1H} - \tau_H F_H T_{Hin} f_H + \tau_H F_H \overline{T}_{1H}(f_H - \overline{f}_H)$$
$$+\tau_H F_H \overline{f}_H (T_{1H} - \overline{T}_{1H}) + UAT_{1C} - UAT_{1H} \quad \text{(C.14)}$$

Then make Equation (C.14) into the deviation variable form or perturbation form.

$$\rho_H V_H C_{pH} \frac{d(\overline{T}_{1H} + T_{1H}^p)}{dt} = \tau_H F_H T_{Hin} - \tau_H F_H (\overline{T}_{1H} + T_{1H}^p) - \tau_H F_H T_{Hin} (\overline{f}_H + f_H^p) + \tau_H F_H \overline{T}_{1H} f_H^p$$
$$+\tau_H F_H \overline{f}_H T_{1H}^p + UA(\overline{T}_{1C} + T_{1C}^p) - UA(\overline{T}_{1H} + T_{1H}^p) \quad \text{(C.15)}$$

$$\rho_H V_H C_{pH} \frac{dT_{1H}^p}{dt} = -\tau_H F_H T_{1H}^p - \tau_H F_H T_{Hin} f_H^p + \tau_H F_H \overline{T}_{1H} f_H^p + \tau_H F_H \overline{f}_H T_{1H}^p + UAT_{1C}^p - UAT_{1H}^p$$
$$+\tau_H F_H T_{Hin} - \tau_H F_H \overline{T}_{1H} - \tau_H F_H T_{Hin} \overline{f}_H + UA\overline{T}_{1C} - UA\overline{T}_{1H} \quad \text{(C.16)}$$

From Equation (C.14), at steady state;

$$0 = \tau_H F_H T_{Hin} - \tau_H F_H \overline{T}_{1H} - \tau_H F_H T_{Hin} \overline{f}_H + 0 + 0 + UA\overline{T}_{1C} - UA\overline{T}_{1H} \quad \text{(C.17)}$$

Combine Equations (C.16) and (C.17) together, let $\xi_H = \rho_H V_H C_{pH}$, and rearrange the equation into the compact form. Then Equation (C.5) becomes:

$$\frac{dT_{1H}^p}{dt} = \frac{UA}{\xi_H} T_{1C}^p + \left(\frac{-UA + \tau_H F_H \overline{f}_H - \tau_H F_H}{\xi_H} \right) T_{1H}^p + \left(\frac{\tau_H F_H \overline{T}_{1H} - \tau_H F_H T_{Hin}}{\xi_H} \right) f_H^p \quad \text{(C.18)}$$

Since most of the time perturbation variables are used, it is intuitively understood that whenever linearization is presented, all variables are perturbation variables. Thus, Equation (C.18) becomes as follows.

$$\frac{dT_{1H}}{dt} = \frac{UA}{\xi_H} T_{1C} + \left(\frac{-UA + \tau_H F_H \overline{f}_H - \tau_H F_H}{\xi_H} \right) T_{1H} + \left(\frac{\tau_H F_H \overline{T}_{1H} - \tau_H F_H T_{Hin}}{\xi_H} \right) f_H \quad \text{(C.19)}$$

The dynamic equation for cold stream will be developed and changed into state space form as the same as hot stream.

Let $\tau_C = \rho_C C_{pC}$ and $\xi_C = \rho_C V_C C_{pC}$ then substitute into Equation (C.6).

$$\xi_C \frac{dT_{1C}}{dt} = \tau_C F_C (T_{Cin} - T_{1C}) + UA(T_{1H} - T_{1C}) \tag{C.20}$$

$$\xi_C \frac{dT_{1C}}{dt} = \tau_C F_C T_{Cin} - \tau_C F_C T_{1C} + UAT_{1H} - UAT_{1C} \tag{C.21}$$

All terms on the right are linear but the second term so this one has to be linearized.

$$\tau_C F_C T_{1C} = \tau_C \overline{F}_C \overline{T}_{1C} + \frac{\partial}{\partial F_C}\left(\tau_C F_C T_{1C}\right)_{\overline{F}_C, \overline{T}_{1C}} (F_C - \overline{F}_C) + \frac{\partial}{\partial T_{1C}}\left(\tau_C F_C T_{1C}\right)_{\overline{F}_C, \overline{T}_{1C}} (T_{1C} - \overline{T}_{1C}) \tag{C.22}$$

$$\tau_C F_C T_{1C} = 0 + \tau_C \overline{T}_{1C} (F_C - \overline{F}_C) + \tau_C \overline{F}_C (T_{1C} - \overline{T}_{1C}) \tag{C.23}$$

Combine Equations (C.21) and (C.23) together. The state equation for cold stream after linearization is Equation (C.24).

$$\xi_C \frac{dT_{1C}}{dt} = \tau_C T_{Cin} F_C - \tau_C \overline{T}_{1C} (F_C - \overline{F}_C) - \tau_C \overline{F}_C (T_{1C} - \overline{T}_{1C}) + UAT_{1H} - UAT_{1C} \tag{C.24}$$

$$\xi_C \frac{d(\overline{T}_{1C} + T_{1C}^p)}{dt} = \tau_C T_{Cin} (\overline{F}_C + F_C^p) - \tau_C \overline{T}_{1C} F_C^p - \tau_C \overline{F}_C T_{1C}^p + UA(\overline{T}_{1H} + T_{1H}^p) - UA(\overline{T}_{1C} + T_{1C}^p) \tag{C.25}$$

$$\xi_C \frac{dT_{1C}^p}{dt} = \tau_C T_{Cin} F_C^p - \tau_C \overline{T}_{1C} F_C^p - \tau_C \overline{F}_C T_{1C}^p + UAT_{1H}^p - UAT_{1C}^p + (\tau_C T_{Cin} \overline{F}_C + UA\overline{T}_{1H} - UA\overline{T}_{1C}) \tag{C.26}$$

From Equation (C.24), at steady state;

$$0 = \tau_C T_{Cin} \overline{F}_C + UA\overline{T}_{1H} - UA\overline{T}_{1C} \tag{C.27}$$

Combine Equations (C.26) and (C.27) together, thus the state equation of cold stream is Equation (C.28).

$$\frac{dT_{1C}}{dt} = \left(\frac{-UA - \tau_C \overline{F}_C}{\xi_C}\right) T_{1C} + \frac{UA}{\xi_C} T_{1H} + \left(\frac{\tau_C T_{Cin} - \tau_C \overline{T}_{1C}}{\xi_C}\right) F_C \tag{C.28}$$

Equations (C.18) and (C.28) have been the dynamics equations or the state equations of a single heat exchanger with single bypass.

C.1.2 Output equations for hot and cold streams of a single heat exchanger with a single bypass on hot side.

An output equation in the form of state space in case of time-invariant system is Equation (C.29).

$$y = Cx + Du \tag{C.29}$$

From Appendix Figure C2, the output equation of hot stream for a single heat exchanger with a single bypass referred from (Mathisen, 1994; Glemmestad *et al*., 1999) is presented in Equation (C.30).

$$T_H = (1 - f_H)T_{1H} + f_H T_{Hin} \tag{C.30}$$

$$T_H = T_{1H} - f_H T_{1H} + f_H T_{Hin} \tag{C.31}$$

Since the second term on the right hand side is nonlinear, this term has to be linearized using Taylor's series (Luyben *et al*., 1997) as shown in Equation (10). The following equation shows the nonlinear term in Equation (C.31) is linearized.

$$f_H T_{1H} = \frac{\partial}{\partial f_H}\left(f_H T_{1H}\right)_{\bar{f}_H, \bar{T}_{1H}} (f_H - \bar{f}_H) + \frac{\partial}{\partial T_{1H}}\left(f_H T_{1H}\right)_{\bar{f}_H, \bar{T}_{1H}} (T_{1H} - \bar{T}_{1H}) \tag{C.32}$$

$$f_H T_{1H} = \bar{T}_{1H}(f_H - \bar{f}_H) + \bar{f}_H (T_{1H} - \bar{T}_{1H}) \tag{C.33}$$

After linearization by using Taylor's series, Equation (C.31) becomes Equation (C.34).

$$T_H = T_{1H} - \bar{T}_{1H}(f_H - \bar{f}_H) - \bar{f}_H (T_{1H} - \bar{T}_{1H})) + f_H T_{Hin} \tag{C.34}$$

Then Equation (C.34) can be made in the deviation variable form or perturbation form as Equation (C.35).

$$\bar{T}_H + T_H^p = (\bar{T}_{1H} + T_{1H}^p) - \bar{T}_{1H} f_H^p - \bar{f}_H T_{1H}^p) + (\bar{f}_H + f_H^p) T_{Hin} \tag{C.35}$$

From Equation (C.34), at steady state;

$$\bar{T}_H = \bar{T}_{1H} + \bar{f}_H T_{Hin} \tag{C.36}$$

Combine Equations (C.35) and (C.36) together, then Equation (C.31) becomes as follows.

$$T_H^p = (1-\bar{f}_H)T_{1H}^p + (T_{Hin} - \bar{T}_{1H})f_H^p \quad \text{(C.37)}$$

From Appendix Figure C.2, the output equation of cold stream for a single heat exchanger with a single bypass on hot side referred from (Hangos *et al*., 2004; Bao and Lee, 2007) is presented in Equation (C.38).

$$T_C = T_{1C} \quad \text{(C.38)}$$

Therefore, the state and output equations for cold and hot streams of a heat exchanger with a single bypass on hot side are summarized in Equations (C.39) to (C.42).

$$\frac{dT_{1C}}{dt} = \left(\frac{-UA-\tau_C\bar{F}_C}{\xi_C}\right)T_{1C} + \frac{UA}{\xi_C}T_{1H} + \left(\frac{\tau_C T_{Cin} - \tau_C\bar{T}_{1C}}{\xi_C}\right)F_C \quad \text{(C.39)}$$

$$\frac{dT_{1H}}{dt} = \frac{UA}{\xi_H}T_{1C} + \left(\frac{-UA+\tau_H F_H\bar{f}_H - \tau_H F_H}{\xi_H}\right)T_{1H} + \left(\frac{\tau_H F_H\bar{T}_{1H} - \tau_H F_H T_{Hin}}{\xi_H}\right)f_H \quad \text{(C.40)}$$

$$T_C = T_{1C} \quad \text{(C.41)}$$

$$T_H = (1-\bar{f}_H)T_{1H} + (T_{Hin} - \bar{T}_{1H})f_H \quad \text{(C.42)}$$

where $\tau_i = \rho_i C_{Pi}$ and $\xi_i = \rho_i V_i C_{Pi}$

C.2 Derivation of a Single Heat Exchanger with a Single Bypass on Cold Side to State Space Model

This model adopts assumptions as the same as previous section in derivation of a single heat exchanger with a single bypass on cold side.

C.2.1 State equations for hot and cold streams of a single heat exchanger with a single bypass on cold side.

Consider a single heat exchanger with a single bypass on cold side as shown in Appendix Figure C3.

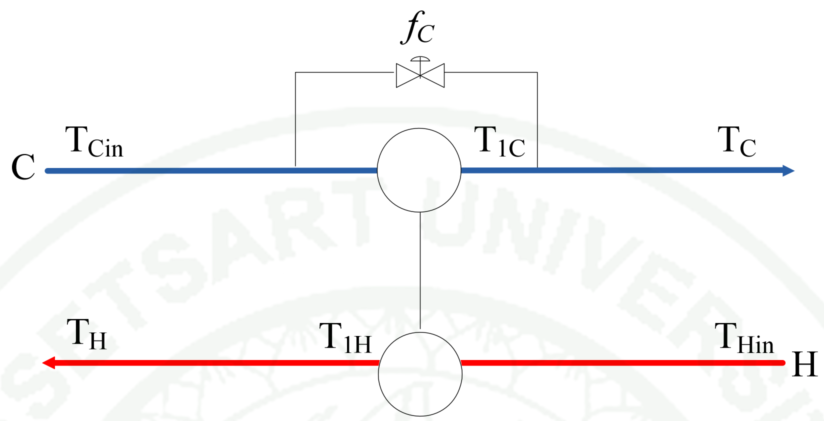

Appendix Figure C3 A single heat exchanger with a single bypass on cold side

Before deriving the equations, it is necessary to specify what state and manipulated variables of this system are. From above figure, the state variables of this system are the outlet temperature of cold and hot streams T_{1C} and T_{1H}, and the manipulated variables are hot flowrate F_H and bypass fraction f_C by assuming constant cold flowrate.

The state equations in Equations (C.43) for hot stream and (C.44) for cold stream

$$\rho_H V_H C_{pH} \frac{dT_{1H}}{dt} = \rho_H F_H C_{pH}(T_{Hin} - T_{1H}) + UA(T_{1C} - T_{1H}) \quad (C.43)$$

$$\rho_C V_C C_{pC} \frac{dT_{1C}}{dt} = \rho_C (1 - f_C) F_C C_{pC}(T_{Cin} - T_{1C}) + UA(T_{1H} - T_{1C}) \quad (C.44)$$

From Equation (C.44), the dynamic equation for cold stream is developed and changed into state space form. Let $\tau_C = \rho_C C_{pC}$ then Equation (C.44) becomes:

$$\rho_C V_C C_{pC} \frac{dT_{1C}}{dt} = \tau_C F_C (T_{Cin} - T_{1C}) - \tau_C F_C f_C (T_{Cin} - T_{1C}) + UA(T_{1H} - T_{1C}) \quad (C.45)$$

$$\rho_C V_C C_{pC} \frac{dT_{1C}}{dt} = \tau_C F_C T_{Cin} - \tau_C F_C T_{1C} - \tau_C F_C f_C T_{Cin} + \tau_C F_C f_C T_{1C} + UA(T_{1H} - T_{1C})$$

(C.46)

From Equation (C.46), although most terms on the right are linear, the forth one is nonlinear due to T_{1C} and f_C which are state and manipulated variables. Therefore, Taylor's series (Luyben *et al*., 1997) for linearization as in Equation (C.11) are presented.

$$\tau_C F_C f_C T_{1C} = \tau_C F_C \bar{f}_C \bar{T}_{1C} + \frac{\partial}{\partial f_C}\left(\tau_C F_C f_C T_{1C}\right)_{\bar{f}_C,\bar{T}_{1C}} (f_C - \bar{f}_C) + \frac{\partial}{\partial T_{1C}}\left(\tau_C F_C f_C T_{1C}\right)_{\bar{f}_C,\bar{T}_{1C}} (T_{1C} - \bar{T}_{1C}) \tag{C.47}$$

At steady state, $\tau_C F_C \bar{f}_C \bar{T}_{1C}$ is usually zero (Seborg *et al*., 2004), thus, Equation (C.47) is reduced into Equation (C.48).

$$\tau_C F_C f_C T_{1C} = \tau_C F_C \bar{T}_{1C}(f_C - \bar{f}_C) + \tau_C F_C \bar{f}_C (T_{1C} - \bar{T}_{1C}) \tag{C.48}$$

After linearization by using Taylor's series, Equation (C.46) becomes:

$$\begin{aligned}\rho_C V_C C_{pC}\frac{dT_{1C}}{dt} &= \tau_C F_C T_{Cin} - \tau_C F_C T_{1C} - \tau_C F_C T_{Cin} f_C + \tau_C F_C \bar{T}_{1C}(f_C - \bar{f}_C) \\ &\quad + \tau_C F_C \bar{f}_C (T_{1C} - \bar{T}_{1C}) + UA(T_{1H} - T_{1C})\end{aligned} \tag{C.49}$$

Then Equation (C.49) can be made into the deviation variable form or perturbation form.

$$\begin{aligned}\rho_C V_C C_{pC}\frac{d(\bar{T}_{1C} + T_{1C}^p)}{dt} &= \tau_C F_C T_{Cin} - \tau_C F_C(\bar{T}_{1C} + T_{1C}^p) - \tau_C F_C T_{Cin}(\bar{f}_C + f_C^p) \\ &\quad + \tau_C F_C \bar{T}_{1C} f_C^p + \tau_C F_C \bar{f}_C T_{1C}^p + UA(\bar{T}_{1H} + T_{1H}^p) - UA(\bar{T}_{1C} + T_{1C}^p)\end{aligned} \tag{C.50}$$

$$\begin{aligned}\rho_C V_C C_{pC}\frac{dT_{1C}^p}{dt} &= -\tau_C F_C T_{1C}^p - \tau_C F_C T_{Cin} f_C^p + \tau_C F_C \bar{T}_{1C} f_C^p + \tau_C F_C \bar{f}_C T_{1C}^p + UAT_{1H}^p \\ &\quad - UAT_{1C}^p + \tau_C F_C T_{Cin} - \tau_C F_C \bar{T}_{1C} - \tau_C F_C T_{Cin}\bar{f}_C + UA\bar{T}_{1H} - UA\bar{T}_{1C}\end{aligned} \tag{C.51}$$

From Equation (C.49), at steady state;

$$0 = \tau_C F_C T_{Cin} - \tau_C F_C \bar{T}_{1C} - \tau_C F_C T_{Cin}\bar{f}_C + UA(\bar{T}_{1H} - \bar{T}_{1C}) \tag{C.52}$$

Combine Equations (C.51) and (C.52) together, let $\xi_C = \rho_C V_C C_{pC}$, and rearrange the equation into the compact form. Then Equation (C.44) becomes:

$$\frac{dT_{1C}}{dt} = \left(\frac{-UA + \tau_C F_C \bar{f}_C - \tau_C F_C}{\xi_C} \right) T_{1C} + \frac{UA}{\xi_C} T_{1H} + \left(\frac{\tau_C F_C \bar{T}_{1C} - \tau_C F_C T_{Cin}}{\xi_C} \right) f_C \tag{C.53}$$

The dynamic equation for hot stream is developed and changed into state space form as the same as cold stream.

Let $\tau_H = \rho_H C_{pH}$ and $\xi_H = \rho_H V_H C_{pH}$ then substitute into Equation (C.43).

$$\xi_H \frac{dT_{1H}}{dt} = \tau_H F_H (T_{Hin} - T_{1H}) + UA(T_{1C} - T_{1H}) \tag{C.54}$$

$$\xi_H \frac{dT_{1H}}{dt} = \tau_H F_H T_{Hin} - \tau_H F_H T_{1H} + UAT_{1C} - UAT_{1H} \tag{C.55}$$

All terms on the right are linear but the second term so this one has to be linearized.

$$\tau_H F_H T_{1H} = \tau_H \bar{F}_H \bar{T}_{1H} + \frac{\partial}{\partial F_H} \left(\tau_H F_H T_{1H} \right)_{\bar{F}_H, \bar{T}_{1H}} (F_H - \bar{F}_H) + \frac{\partial}{\partial T_{1H}} \left(\tau_H F_H T_{1H} \right)_{\bar{F}_H, \bar{T}_{1H}} (T_{1H} - \bar{T}_{1H}) \tag{C.56}$$

$$\tau_H F_H T_{1H} = \tau_H \bar{T}_{1H} (F_H - \bar{F}_H) + \tau_H \bar{F}_H (T_{1H} - \bar{T}_{1H}) \tag{C.57}$$

Combine Equations (C.55) and (C.57) together. The state equation for hot stream after linearization is Equation (C.58).

$$\xi_H \frac{dT_{1H}}{dt} = \tau_H T_{Hin} F_H - \tau_H \bar{T}_{1H} (F_H - \bar{F}_H) - \tau_H \bar{F}_H (T_{1H} - \bar{T}_{1H}) + UAT_{1C} - UAT_{1H} \tag{C.58}$$

$$\xi_H \frac{d(\bar{T}_{1H} + T_{1H}^p)}{dt} = \tau_H T_{Hin} (\bar{F}_H + F_H^p) - \tau_H \bar{T}_{1H} F_H^p - \tau_H \bar{F}_H T_{1H}^p + UA(\bar{T}_{1C} + T_{1C}^p) - UA(\bar{T}_{1H} + T_{1H}^p) \tag{C.59}$$

$$\xi_H \frac{dT_{1H}^p}{dt} = \tau_H T_{Hin} F_H^p - \tau_H \bar{T}_{1H} F_H^p - \tau_H \bar{F}_H T_{1H}^p + UAT_{1C}^p - UAT_{1H}^p + (\tau_H T_{Hin} \bar{F}_H + UA\bar{T}_{1C} - UA\bar{T}_{1H}) \tag{C.60}$$

From Equation (C.58), at steady state;

$$0 = \tau_H T_{Hin} \overline{F}_H + UA\overline{T}_{1C} - UA\overline{T}_{1H} \tag{C.61}$$

Combine Equations (C.60) and (C.61) together, thus the state equation of hot stream is Equation (C.62).

$$\frac{dT_{1H}}{dt} = \frac{UA}{\xi_H} T_{1C} + \left(\frac{-UA - \tau_H \overline{F}_H}{\xi_H} \right) T_{1H} + \left(\frac{\tau_H T_{Hin} - \tau_H \overline{T}_{1H}}{\xi_H} \right) F_H \tag{C.62}$$

Equations (C.53) and (C.62) have been the dynamics equations or the state equations of a single heat exchanger with a single bypass on cold side.

C.2.2 Output equations for hot and cold streams of a single heat exchanger with a single bypass on cold side.

An output equation in the form of state space in case of time-invariant system is Equation (C.29).

$$y = Cx + Du \tag{C.29}$$

From Appendix Figure C2, the output equation of cold stream for a single heat exchanger with a single bypass referred from (Mathisen, 1994; Glemmestad *et al*., 1999) is presented in Equation (C.63).

$$T_C = (1 - f_C) T_{1C} + f_C T_{Cin} \tag{C.63}$$

$$T_C = T_{1C} - f_C T_{1C} + f_C T_{Cin} \tag{C.64}$$

Since the second term on the right hand side is nonlinear, this term has to be linearized using Taylor's series (Luyben *et al*., 1997) as shown in Equation (10). The following equation shows the nonlinear term in Equation (C.64) is linearized.

$$f_C T_{1C} = \frac{\partial}{\partial f_C} \left(f_C T_{1C} \right)_{\overline{f}_C, \overline{T}_{1C}} (f_C - \overline{f}_C) + \frac{\partial}{\partial T_{1C}} \left(f_C T_{1C} \right)_{\overline{f}_C, \overline{T}_{1C}} (T_{1C} - \overline{T}_{1C}) \tag{C.65}$$

$$f_C T_{1C} = \overline{T}_{1C} (f_C - \overline{f}_C) + \overline{f}_C (T_{1C} - \overline{T}_{1C}) \tag{C.66}$$

After linearization by using Taylor's series, Equation (C.64) becomes Equation (C.67).

$$T_C = T_{1C} - \overline{T}_{1C}(f_C - \overline{f}_C) - \overline{f}_C(T_{1C} - \overline{T}_{1C})) + f_C T_{Cin} \quad \text{(C.67)}$$

Then Equation (C.67) can be made in the deviation variable form or perturbation form as Equation (C.68).

$$\overline{T}_C + T_C^p = (\overline{T}_{1C} + T_{1C}^p) - \overline{T}_{1C} f_C^p - \overline{f}_C T_{1C}^p) + (\overline{f}_C + f_C^p) T_{Cin} \quad \text{(C.68)}$$

From Equation (C.67), at steady state;

$$\overline{T}_C = \overline{T}_{1C} + \overline{f}_C T_{Cin} \quad \text{(C.69)}$$

Combine Equations (C.68) and (C.69) together, then Equation (C.64) becomes as follows.

$$T_C^p = (1 - \overline{f}_C) T_{1C}^p + (T_{Cin} - \overline{T}_{1C}) f_C^p \quad \text{(C.70)}$$

From Appendix Figure C2, the output equation of hot stream for a single heat exchanger with a single bypass on cold side referred from (Hangos *et al*., 2004; Bao and Lee, 2007) is presented in Equation (C.71).

$$T_H = T_{1H} \quad \text{(C.71)}$$

Therefore, the state and output equations for cold and hot streams of a heat exchanger with a single bypass on cold side are summarized in Equations (C.72) to (C.75).

$$\frac{dT_{1C}}{dt} = \left(\frac{-UA + \tau_C F_C \overline{f}_C - \tau_C F_C}{\xi_C} \right) T_{1C} + \frac{UA}{\xi_C} T_{1H} + \left(\frac{\tau_C F_C \overline{T}_{1C} - \tau_C F_C T_{Cin}}{\xi_C} \right) f_C \quad \text{(C.72)}$$

$$\frac{dT_{1H}}{dt} = \frac{UA}{\xi_H} T_{1C} + \left(\frac{-UA - \tau_H \overline{F}_H}{\xi_H} \right) T_{1H} + \left(\frac{\tau_H T_{Hin} - \tau_H \overline{T}_{1H}}{\xi_H} \right) F_H \quad \text{(C.73)}$$

$$T_C = (1 - \overline{f}_C) T_{1C} + (T_{Cin} - \overline{T}_{1C}) f_C \quad \text{(C.74)}$$

$$T_H = T_{1H} \quad \text{(C.75)}$$

where $\tau_i = \rho_i C_{Pi}$ and $\xi_i = \rho_i V_i C_{Pi}$

C.3 Derivation of a Single Heat Exchanger without Bypass Concerning Volumetric Flowrates as Manipulated Variables into State Space Model

This section shows the derivation of a single heat exchanger without bypass by concerning volumetric flowrates as manipulated variables into state space model. The original equations for this model referred from Equations (C.1) to (C.4).

$$\rho_C V_C C_{pC} \frac{dT_{1C}}{dt} = \rho_C F_C C_{pC}(T_{Cin} - T_{1C}) + UA(T_{1H} - T_{1C}) \quad \text{(C.1)}$$

$$\rho_H V_H C_{pH} \frac{dT_{1H}}{dt} = \rho_H F_H C_{pH}(T_{Hin} - T_{1H}) + UA(T_{1C} - T_{1H}) \quad \text{(C.2)}$$

$$T_C = T_{1C} \quad \text{(C.3)}$$

$$T_H = T_{1H} \quad \text{(C.4)}$$

The state variables are output cold and hot temperature (T_{1C}, T_{1H}), and the manipulated variables are cold and hot flowrates (F_C, F_H).

Let $\tau_C = \rho_C C_{pC}$ and $\xi_C = \rho_C V_C C_{pC}$ then Equation (C.1) becomes;

$$\xi_C \frac{dT_{1C}}{dt} = \tau_C F_C (T_{Cin} - T_{1C}) + UA(T_{1H} - T_{1C}) \quad \text{(C.76)}$$

$$\xi_C \frac{dT_{1C}}{dt} = \tau_C F_C T_{Cin} - \tau_C F_C T_{1C} + UAT_{1H} - UAT_{1C} \quad \text{(C.77)}$$

From Equation (C.77), although most terms on the right are linear, the second one is nonlinear due to T_{1C} and F_C which are state and manipulated variables. Therefore, Taylor's series (Luyben *et al.*, 1997) for linearization are presented. After linearization, Equation (C.77) becomes;

$$\xi_C \frac{dT_{1C}}{dt} = \tau_C F_C T_{Cin} - \tau_C \overline{F}_C (T_{1C} - \overline{T}_{1C}) - \tau_C \overline{T}_{1C}(F_C - \overline{F}_C) + UAT_{1H} - UAT_{1C} \quad \text{(C.78)}$$

Then Equation (C.78) can be made into the deviation variable form or perturbation form.

$$\xi_C \frac{d(\overline{T}_{1C} + T_{1C}^p)}{dt} = \tau_C T_{Cin}(\overline{F}_C + F_C^p) - \tau_C \overline{F}_C T_{1C}^p - \tau_C \overline{T}_{1C} F_C^p + UA(\overline{T}_{1H} + T_{1H}^p) - UA(\overline{T}_{1C} - T_{1C}^p) \tag{C.79}$$

$$\xi_C \frac{dT_{1C}^p}{dt} = -\tau_C \overline{F}_C T_{1C}^p - \tau_C \overline{T}_{1C} F_C^p + UAT_{1H}^p - UAT_{1C}^p + \tau_C T_{Cin} F_C^p + \tau_C T_{Cin} \overline{F}_C + UA\overline{T}_{1H} - UA\overline{T}_{1C} \tag{C.80}$$

From Equation (C.79), at steady state;

$$0 = \tau_C T_{Cin} \overline{F}_C + UA\overline{T}_{1H} - UA\overline{T}_{1C} \tag{C.81}$$

Combine Equations (C.80) and (C.81) together and rearrange the equation into the following form. Then Equation (C.76) becomes;

$$\frac{dT_{1C}^p}{dt} = \left(\frac{-UA - \tau_C \overline{F}_C}{\xi_C}\right) T_{1C}^p + \left(\frac{UA}{\xi_C}\right) T_{1H}^p + \left(\frac{\tau_C T_{Cin} - \tau_C \overline{T}_{1C}}{\xi_C}\right) F_C^p \tag{C.82}$$

Equation (C.82) is the state equation for cold stream of a single heat exchanger without bypass concerning volumetric flowrate as manipulated variable. Likewise, the state equation for hot stream is followed the above development which is resulted in the following equation.

$$\frac{dT_{1H}^p}{dt} = +\left(\frac{UA}{\xi_H}\right) T_{1C}^p + \left(\frac{-UA - \tau_H \overline{F}_H}{\xi_H}\right) T_{1H}^p + \left(\frac{\tau_H T_{Hin} - \tau_H \overline{T}_{1H}}{\xi_H}\right) F_H^p \tag{C.83}$$

For the output equations for this system, they are the same as Equations (78) and (79).

$$T_C = T_{1C} \tag{C.84}$$

$$T_H = T_{1H} \tag{C.85}$$

C.4 Linearized State Space Equation Forms

This part shows another way which is referred from Hangos and Cameron (2001) to linearize models and change into state space forms. The advantage of this part is to ensure that the models derived in section C.1 to C.3 are correct.

Consider the set of nonlinear state space equations given by Equations (C.86) and (C.87).

$$\frac{dx(t)}{dt} = f(x(t), u(t)) \tag{C.86}$$

$$y(t) = h(x(t), u(t)) \tag{C.87}$$

or in expanded form as

$$\begin{pmatrix} \frac{dx_1}{dt} \\ \frac{dx_2}{dt} \\ \vdots \\ \frac{dx_n}{dt} \end{pmatrix} = \begin{pmatrix} f_1(x_1,\ldots,x_n,u_1,\ldots u_m) \\ f_2(x_1,\ldots,x_n,u_1,\ldots u_m) \\ \vdots \\ f_n(x_1,\ldots,x_n,u_1,\ldots u_m) \end{pmatrix} \tag{C.88}$$

and

$$\begin{pmatrix} y_1 \\ y_2 \\ \vdots \\ y_k \end{pmatrix} = \begin{pmatrix} h_1(x_1,\ldots,x_n,u_1,\ldots u_m) \\ h_2(x_1,\ldots,x_n,u_1,\ldots u_m) \\ \vdots \\ h_n(x_1,\ldots,x_n,u_1,\ldots u_m) \end{pmatrix} \tag{C.89}$$

If this state space models are regarded as LTI system as being written in deviation form, then the state space matrices are the partial derivatives of the state and input variables as follows:

$$A = \left.\frac{\partial f}{\partial x}\right|_{x_o, u_o} = \begin{pmatrix} \frac{\partial f_1}{\partial x_1} & \frac{\partial f_1}{\partial x_2} & \cdots & \frac{\partial f_1}{\partial x_n} \\ \frac{\partial f_2}{\partial x_1} & \frac{\partial f_2}{\partial x_2} & \cdots & \frac{\partial f_2}{\partial x_n} \\ \vdots & \vdots & \ddots & \vdots \\ \frac{\partial f_n}{\partial x_1} & \frac{\partial f_n}{\partial x_2} & \cdots & \frac{\partial f_n}{\partial x_n} \end{pmatrix} = \begin{pmatrix} a_{11} & a_{12} & \cdots & a_{1n} \\ a_{21} & a_{22} & \cdots & a_{2n} \\ \vdots & \vdots & \ddots & \vdots \\ a_{n1} & a_{n2} & \cdots & a_{nn} \end{pmatrix} \tag{C.90}$$

$$B = \left.\frac{\partial f}{\partial u}\right|_{x_o, u_o} = \begin{pmatrix} \frac{\partial f_1}{\partial u_1} & \frac{\partial f_1}{\partial u_2} & \cdots & \frac{\partial f_1}{\partial u_m} \\ \frac{\partial f_2}{\partial u_1} & \frac{\partial f_2}{\partial u_2} & \cdots & \frac{\partial f_2}{\partial u_m} \\ \vdots & \vdots & \ddots & \vdots \\ \frac{\partial f_n}{\partial u_1} & \frac{\partial f_n}{\partial u_2} & \cdots & \frac{\partial f_n}{\partial u_m} \end{pmatrix} = \begin{pmatrix} b_{11} & b_{12} & \cdots & b_{1m} \\ b_{21} & b_{22} & \cdots & b_{2m} \\ \vdots & \vdots & \ddots & \vdots \\ b_{n1} & b_{n2} & \cdots & b_{nm} \end{pmatrix} \tag{C.91}$$

$$C = \left.\frac{\partial h}{\partial x}\right|_{x_o, u_o} = \begin{pmatrix} \frac{\partial h_1}{\partial x_1} & \frac{\partial h_1}{\partial x_2} & \cdots & \frac{\partial h_1}{\partial x_n} \\ \frac{\partial h_2}{\partial x_1} & \frac{\partial h_2}{\partial x_2} & \cdots & \frac{\partial h_2}{\partial x_n} \\ \vdots & \vdots & \ddots & \vdots \\ \frac{\partial h_k}{\partial x_1} & \frac{\partial h_k}{\partial x_2} & \cdots & \frac{\partial h_k}{\partial x_n} \end{pmatrix} = \begin{pmatrix} c_{11} & c_{12} & \cdots & c_{1n} \\ c_{21} & c_{22} & \cdots & c_{2n} \\ \vdots & \vdots & \ddots & \vdots \\ c_{k1} & c_{k2} & \cdots & c_{kn} \end{pmatrix} \tag{C.92}$$

$$D = \left.\frac{\partial h}{\partial u}\right|_{x_o, u_o} = \begin{pmatrix} \frac{\partial h_1}{\partial u_1} & \frac{\partial h_1}{\partial u_2} & \cdots & \frac{\partial h_1}{\partial u_m} \\ \frac{\partial h_2}{\partial u_1} & \frac{\partial h_2}{\partial u_2} & \cdots & \frac{\partial h_2}{\partial u_m} \\ \vdots & \vdots & \ddots & \vdots \\ \frac{\partial h_k}{\partial u_1} & \frac{\partial h_k}{\partial u_2} & \cdots & \frac{\partial h_k}{\partial u_m} \end{pmatrix} = \begin{pmatrix} d_{11} & d_{12} & \cdots & d_{1m} \\ d_{21} & d_{22} & \cdots & d_{2m} \\ \vdots & \vdots & \ddots & \vdots \\ d_{k1} & d_{k2} & \cdots & d_{km} \end{pmatrix} \tag{C.93}$$

These entries are evaluated at the chosen operating point of x_0, u_0. Next, the derivation of state and output equations for hot stream of a single heat exchanger with a single bypass on hot side is considered.

From Equations (C.8), (C.21), (C.31) and (C.38), the state variables are $x=[T_{1C}\ T_{1H}]^T$; the input (manipulated) variables are $u=[F_C\ f_H]^T$; the output variables are $y=[T_C\ T_H]^T$. Let Equation (C.21) be $f_1(x,u)$, Equation (C.8) be $f_2(x,u)$, Equation (C.38) be $h_1(x,u)$ and Equation (C.31) be $h_2(x,u)$. The elements of A, B, C, D matrices are determined as follows.

$$a_{11}=\frac{\partial f_1}{\partial x_1}=\frac{\partial f_1}{\partial T_{1C}}=\frac{\partial}{\partial T_{1C}}\left(\frac{\tau_C F_C T_{Cin}-\tau_C F_C T_{1C}+UAT_{1H}-UAT_{1C}}{\xi_C}\right) \tag{C.94}$$

$$=\frac{-UA-\tau_C\bar{F}_C}{\xi_C} \tag{C.95}$$

$$a_{12}=\frac{\partial f_1}{\partial x_2}=\frac{\partial f_1}{\partial T_{1H}}=\frac{\partial}{\partial T_{1H}}\left(\frac{\tau_C F_C T_{Cin}-\tau_C F_C T_{1C}+UAT_{1H}-UAT_{1C}}{\xi_C}\right) \tag{C.96}$$

$$=\frac{UA}{\xi_C} \tag{C.97}$$

$$a_{21}=\frac{\partial f_2}{\partial x_1}=\frac{\partial f_2}{\partial T_{1C}}=\frac{\partial}{\partial T_{1C}}\left(\frac{\tau_H F_H(T_{Hin}-T_{1H})-\tau_H F_H f_H(T_{Hin}-T_{1H})+UA(T_{1C}-T_{1H})}{\xi_H}\right) \tag{C.98}$$

$$=\frac{UA}{\xi_H} \tag{C.99}$$

$$a_{22}=\frac{\partial f_2}{\partial x_2}=\frac{\partial f_2}{\partial T_{1H}}=\frac{\partial}{\partial T_{1H}}\left(\frac{\tau_H F_H(T_{Hin}-T_{1H})-\tau_H F_H f_H(T_{Hin}-T_{1H})+UA(T_{1C}-T_{1H})}{\xi_H}\right) \tag{C.100}$$

$$=\frac{-UA-\tau_H F_H+\tau_H F_H\bar{f}_H}{\xi_H} \tag{C.101}$$

$$b_{11}=\frac{\partial f_1}{\partial u_1}=\frac{\partial f_1}{\partial F_C}=\frac{\partial}{\partial F_C}\left(\frac{\tau_C F_C T_{Cin}-\tau_C F_C T_{1C}+UAT_{1H}-UAT_{1C}}{\xi_C}\right) \tag{C.102}$$

$$=\frac{\tau_C T_{Cin}-\tau_C\bar{T}_{1C}}{\xi_C} \tag{C.103}$$

$$b_{12}=\frac{\partial f_1}{\partial u_2}=\frac{\partial f_1}{\partial f_H}=\frac{\partial}{\partial f_H}\left(\frac{\tau_C F_C T_{Cin}-\tau_C F_C T_{1C}+UAT_{1H}-UAT_{1C}}{\xi_C}\right) \tag{C.104}$$

$$=0 \tag{C.105}$$

$$b_{21} = \frac{\partial f_2}{\partial u_1} = \frac{\partial f_2}{\partial F_C} = \frac{\partial}{\partial F_C}\left(\frac{\tau_H F_H (T_{Hin} - T_{1H}) - \tau_H F_H f_H (T_{Hin} - T_{1H}) + UA(T_{1C} - T_{1H})}{\xi_H}\right) \quad (C.106)$$

$$= 0 \quad (C.107)$$

$$b_{22} = \frac{\partial f_2}{\partial u_2} = \frac{\partial f_2}{\partial f_H} = \frac{\partial}{\partial f_H}\left(\frac{\tau_H F_H (T_{Hin} - T_{1H}) - \tau_H F_H f_H (T_{Hin} - T_{1H}) + UA(T_{1C} - T_{1H})}{\xi_H}\right) \quad (C.108)$$

$$= \frac{\tau_H F_H \overline{T}_{1H} - \tau_H F_H T_{Hin}}{\xi_H} \quad (C.109)$$

$$c_{11} = \frac{\partial h_1}{\partial x_1} = \frac{\partial h_1}{\partial T_{1C}} = \frac{\partial T_{1C}}{\partial T_{1C}} = 1 \quad (C.110)$$

$$c_{12} = \frac{\partial h_1}{\partial x_2} = \frac{\partial h_1}{\partial T_{1H}} = \frac{\partial T_{1C}}{\partial T_{1H}} = 0 \quad (C.111)$$

$$c_{21} = \frac{\partial h_2}{\partial x_1} = \frac{\partial h_2}{\partial T_{1C}} = \frac{\partial}{\partial T_{1C}}\left(T_{1H} - f_H T_{1H} + f_H T_{Hin}\right) = 0 \quad (C.112)$$

$$c_{22} = \frac{\partial h_2}{\partial x_2} = \frac{\partial h_2}{\partial T_{1H}} = \frac{\partial}{\partial T_{1H}}\left(T_{1H} - f_H T_{1H} + f_H T_{Hin}\right) = 1 - \overline{f}_H \quad (C.113)$$

$$d_{11} = \frac{\partial h_1}{\partial u_1} = \frac{\partial h_1}{\partial F_C} = \frac{\partial T_{1C}}{\partial F_C} = 0 \quad (C.114)$$

$$d_{12} = \frac{\partial h_1}{\partial u_2} = \frac{\partial h_1}{\partial f_H} = \frac{\partial T_{1C}}{\partial f_H} = 0 \quad (C.115)$$

$$d_{21} = \frac{\partial h_2}{\partial u_1} = \frac{\partial h_2}{\partial F_C} = \frac{\partial}{\partial F_C}\left(T_{1H} - f_H T_{1H} + f_H T_{Hin}\right) = 0 \quad (C.116)$$

$$d_{22} = \frac{\partial h_2}{\partial u_2} = \frac{\partial h_2}{\partial f_H} = \frac{\partial}{\partial f_H}\left(T_{1H} - f_H T_{1H} + f_H T_{Hin}\right) = T_{Hin} - \overline{T}_{1H} \quad (C.117)$$

Therefore, the state space equation in the deviation variable form of a single heat exchanger with a single bypass on hot side is Equations (C.118) and (C.119)) which are the same as Equations (C.39) to (C.42).

$$\begin{pmatrix} \dfrac{dT_{1C}}{dt} \\ \dfrac{dT_{1H}}{dt} \end{pmatrix} = \begin{pmatrix} \dfrac{-UA-\tau_C\bar{F}_C}{\xi_C} & \dfrac{UA}{\xi_C} \\ \dfrac{UA}{\xi_H} & \dfrac{-UA+\tau_H F_H \bar{f}_H - \tau_H F_H}{\xi_H} \end{pmatrix} \begin{pmatrix} T_{1C} \\ T_{1H} \end{pmatrix} + \begin{pmatrix} \dfrac{\tau_C T_{Cin} - \tau_C \bar{T}_{1C}}{\xi_C} & 0 \\ 0 & \dfrac{\tau_H F_H \bar{T}_{1H} - \tau_H F_H T_{Hin}}{\xi_H} \end{pmatrix} \begin{pmatrix} F_C \\ f_H \end{pmatrix}$$

(C.118)

$$\begin{pmatrix} T_C \\ T_H \end{pmatrix} = \begin{pmatrix} 1 & 0 \\ 0 & 1-\bar{f}_H \end{pmatrix} \begin{pmatrix} T_{1C} \\ T_{1H} \end{pmatrix} + \begin{pmatrix} 0 & 0 \\ 0 & T_{Hin}-\bar{T}_{1H} \end{pmatrix} \begin{pmatrix} F_C \\ f_H \end{pmatrix} \qquad \text{(C.119)}$$

Appendix D
Theorem proof

This appendix shows the full proof of the theorems or equations as resulted in previous part.

1. *Theorem 2:* (Bao and Lee, 2007) For a given stable non-passive process with a transfer function matrix of G(s), there exists a diagonal, stable, and passive transfer function matrix W(s) = *w(s)I* such that H(s) = G(s) + W(s) is passive.

Proof: Since both G(s) and W(s) are analytic in $\mathrm{Re}(s) \geq 0$, so is H(s). Therefore, H(s) is passive if the minimum eigenvalue of $[H(j\omega)+H^*(j\omega)]$ is non-negative for any $\omega \in [-\infty, +\infty]$,

$$\lambda_{\min}\left(H(j\omega)+H^*(j\omega)\right)=\lambda_{\min}\left(\left[G(j\omega)+G^*(j\omega)\right]+\left[W(j\omega)+W^*(j\omega)\right]\right) \qquad (D.1)$$

Because both $\left[G(j\omega)+G^*(j\omega)\right]$ and $\left[W(j\omega)+W^*(j\omega)\right]$ are Hermitian, from the Weyl inequality (Amir-Moez, 1956), we have

$$\lambda_{\min}\left(H(j\omega)+H^*(j\omega)\right)\geq\lambda_{\min}\left(G(j\omega)+G^*(j\omega)\right)+\lambda_{\min}\left(W(j\omega)+W^*(j\omega)\right)$$

$$\lambda_{\min}\left(H(j\omega)+H^*(j\omega)\right)=\lambda_{\min}\left(G(j\omega)+G^*(j\omega)\right)+2\{\mathrm{Re}\}\left(w(j\omega)\right) \qquad (D.2)$$

If w(s) is chosen to be "passive enough" such that

$$\mathrm{Re}\left(w(j\omega)\right)\geq-\frac{1}{2}\lambda_{\min}\left(G(j\omega)+G^*(j\omega)\right) \qquad (D.3)$$

For any $\omega \in [-\infty, +\infty]$, then H(s) = G(s) + W(s) can be rendered passive. If $\mathrm{Re}\left(w(j\omega)\right)>-\frac{1}{2}\lambda_{\min}\left(G(j\omega)+G^*(j\omega)\right)$, then H(s) will be strictly passive□

2. *Theorem 3:* (Bao *et al.*, 2002a) For an interconnected system (as shown in Figure 3) comprising a stable subsystem G(*s*) and a decentralized controller K(*s*) = diag{$k_i(s)$}, *i* = 1, ..., *n,* if a stable and minimum phase transfer function *w*(*s*) is chosen such that $\nu(w(s),\omega)<-\nu(G^+(s),\omega)$, then the closed-loop system will be decentralized unconditionally stable if for any loop *i* = 1, ..., *n*, $k'_i(s) = k^+_I(s)[1-w(s)k^+_I(s)]^{-1}$ is passive, where $k_I^+(s) = U_{ii}k_I(s)$ and U = diag{U_{ii}}, i = 1, …, n

Proof: When loop shifting is used, a closed-loop system equal to that in Figure 3 is obtained, as shown in Appendix Figure D1,

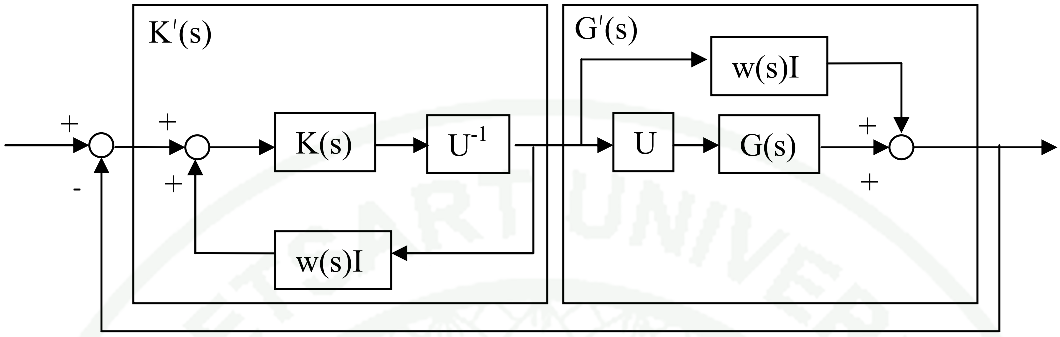

Appendix Figure D1 Loop shifting

Source: Bao *et al*. (2002a)

where $$G'(s) = G(s)U + w(s)I \quad \text{(D.4)}$$

and

$$K'(s) = U^{-1}K(s)[I - w(s)U^{-1}K(s)]^{-1} \quad \text{(D.5)}$$

From Theorem 1, if G'(*s*) is SPR and K'(*s*) is PR, the closed-loop system will be stable. Because $K^{+}(s)$ is diagonal, so is the subsystem K'(*s*). Then, K'(*s*) is passive if and only if its diagonal element $k_i'(s)$ is passive for each loop $i = 1, ..., n$. In addition, when $k_i'(s)$ is passive, K'(*s*) will remain passive when its gain matrix is reduced to $K'(s)E = \mathrm{diag}\{k_i'(s)\varepsilon_i\}$, $0 \le \epsilon_i \le 1$, $i = 1, ..., n$. Therefore, the positive realness of $k_i'(s)$ ensures the decentralized unconditional stability of the closed-loop system.□

3. ***Theorem 5:*** (Necessary condition for decentralized integral controllability (DIC)) (Morari and Zafiriou, 1989). An $m \times m$ LTI stable process G(s) is DIC only if

$$\Lambda_{ii}(G(0)) \ge 0, \forall i = 1, ..., m \quad (50)$$

where $\Lambda_{ii}(G(0))$ is the *i*th diagonal element of the RGA matrix of G(0).

Proof: Follows from Theorem 6 in Grosdidier *et al*. (1985).

The rule of avoiding pairings corresponding to negative RGA elements goes back to Bristol (1966), but it was proved rigorously in recent. Note that *ij*-th element of the RGA is defined as

$$RGA_{ij} = \frac{(\partial y_i / \partial u_j)_{u_{k,k\neq j}}}{(\partial y_i / \partial u_j)_{y_{l,l\neq i}}} = \frac{gOL}{gCL} \tag{D.6}$$

where *gOL* is open-loop steady-state gain matrix and *gCL* is closed-loop steady-state gain matrix

Equation (D.6) represents the ratio of the gain from u_j to y_i in open-loop (other *u*'s constant) and closed-loop (other *y*'s constant). If the sign of this gain changes as we change or close other loops, then we are not able to apply negative feedback in all cases, and the plant is not DIC.

4. Derivation from Problem 1 to Problem 2

Problem 1 (Bao *et al*., 2002a)

$$\min_{\mathrm{D}}\{\mathrm{t}\} \tag{51}$$

subject to:

$$\mathrm{D}(\omega)^{-1}\,\mathrm{G}^{+}(\mathrm{j}\omega)\mathrm{D}(\omega)+\mathrm{D}(\omega)\left[\mathrm{G}^{+}(\mathrm{j}\omega)\right]^{*}\mathrm{D}(\omega)^{-1}+\mathrm{tI}>0 \tag{52}$$

$$\mathrm{D}(\omega)>0 \tag{53}$$

where $\mathrm{D}(\omega)\in \mathrm{R}^{\mathrm{n}\times\mathrm{n}}$ is a diagonal matrix and *t* is a real scalar variable

Because $\mathrm{D}(\omega)$ is nonsingular; therefore Equation (52) is equivalent to the following equation.

$$D(\omega)\left\{D(\omega)^{-1}G^{+}(j\omega)D(\omega)+D(\omega)[G^{+}(j\omega)]^{*}D(\omega)^{-1}\right\}D(\omega)+tD(\omega)D(\omega)>0 \tag{D.7}$$

$$G^{+}(j\omega)D(\omega)D(\omega)+D(\omega)D(\omega)[G^{+}(j\omega)]^{*}+tD(\omega)D(\omega)>0 \tag{D.8}$$

Due to $M = D(\omega)D(\omega)$ as defined before, Equation (D.8) becomes Equation (D.9).

$$G^{+}(j\omega)M + M[G^{+}(j\omega)]^{*} + tM > 0 \tag{D.9}$$

Due to $G^{+}(j\omega) = X(\omega) + jY(j\omega)$, where both $X(\omega)$ and $Y(\omega)$ are real matrices, as defined before, This leads Equation (D.9) to Equation (D.10).

$$(X(\omega)M + MX(\omega)^{T}) + j(Y(\omega)M - MY(\omega)^{T}) + tM > 0 \tag{D.10}$$

or quaivalently,

$$-(X(\omega)M + MX(\omega)^{T}) - j(Y(\omega)M - MY(\omega)^{T}) - tM < 0 \tag{D.11}$$

The above equation holds if and only if

$$\begin{bmatrix} -X(\omega)M - MX(\omega)^{T} & Y(\omega)M - MY(\omega)^{T} \\ -Y(\omega)M + MY(\omega)^{T} & -X(\omega)M - MX(\omega)^{T} \end{bmatrix} - t\begin{bmatrix} M & 0 \\ 0 & M \end{bmatrix} < 0 \tag{D.12}$$

Therefore, Problem 1 can be converted into the following generalized eigenvalue problem with constraints described in real matrix inequalities.

Problem 2 (Bao *et al*., 2002b)

$$\min_{\mathrm{M}}\{\mathrm{t}\} \tag{54}$$

subject to:

$$\begin{bmatrix} -\mathrm{X}(\omega)\mathrm{M} - \mathrm{M}\mathrm{X}^{\mathrm{T}}(\omega) & \mathrm{Y}(\omega)\mathrm{M} - \mathrm{M}\mathrm{Y}^{\mathrm{T}}(\omega) \\ -\mathrm{Y}(\omega)\mathrm{M} + \mathrm{M}\mathrm{Y}^{\mathrm{T}}(\omega) & -\mathrm{X}(\omega)\mathrm{M} - \mathrm{M}\mathrm{X}^{\mathrm{T}}(\omega) \end{bmatrix} < \mathrm{t}\begin{bmatrix} \mathrm{M} & 0 \\ 0 & \mathrm{M} \end{bmatrix} \tag{55}$$

$$\mathrm{M} \text{ is diagonal and } \mathrm{M} > 0 \tag{56}$$

Appendix E
Code validation

Since the main part of this work uses the passivity concept via MATLAB program, codes determining or optimizing is verified through some examples from Bao and Lee (2007) and Boonkhao (2004).

E.1 Code Validation of Definition 2.1: Passivity Index

The equation used to determine the passivity index is Equation (57)

$$\nu_s\left(G^+(s),\omega\right) = -\lambda_{\min}\left(\frac{1}{2}\left[M^{-\frac{1}{2}}G^+(j\omega)M^{\frac{1}{2}} + M^{\frac{1}{2}}\left(G^+(j\omega)\right)^* M^{-\frac{1}{2}}\right]\right) \tag{57}$$

The example used to validate, which is referred from Bao and Lee (2007), has a system as follows.

$$\begin{aligned} \dot{x} &= \begin{pmatrix} -690.87 & 279.17 \\ 69.254 & -375.29 \end{pmatrix} x + \begin{pmatrix} 411.7 & 0 \\ 0 & 306.03 \end{pmatrix} u \\ y &= \begin{pmatrix} 1 & 0 \\ 0 & 1 \end{pmatrix} x \end{aligned} \tag{E.1}$$

After validating with the author's code, it give the same results as shown in Appendix Figure E1.

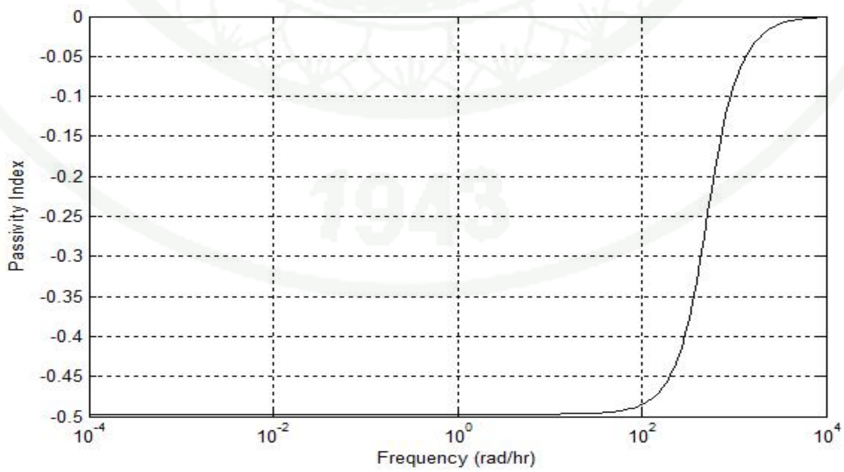

Appendix Figure E1 Code validation of passivity index of the example

Source: Bao and Lee (2007)

E.2 Code Validation of Definition 2.5: Weighting Function

The equations used to determine the weighting function parameter are Equations (59) and (60).

$$\min_{a,b,c,k} \sum_{i=1}^{m} \Big(\mathrm{Re}\big(w(j\omega_i)\big) - \upsilon_s\big(G^{+}(s), \omega_i\big) \Big)^2 \qquad (59)$$

subject to

$$\mathrm{Re}\big(w(j\omega_i)\big) > \upsilon_s\big(G^{+}(s), \omega_i\big), \quad \forall i = 1 \ldots m \qquad (60)$$

The example used to validate, which is referred from Boonkhao (2004), has a system as follows.

$$G(s) = \begin{bmatrix} \dfrac{4.05}{50s+1}e^{-27s} & \dfrac{1.77}{60s+1}e^{-28s} \\ \dfrac{5.39}{50s+1}e^{-18s} & \dfrac{5.72}{60s+1}e^{-14s} \end{bmatrix} \qquad (E.2)$$

This system is tested by passivity index as in section E.1. The result is shown in Appendix Figure E2.

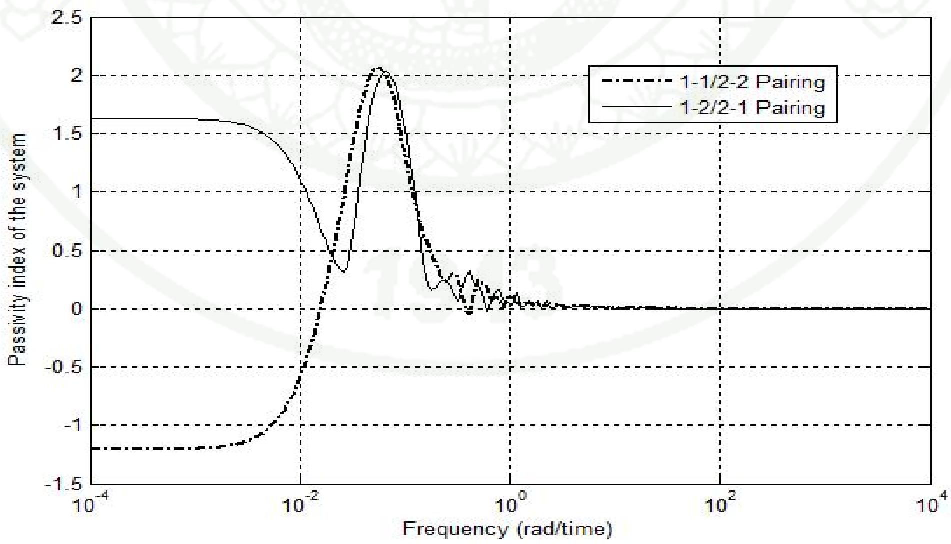

Appendix Figure E2 Code validation of the passivity index of the system

Source: Boonkhao (2004)

The above graph results that the system is non-passive; therefore, the weighting function has to add into this system and make it passive. After validating with the author's code in Appendix F, it gives the same results as shown in Appendix Figures E3 and E4.

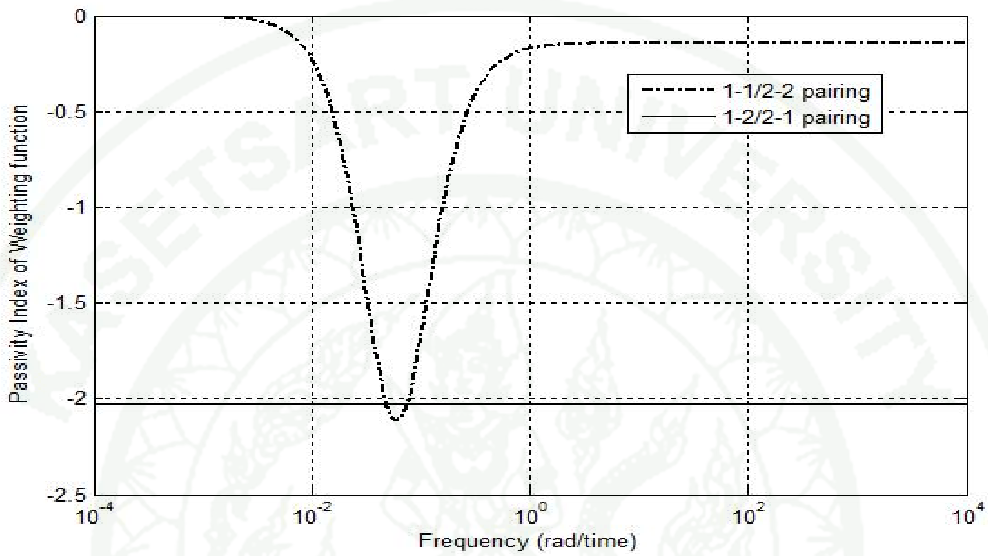

Appendix Figure E3 Code validation of the passivity index of weighting function

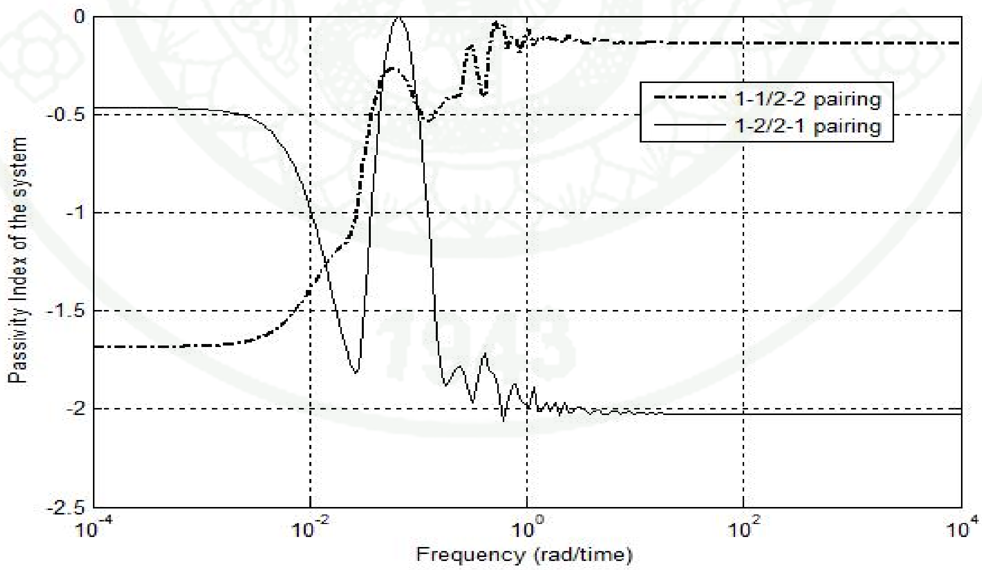

Appendix Figure E4 Code validation of passivity index after adding weighting Function

Source: Boonkhao (2004)

E.3 Code Validation of Problem 2: Diagonal Scaling Passivity Index

The equations used to calculate diagonal scaling passivity index are Equations (54) to (57) as follows.

$$\min_{\mathrm{M}}\{\mathrm{t}\} \tag{54}$$

subject to:

$$\begin{bmatrix} -\mathrm{X}(\omega)\mathrm{M}-\mathrm{M}\mathrm{X}^{\mathrm{T}}(\omega) & \mathrm{Y}(\omega)\mathrm{M}-\mathrm{M}\mathrm{Y}^{\mathrm{T}}(\omega) \\ -\mathrm{Y}(\omega)\mathrm{M}+\mathrm{M}\mathrm{Y}^{\mathrm{T}}(\omega) & -\mathrm{X}(\omega)\mathrm{M}-\mathrm{M}\mathrm{X}^{\mathrm{T}}(\omega) \end{bmatrix} < \mathrm{t}\begin{bmatrix} \mathrm{M} & 0 \\ 0 & \mathrm{M} \end{bmatrix} \tag{55}$$

$$\mathrm{M} \text{ is diagonal and } \mathrm{M} > 0 \tag{56}$$

$$\nu_s\left(\mathrm{G}^+(\mathrm{s}),\omega\right) = -\lambda_{\min}\left(\frac{1}{2}\left[\mathrm{M}^{-\frac{1}{2}}\mathrm{G}^+(\mathrm{j}\omega)\mathrm{M}^{\frac{1}{2}} + \mathrm{M}^{\frac{1}{2}}\left(\mathrm{G}^+(\mathrm{j}\omega)\right)^*\mathrm{M}^{-\frac{1}{2}}\right]\right) \tag{57}$$

The example used to validate, which is referred from Bao and Lee (2007), has a system as follows.

$$G(s) = \begin{bmatrix} \dfrac{4.09e^{-1.3s}}{(33s+1)(8.3s+1)} & \dfrac{-6.36e^{-0.2s}}{(31.6s+1)(20s+1)} & \dfrac{0.25e^{-0.4s}}{21s+1} & \dfrac{-0.49e^{-5s}}{(22s+1)^2} \\ \dfrac{-4.17e^{-4s}}{45s+1} & \dfrac{6.93e^{-1.01s}}{44.6s+1} & \dfrac{-0.05e^{-5s}}{(34.5s+1)^2} & \dfrac{1.53e^{-2.8s}}{(48s+1)} \\ \dfrac{-1.73e^{-17s}}{(13s+1)^2} & \dfrac{5.11e^{-11s}}{(13.3s+1)^2} & \dfrac{4.61e^{-1.02s}}{18.5s+1} & \dfrac{-5.48e^{-0.5s}}{15s+1} \\ \dfrac{-11.18e^{-2.6s}}{(43s+1)(6.5s+1)} & \dfrac{14.04e^{-0.2s}}{(45s+1)(10s+1)} & \dfrac{-0.1e^{-0.05s}}{(31.6s+1)(5s+1)} & \dfrac{4.49e^{-0.06s}}{(48s+1)(6.3s+1)} \end{bmatrix} \tag{E.3}$$

This system is tested by both passivity index as in section E.1 and diagonal scaling passivity index as in this section. The results are shown in Appendix Figure E5.

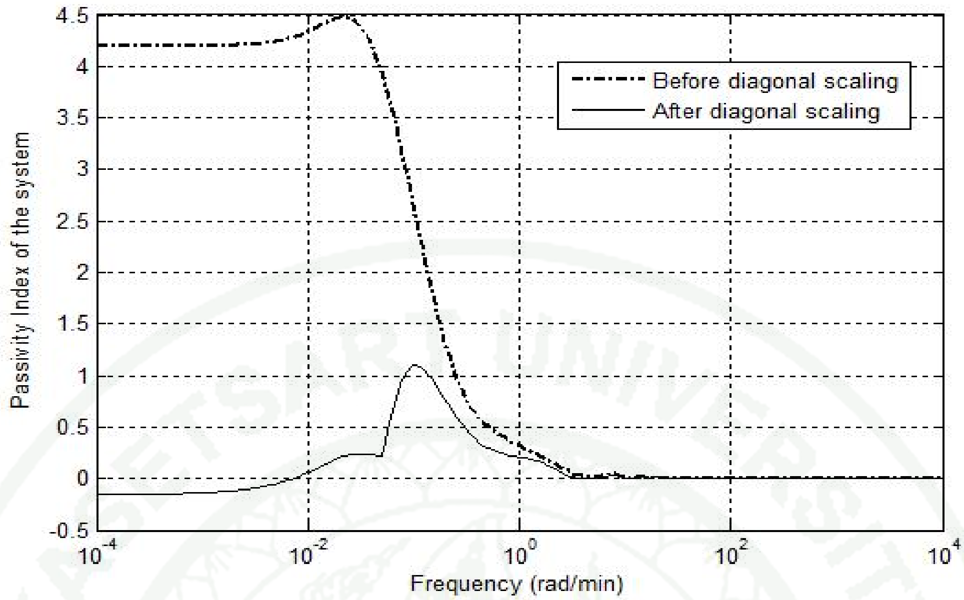

Appendix Figure E5 Code validation of before and after diagonal scaling passivity Index

Source: Bao and Lee (2007)

CURRICULUM VITAE

NAME	: Mr.Nitipat Chaiwattanapong		
BIRTH DATE	: September 21, 1985		
BIRTH PLACE	: Chonburi, Thailand		
EDUCATION	: **YEAR**	**INSTITUTE**	**DEGREE**
	2004	Kasetsart University	B.Eng (Chem Eng)
WORK PLACE	: Department of Chemical Engineering, Kasetsart University		
SCHOLARSHIP	: Chemical Engineering Scholarship, Kasetsart University		